CONTENTS

PREFACE	iii	1/A4
1. LANGLEY RESEARCH CENTER FLEXIBLE BEAM EXPERIMENT Raymond C. Montgomery	1	1/A8
2. STRUCTURAL DYNAMICS RESEARCH IN ACTUATOR/SENSOR LOCATIONS G. C. Horner	5	1/A12
3. REDUCED ORDER ADAPTIVE REGULATION STRATEGIES FOR THE NASA BEAM CONTROL EXPERIMENT C. Richard Johnson, Jr.	13	1/B6
4. DYNAMICS AND CONTROL OF COUPLED RIGID/FLEXIBLE BODIES Elias G. Abu-Saba	21	1/B14
5. ADJUSTED FEEDBACK CONTROL FOR INCOMPLETE DECOUPLING PROCEDURES Harold A. Hamer	27	1/C6
6. INVESTIGATIONS OF ALGORITHMS FOR LARGE SPACE STRUCTURES E. D. Denman	47	1/D12
7. IDENTIFICATION AND CONTROL FOR FLEXIBLE VEHICLES Christopher S. Greene	57	1/E8
8. RELIABILITY ISSUES IN ACTIVE CONTROL OF FLEXIBLE SPACE STRUCTURES W. E. VanderVelde	73	1/F10
9. HARDWARE DEMONSTRATION OF FLEXIBLE BEAM CONTROL David B. Schaechter	85	1/G8
10. THE ADAPTIVE/LEARNING CONTROL SYSTEM APPROACH Frederick E. Thau	93	2/A4
11. SOME EARLY EXPERIMENTS WITH NONCOLOCATED CONTROLS OF FLEXIBLE SYSTEMS R. H. Cannon, Jr.	101	2/A12
12. REVIEW OF AD HOC COMMITTEE REPORT ON TECHNOLOGY OF LARGE SPACE STRUCTURES H. Ashley	107	2/B4
13. ATTITUDE CONTROL OF A FLEXIBLE TRIANGULAR TRUSS IN SPACE Bong Wie and Arthur E. Bryson, Jr.	113	2/B10
14. LARGE MOTIONS OF DEFORMABLE SPACECRAFT T. R. Kane	127	2/C10
ATTENDEES	133	2/D2

Item 830-H-10 NAS 1.55:2187

NASA Conference Publication 2187

COMPLETED ORIGINAL

Structural Dynamics and Control of Large Space Structures

Proceedings of a workshop
held at NASA Langley Research Center
Hampton, Virginia
October 30-31, 1980

NASA

143

NASA Conference Publication 2187

Structural Dynamics and Control of Large Space Structures

E. Burton Lightner, *Compiler*
Langley Research Center
Hampton, Virginia

Proceedings of a workshop
held at NASA Langley Research Center
Hampton, Virginia
October 30-31, 1980

NASA
National Aeronautics
and Space Administration

Scientific and Technical
Information Branch

1981

PREFACE

This publication contains the proceedings of a workshop conducted at the NASA Langley Research Center on the technology for controlling large space structures currently being conceived for space applications by the year 2000. The purpose of the program was to address the fundamental technology deficiencies that were identified in several studies on large space systems (LSS) conducted by NASA in the last several years. Two such studies have pointed out the need for distributed control technology and technology for adaptive surface control. During the course of the workshop, additional technological deficiencies were uncovered, the most notable being the lack of experience in managing large numbers of control system components and maintaining system level functions in the presence of failed actuator or sensor components. At present, these issues are of primary concern because there is little or no experience with them in the space program but the missions studies are critically dependent upon these technology items for their mission economy or success.

A basic research program has been assembled at NASA Langley Research Center to address the technology deficiencies discussed previously. It consists of an in-house effort, university grants, and industry contracts. The staffs of the respective participants were assembled at the workshop to review the current state of research in the control technology for large structural systems and to plan the efforts that would be pursued by their respective organizations. This document contains the more important slides that were used by each participant with a word description where required for clarity. It is our intention to review the progress of the activity and have another workshop to plan the program for the following year at the close of the 1981 fiscal year (about October 1981).

Use of trade names or names of manufacturers in this report does not constitute an official endorsement of such products or manufacturers, either expressed or implied, by the National Aeronautics and Space Administration.

Raymond C. Montgomery, Cochairman
Garnett C. Horner, Cochairman
E. Burton Lightner, Coordinator

Blank Page

CONTENTS

PREFACE iii

1. LANGLEY RESEARCH CENTER FLEXIBLE BEAM EXPERIMENT 1
Raymond C. Montgomery

2. STRUCTURAL DYNAMICS RESEARCH IN ACTUATOR/SENSOR LOCATIONS 5
G. C. Horner

3. REDUCED ORDER ADAPTIVE REGULATION STRATEGIES FOR THE NASA BEAM CONTROL EXPERIMENT 13
C. Richard Johnson, Jr.

4. DYNAMICS AND CONTROL OF COUPLED RIGID/FLEXIBLE BODIES 21
Elias G. Abu-Saba

5. ADJUSTED FEEDBACK CONTROL FOR INCOMPLETE DECOUPLING PROCEDURES 27
Harold A. Hamer

6. INVESTIGATIONS OF ALGORITHMS FOR LARGE SPACE STRUCTURES 47
E. D. Denman

7. IDENTIFICATION AND CONTROL FOR FLEXIBLE VEHICLES 57
Christopher S. Greene

8. RELIABILITY ISSUES IN ACTIVE CONTROL OF FLEXIBLE SPACE STRUCTURES . . . 73
W. E. VanderVelde

9. HARDWARE DEMONSTRATION OF FLEXIBLE BEAM CONTROL 85
David B. Schaechter

10. THE ADAPTIVE/LEARNING CONTROL SYSTEM APPROACH 93
Frederick E. Thau

11. SOME EARLY EXPERIMENTS WITH NONCOLOCATED CONTROLS OF FLEXIBLE SYSTEMS 101
R. H. Cannon, Jr.

12. REVIEW OF AD HOC COMMITTEE REPORT ON TECHNOLOGY OF LARGE SPACE STRUCTURES 107
H. Ashley

13. ATTITUDE CONTROL OF A FLEXIBLE TRIANGULAR TRUSS IN SPACE 113
Bong Wie and Arthur E. Bryson, Jr.

14. LARGE MOTIONS OF DEFORMABLE SPACECRAFT 127
T. R. Kane

ATTENDEES 133

BLANK

PAGE

LANGLEY RESEARCH CENTER FLEXIBLE BEAM EXPERIMENT

Raymond C. Montgomery
NASA Langley Research Center
Hampton, VA

Workshop on the Structural Dynamics and Control
of Large Space Structures
October 30-31, 1980

LaRC FLEXIBLE BEAM EXPERIMENT

To verify some of the optimization results and other control algorithms, a flexible beam experiment has been initiated at LaRC. In figure 1, the flexible beam experiment consists of a 3.66 m (12 ft) long aluminum beam with a 4.76 mm (3.16 in.) by 15 cm (6 in.) cross section. The beam is suspended by two small flexible cables so that free-free end conditions are approximated. Located in front of the beam are four electromagnetic shakers (actuators) which can be repositioned along the beam by sliding them along the platform which supports them. The console on the left contains the power amplifiers for the shakers.

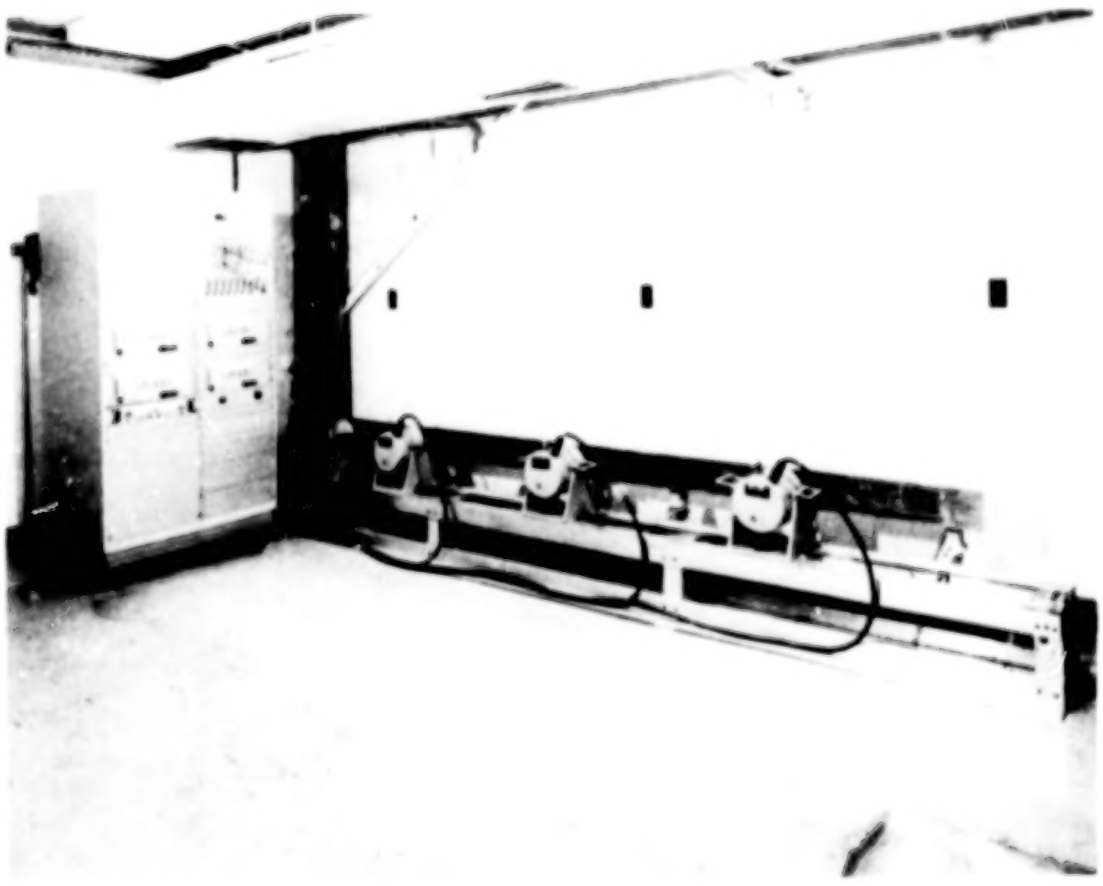

Figure 1

Figure 2 shows another picture of the experimental setup. On one side of the beam the four shakers are located and on the other side of the beam there are nine noncontacting displacement probes. With the experiment being tied in with the CDC Cyber 175 computer, real-time calculations may be made. For example, the output of the displacement probes can be made available to the computer. Using state estimation, the velocity at the shaker locations can be approximated. Knowing the damping rate or gain from the optimization program and the velocity, the desired force output of the shakers can be calculated.

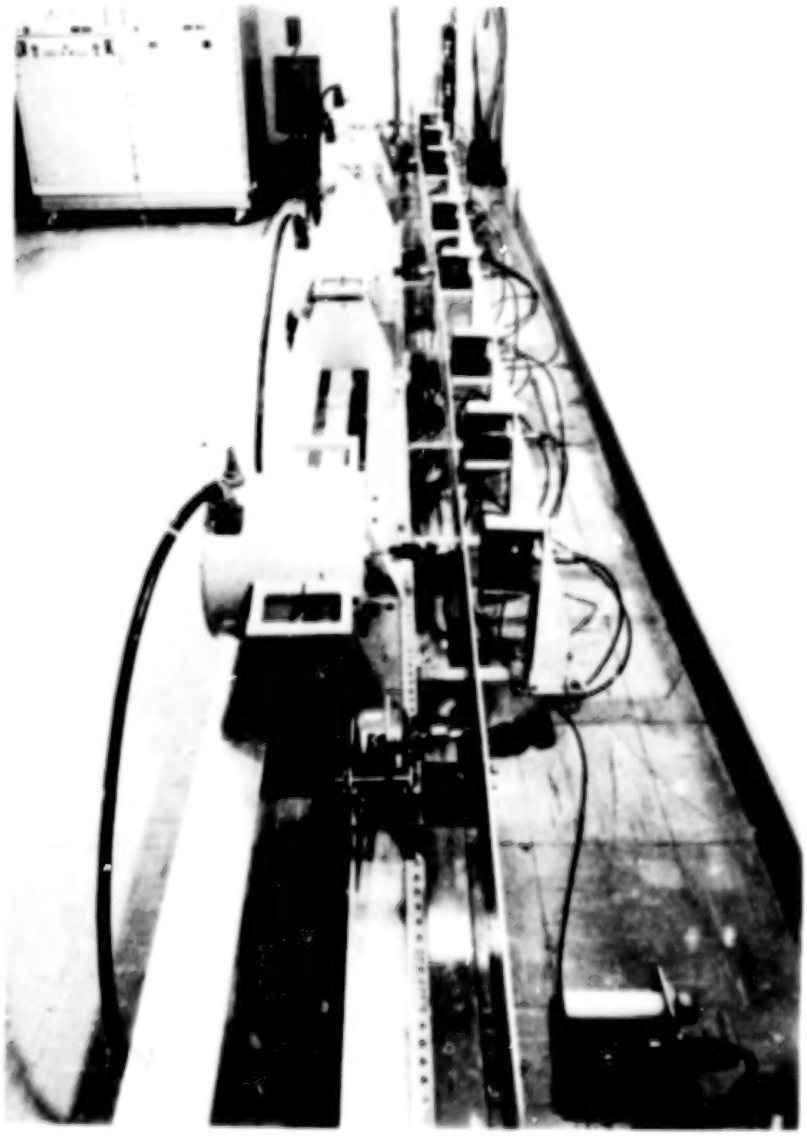

Figure 2

Blank Page

STRUCTURAL DYNAMICS RESEARCH

IN ACTUATOR/SENSOR LOCATIONS

G. C. Horner
NASA Langley Research Center
Hampton, VA

Workshop on the Structural Dynamics and Control
of Large Space Structures
October 30-31, 1980

OPTIMUM DAMPER LOCATIONS FOR A FREE-FREE BEAM

The objectives of this research are to identify optimum locations for sensors and actuators on large space structures. If it is assumed that large platforms and antennae will have many potential actuator/sensor locations, we may logically ask "Where should actuators and sensors be placed?" Not only should the optimum placement be determined, but also the dynamic characteristics of actuators may also be necessary.

OBJECTIVES

- o DEVELOP ALGORITHMS TO OPTIMALLY LOCATE AND DESIGN DAMPERS FOR LARGE SPACE STRUCTURES
- o DETERMINE REQUIREMENTS FOR DISTRIBUTED SENSING AND ACTUATION (AS OPPOSED TO COLOCATED SENSOR AND ACTUATOR) IN CONTROL OF STRUCTURAL SYSTEMS

APPROACH

- o USE MATHEMATICAL PROGRAMMING TO SOLVE FOR OPTIMUM DAMPING RATE AND LOCATION.
- o CONSIDER ACTUATOR DYNAMICS TO SOLVE FOR OPTIMUM ACTUATOR MASS.

Figure 1

DAMPING CHARACTERISTICS OF A FREE-FREE BEAM

To get an understanding of the behavior of large space structures, we first look at the damping characteristics of a uniform beam. A dash pot is located at one end of a free-free beam. This is an ideal dash pot which is characterized by a damping rate, C, and no other dynamic characteristics. In figure 2 it is seen that for small values of C (<.005), the damping ratio, ζ, and damping rate are linearily related. This is denoted as perturbation theory. As the damping rate is increased, the damping ratio reaches a peak value and then decreases. The peak value of the damping ratio is about 0.2 for the first flexible mode. Suppose a design problem were stated which required that the first mode have a damping ratio greater than 0.2. This requirement may be a result of mission performance specifications. To achieve more than the 0.2 damping ratio in the first mode, one or more dash pots are required. Since the design problem being addressed here is one in which the damping ratio is prescribed for each mode to be damped, the damping rate of the dash pots is determined.

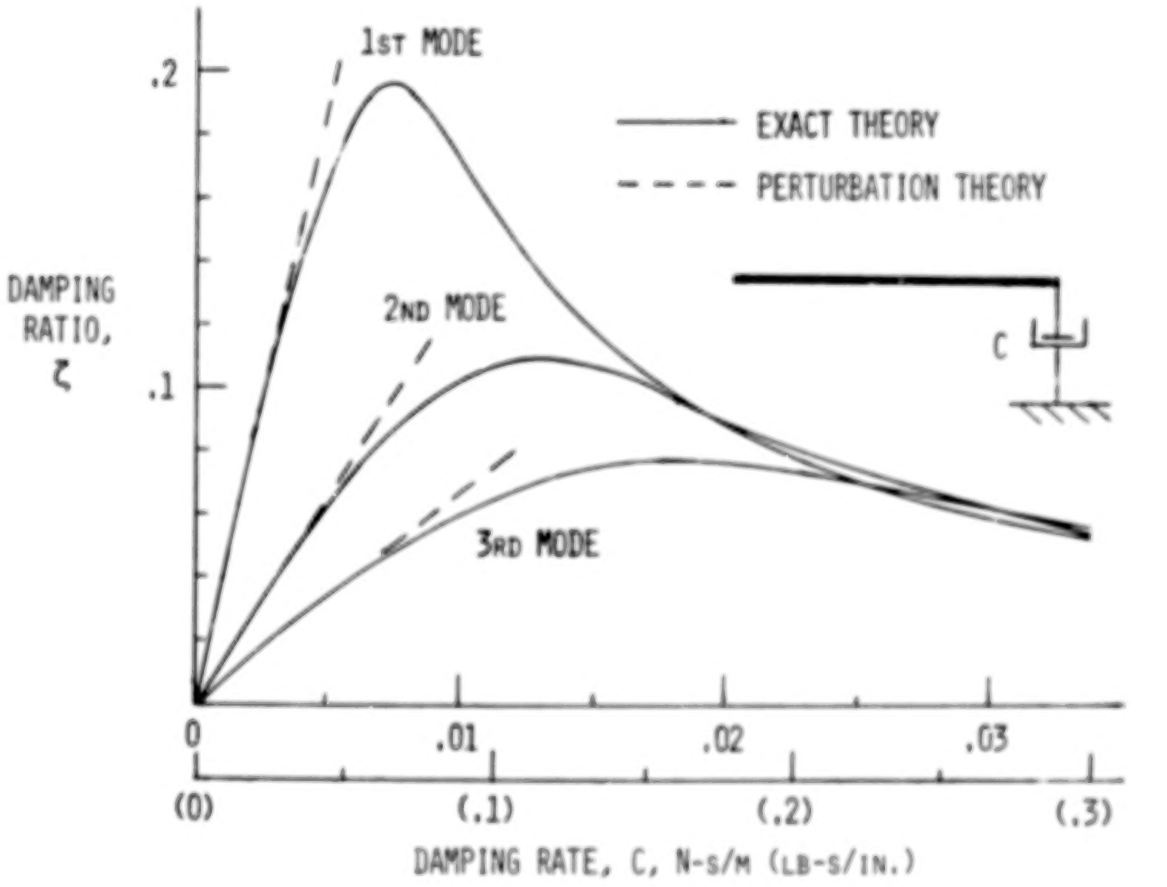

Figure 2

DAMPING CHARACTERISTICS OF A CLAMPED-FREE BEAM

The results are essentially the same as for the free-free beam in figure 2.

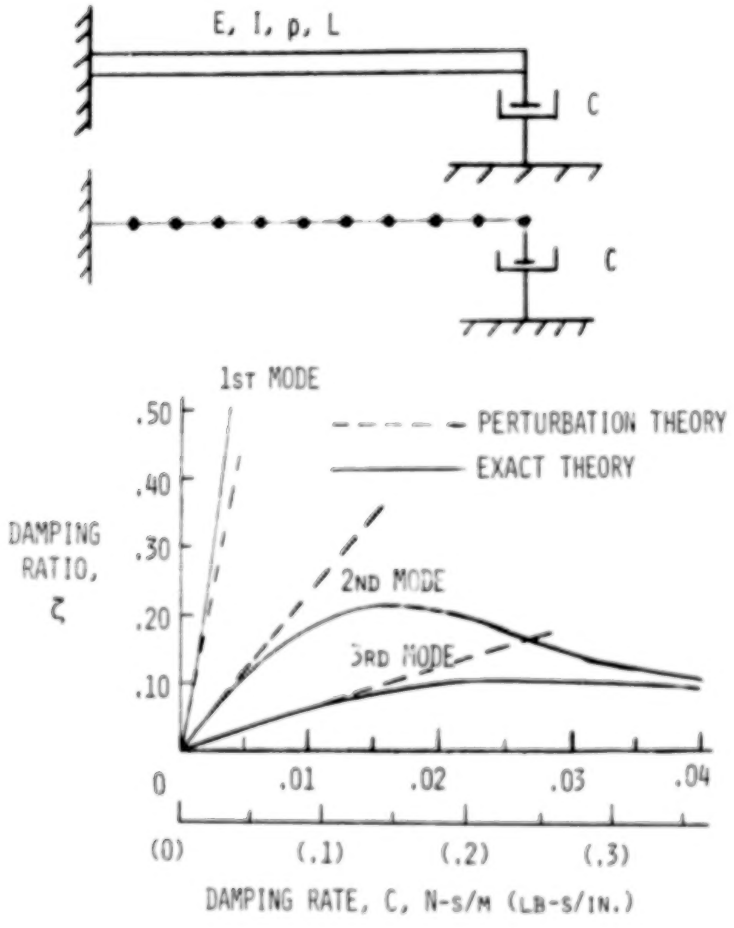

Figure 3

NONLINEAR OPTIMIZATION PROBLEM

A design problem is posed which states that given the prescribed modal damping ratio for N modes, what are the optimum damping locations and sizes? The design problem is now cast as a nonlinear optimization problem. Since it is not known where the dash pots should be located on a structure, the initial step is to put a dash pot at every location of the beam. The objective function is to minimize the total dissipative effort. The constraints are that the actual computed modal damping ratios must be greater than or equal to the prescribed value. Another constraint is that the damping rate must be positive. This guarantees stability.

- FOR PRESCRIBED MODAL DAMPING RATIO IN N MODES, WHAT ARE THE BEST DAMPING SIZES AND LOCATIONS?

- OBJECTIVE

  MINIMIZE TOTAL DISSIPATION $\quad \text{MIN} \sum_i C_i$

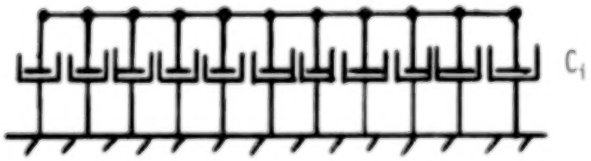

- CONSTRAINTS

  $(\text{COMPUTED MODAL DAMPING RATIO})_j \geq (\text{DESIGN VALUE})_j$

  C_i MUST BE POSITIVE

Figure 4

OPTIMUM DAMPING LOCATIONS AND SIZES FOR A FREE-FREE BEAM

Some results are presented in figure 5 for a free-free beam. The design problem consisted of prescribing a modal damping ratio of 0.5 in N modes. The results are shown for N = 1, 2, 3, 4. The results are also split between symmetric solutions and nonsymmetric solutions. The symmetric solutions are obtained by minimizing the total dissipation while imposing symmetry in the solution. The horizontal lines represent the length of the beam. The vertical lines are proportional to the magnitude of the damping rate at the location shown on the beam axis. The nonsymmetric solution is obtained by removing the symmetry requirement and the smallest damper location. Thus, nonsymmetric solutions will have no more than one fewer dampers than the symmetric case. In some cases the objective function for the nonsymmetric solution is less than that for the symmetric case.

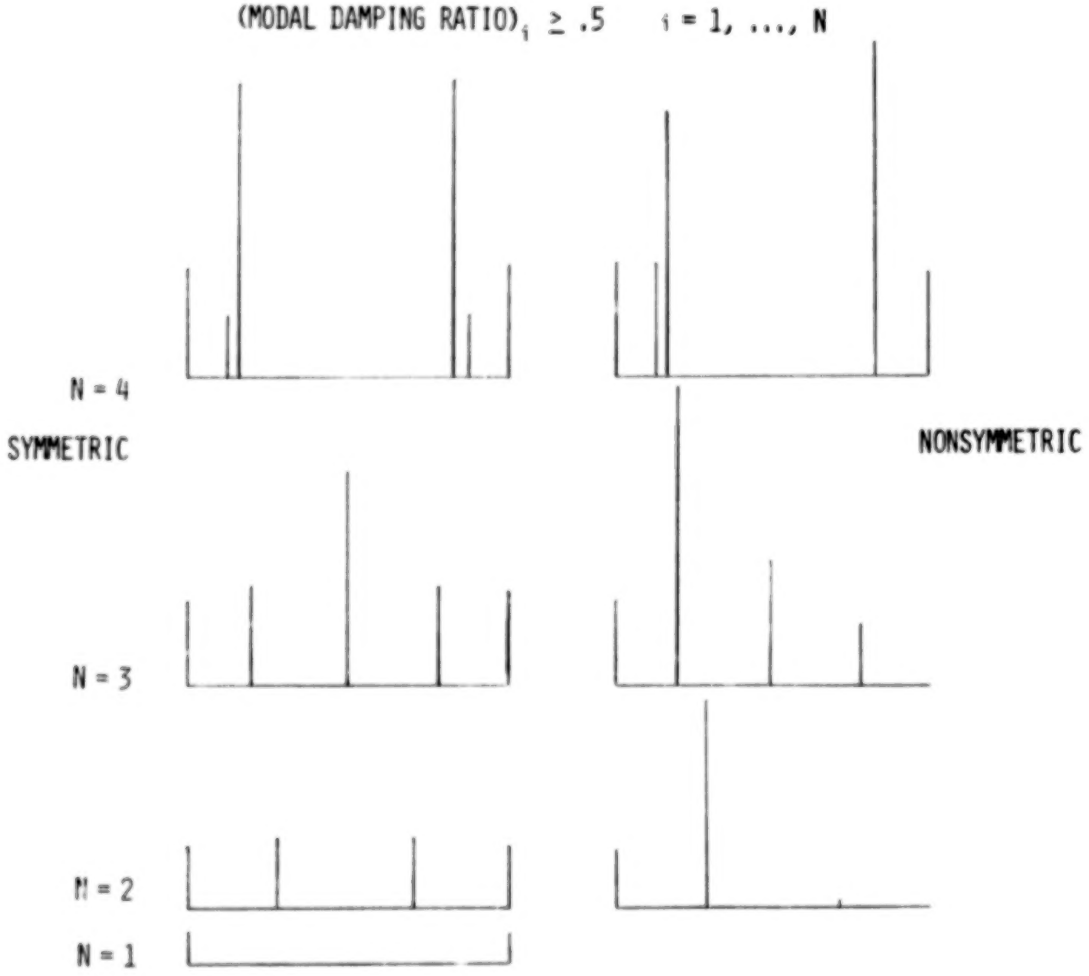

Figure 5

The results shown in figure 6 are similar to those in figure 5.

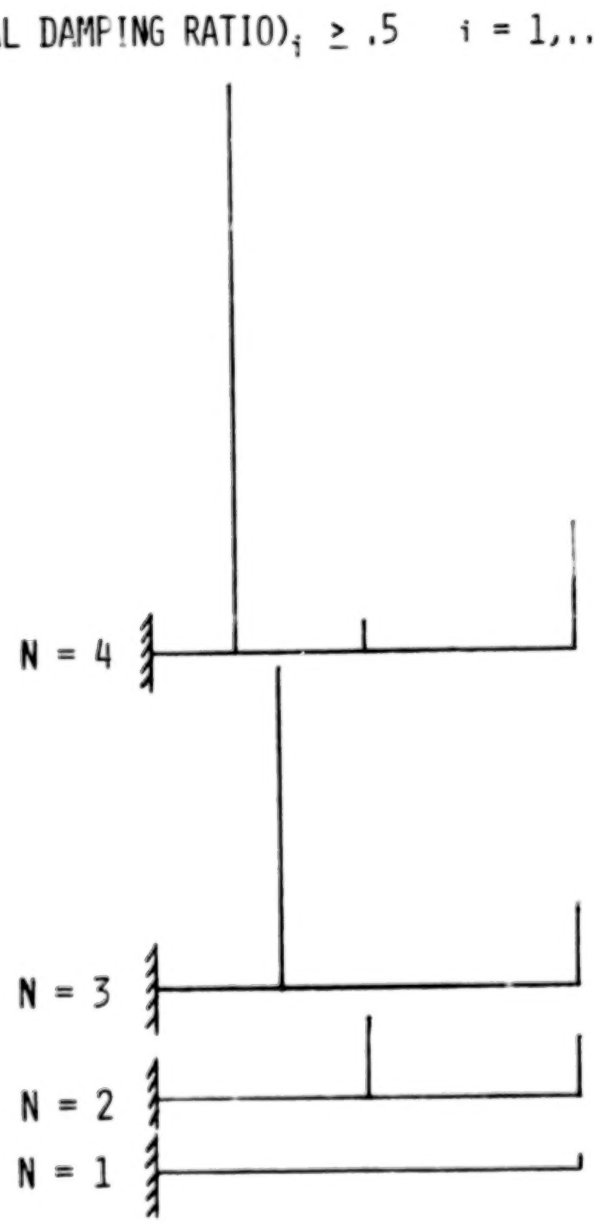

Figure 6

FUTURE RESEARCH

The future research thrusts will involve the addition of actuator dynamics to the structural dynamic models. This will allow the mass and stiffness as well as the damping rate of the damper to be design variables. Thus this will be the actuator design phase.

Next, a 2-dimensional structural model which has a higher modal density will be developed.

- NONCOLOCATED SENSORS AND ACTUATORS
- ADDITION OF ACTUATOR DYNAMICS
- 2-DIMENSIONAL STRUCTURAL MODEL

Figure 7

REDUCED ORDER ADAPTIVE REGULATION STRATEGIES FOR THE NASA BEAM CONTROL EXPERIMENT

C. Richard Johnson, Jr.
Department of Electrical Engineering
Virginia Polytechnic Institute and State University
Blacksburg, VA 24061

Workshop on the Structural Dynamics and Control
of Large Space Structures
NASA Langley Research Center
Hampton, VA 23665

October 30, 1980

REASONS FOR ADAPTIVE REGULATION

- Uncertainty in modal frequency (and mode shape) prespecification
- Inability to perform identification prior to deployment
- Time-variations in system dynamics during operation (especially construction)

NASA BEAM MODE FREQUENCIES

mode	continuum analysis (w/w_1)	finite element analysis	W_1 based on		
			W_1	W_2	W_3
1	1	1.8173	-	1.8107	1.8042
2	2.7565	4.9911	5.0094	-	4.9732
3	5.4039	9.7496	9.8205	9.7847	-

REASONS FOR MODAL DESCRIPTION

- Decoupled dynamics convert multi-input, multi-output problem to several single-input, single-output problems
- Parallel computation for real-time control implementation
- Common form of models of large flexible structures

MODAL DESCRIPTION OF FREE-FREE BEAM

$$y(x,t) = \sum_i y_i(x,t)$$

$$y_i(x,t) = \phi_i(x)\,\psi_i(t)$$

$$\ddot{\psi}_i(t) + w_i^2\,\psi_i(t) = F_i(t)$$

$$F_i(t) = \sum_j \phi_i(x_j)\,f_j(x_j, t)$$

$$\phi_i(x) = [\cosh w_i x + \cos w_i x - \frac{(\cosh w_i l - \cos w_i l)}{(\sinh w_i l - \sin w_i l)}(\sinh w_i x + \sin w_i x)]$$

Note: ϕ_i dependent on w_i

y : vertical deflection
x : horizontal beam point location
t : time
y_i : ith mode deflection
ϕ_i : ith mode shape (characteristic function)
ψ_i : ith mode amplitude
w_i : ith mode natural frequency
F_i : ith mode forcing function
$f_j(x_j, \cdot)$: jth point actuator force applied at x_j
l : beam length

QUESTIONS

- How do currently available single - input, single-output adaptive control schemes behave when applied as modal controllers of flexible structures?

- Can adaptive regulation (stabilization) be achieved with reasonable control levels despite inexact mode frequency (and shape) prespecification?

- How close must initial estimates be?

- Is adaptive regulation "better" (i.e. faster, closer to some desired behavior, ...) than fixed or gain scheduled control of comparable complexity designed for some bounded uncertainty in mode frequencies(and shapes)?

- What (if any) augmentations to currently available adaptive controllers improve their performance with application to flexible structures?

ADAPTIVE MODAL REGULATION CANDIDATE

Given: expansion basis $\{\phi_i\}$, finite expansion limit N, sensor and actuator locations, and modal control objectives

(1) Apply previously calculated actuation forces $f_j(x_j, t)$ and sense $y(x, t)$

(2) Process sensor data to estimate M modal amplitudes $y_i(x, t)$

(3) Select C modes requiring control

(4) Process applied forces $f_j(x_j, t)$ to determine achieved modal forces $F_i(t)$

(5) Improve the identification of the discretization of the ψ_i dynamics (i.e. essentially the modal frequencies w_i)

(6) Parameterize modal controllers using current plant parameter estimates to meet modal performance objectives and calculate $F_i(t + 1)$

(7) Convert desired modal forces $F_i(t + 1)$ to actuator commands $f_j(x_j, t + 1)$

(8) Repeat (1) - (7)

Source: Johnson, "Adaptive modal control of large flexible spacecraft," J. of Guid. and Control, July-August 1980.

PROBLEMS

- Finite number of modes accurately describing system N $\geq$ number of modes identifiable M due to number of point sensors $\geq$ number of modes controllable C, i.e., the reduced-order adaptive identification/control problem.

- Disregard of coupling due to inexact modal shape ϕ_i specification.

- Unbounded control effort request due to momentary uncontrollability of estimated plant parameterization.

- Lack of guaranteed parameter identifiability without sufficient excitation.

- Misinterpretation of deflection due to short-term disturbances as caused by parameter estimate inaccuracy.

- Meaningful prespecification of modal control objectives (e.g., pole placement for quadratic cost function minimization) given modal frequency and shape uncertainty.

ALTERNATE ADAPTIVE STRATEGIES

- Asymptotic feedback matrix synthesis can bypass momentary estimated plant uncontrollability.
  Source: Kreisselmeier, "Adaptive control via adaptive observation and asymptotic feedback matirx synthesis," IEEE Trans. on Auto. Control, August 1980.

- Avoid modal decomposition and treat as multi-input (C actuators), multi-output (M sensors) problem to accomodate "modal" coupling with loss of computational advantages.
  Source: Goodwin, Ramadge, and Caines, "Discrete-time multivariable adaptive control, "IEEE Trans. on Auto. Control, June 1980.

- Use direct adaptive controllers to bypass perturbation necessity for identifiability.
  Source: Johnson and Tse, "Adaptive implementation of one-step-ahead optimal control via input matching, "IEEE Trans. on Auto. Control, October 1978.

- Use off-line parameter estimation with verification prior to alteration of gain schedule to avoid reaction to non-parameter-estimate errors such as deterministic disturbances.
  Source: Hall, "A learning control system extension to the modal control of large flexible rotating spacecraft," Proc. 1979 AIAA Guid. and Control Conf., August 1979.

- Limit controller parameterizations to positive real operators with subsequent loss in objective range in order to assure stabilization despite reduced-order usage.
  Source: Benhabib, Iwens, and Jackson, "Active vibration control of a flat plate using model reference adaptive techniques," Proc. 2nd VPI&SU/AIAA Symp. on Dyn, and Control of Large Flexible Spacecraft, June 1979.

SPECIFIC QUESTIONS TO BE ADDRESSED

- How many modes (with N = M = C) are required in a modal, simultaneous identifier-controller, initialized with the ideal description of a free-free beam, to satisfactorily regulate Langley's flexible beam?

- Using only displacement measurements what order actuator-input, sensor-output, matrix-ARMA model is satisfactory for non-modal, multivariable adaptive regulation of Langley's flexible beam?

- By describing the effects of reduced-order modeling as a perturbation to the time-varying, nonlinear, parameter-estimate-error system, can the theoretical limitations of reduced-order adaptive control, especially in terms of initial estimate accuracy, be interpreted?

- Using a singular perturbation separation of the modes of a flexible structure, can the effects of reduced-order adaptive control be quantified?

DYNAMICS AND CONTROL OF

COUPLED RIGID/FLEXIBLE BODIES

Elias G. Abu-Saba
Associate Professor of Architectural Engineering
North Carolina A & T State University
Greensboro, North Carolina

Workshop on the Structural Dynamics and Control
of Large Space Structures
October 30-31, 1980

MILESTONES

1. Select and prepare a mission model
2. Write a set of equations of motion
3. Determine elastic constants of model components
4. Write a computer program for open loop input
5. Set up control block diagram
6. Simulate the dynamic system on the computer

MISSION MODEL

The Orbiter and the SEP solar array are represented by the model shown in figure 1. The coordinate system is shown on the diagram.

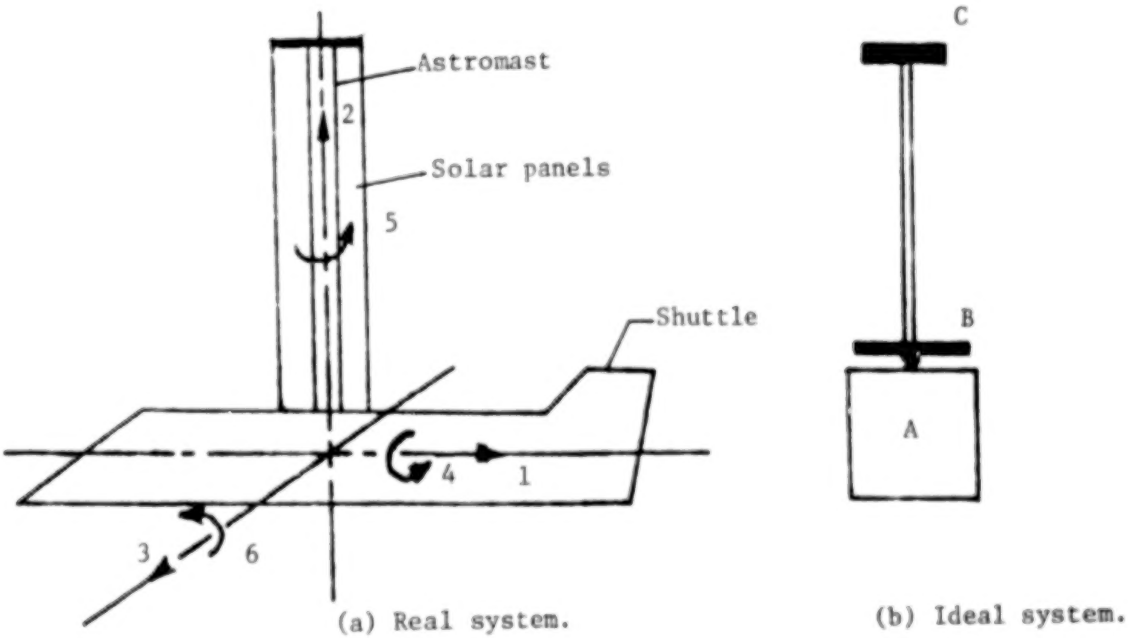

(a) Real system.

(b) Ideal system.

Figure 1

KINEMATICS OF RIGID BODIES

$$\vec{V}_B = \vec{V}_A + \vec{V}_{B/R}$$

$$\vec{V}_{B/R} = \vec{w} \times \vec{r}$$

$\vec{w}$ = rotation vector

$\vec{r}$ = position vector

$$\vec{a}_B = \frac{d}{dt}(V_B)$$

SEP SOLAR ARRAY MODEL

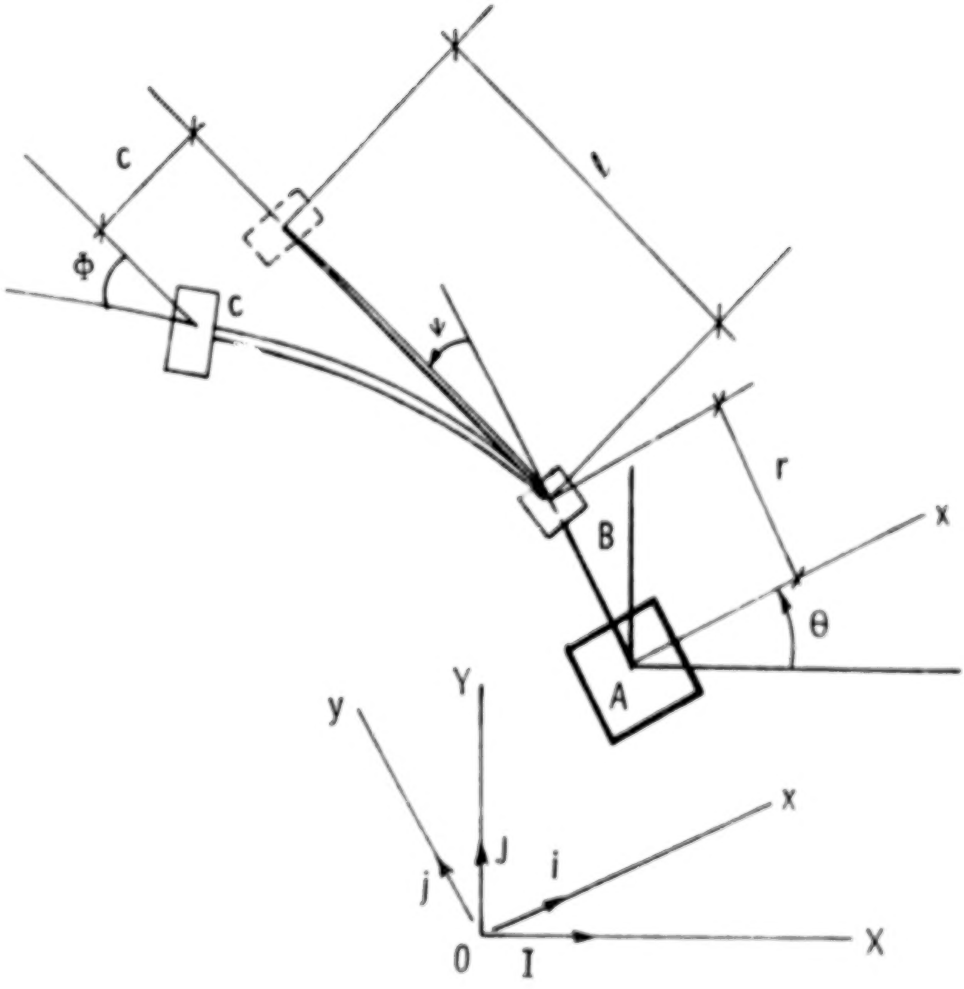

Figure 2

MAST MODEL

Assumptions:

1. The total mass of the mast is concentrated at each level.
2. Lateral members are relatively much stiffer than longitudinal ones.
3. The deformations in the mast do not depend on axial forces present in the londitudinal members.

Model:

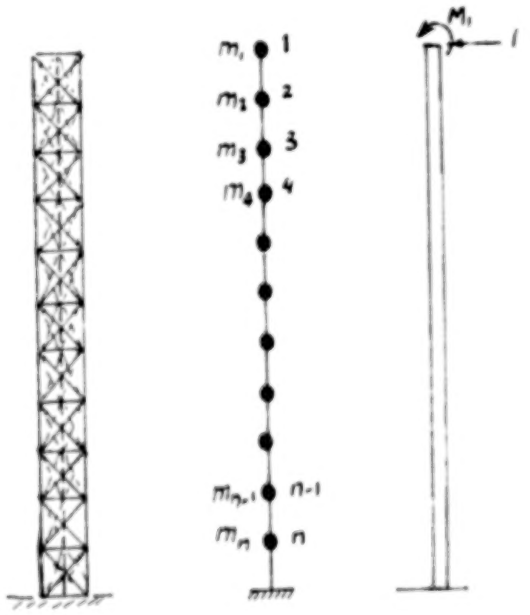

$$\delta_{ij} = \frac{x_j^2(\ell_i - x_j)}{2EI} + \frac{x_j^3}{3EI} + \frac{M_1 x_j^2}{2EI}$$

FLEXIBILITY MATRIX = $[\delta]$

STIFFNESS MATRIX = $[K] = [\delta]^{-1}$

MASS MATRIX (DIAGONAL) = $[M]$

FORCE MATRIX = $[F]$

$$[M][\ddot{X}] + [K][X] = [F]$$

FREE VIBRATIONS

$$[M][\ddot{X}] + [K][X] = 0$$

Figure 3

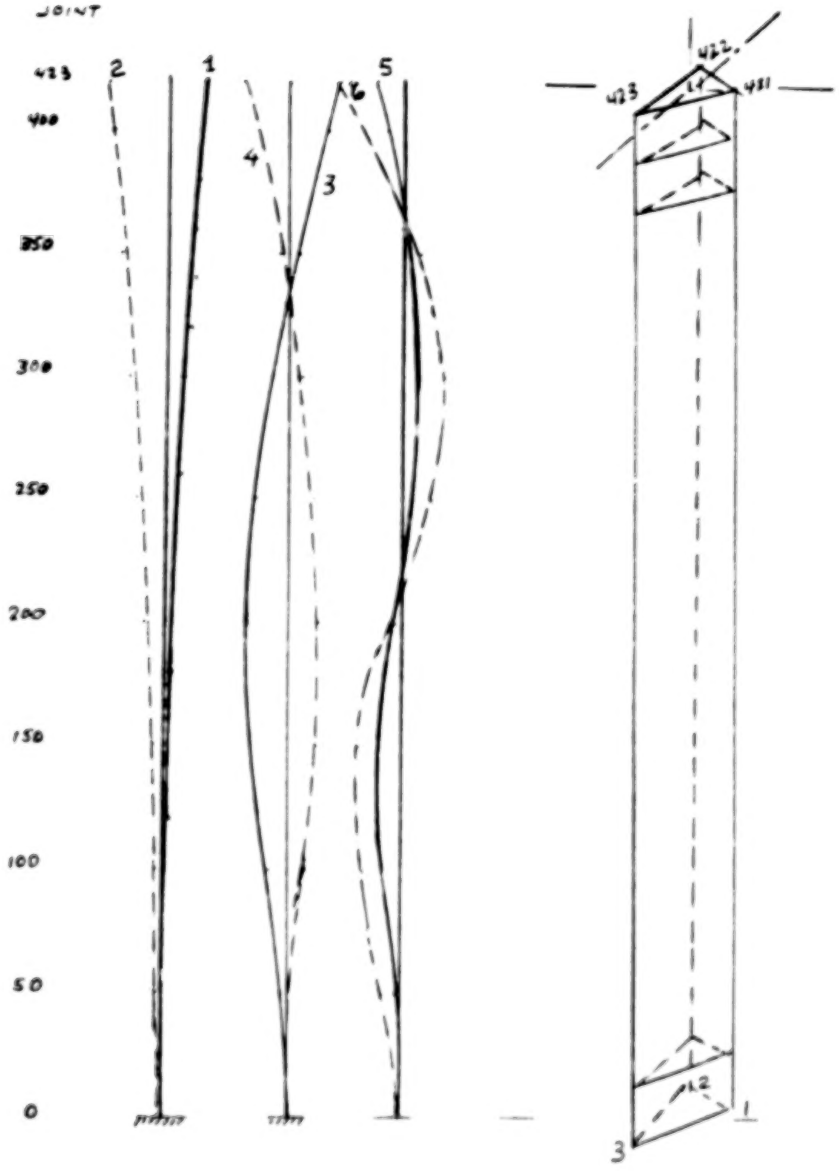

Figure 4

MODAL FREQUENCIES

Modal frequency, Hz		Modal frequency, Hz	
f_1 =	0.0874	f_6 =	1.5334
f_2 =	.0874	f_7 =	3.0030
f_3 =	.5478	f_8 =	3.0031
f_4 =	.5478	f_9 =	4.9644
f_5 =	1.5334	f_{10} =	5.0242

BLANK PAGE

ADJUSTED FEEDBACK CONTROL FOR INCOMPLETE DECOUPLING PROCEDURES

Harold A. Hamer
NASA Langley Research Center
Hampton, Va.

Workshop on the Structural Dynamics and Control
of Large Space Structures
October 30-31, 1980

INTRODUCTION

Complete decoupled control requires the number of control actuators to equal the number of modes in the model, which is a basic limitation in applying decoupling theory to the control of large space structures. Complete decoupled control is usually not achievable in practical application because a large space structure may have an infinite number of flexible modes; hence, procedures must be developed which maintain control of the structure with a small number of control actuators. The present analysis presents techniques which use decoupling theory and state-variable feedback to control the pitch attitude and the flexible-mode amplitudes of the beam. Approximations are incorporated into the decoupling procedure to permit control with a small number of actuators. The approximations involve adjustments in the control-influence coefficients and in the feedback gains which produce simplified procedures for achieving overall control of the system.

EQUATIONS OF MOTION

Figure 1 shows the linearized equations of motion used for a decoupled-control analysis of a 100-m long thin, flexible beam in low Earth orbit. The equations are in modal form where n represents the number of flexible modes included in the model. Although not required, the damping term $2\zeta\omega A_n$ is included in the model. The top equation represents the rigid-body (pitch) mode and includes the gravity-gradient effect, where ω_c is the orbital frequency.

$$\frac{d^2\theta}{dt^2} + 3\omega_c^2\theta = \frac{T_p}{J}$$

$$\frac{d^2A_n}{dt^2} + 2\zeta\omega_n\frac{dA_n}{dt} + \omega_n^2 A_n = \frac{E_n}{M_n}$$

$$n = 1, 2, 3, \cdots$$

Figure 1

DECOUPLED CONTROL EQUATIONS

Figure 2 shows the equations in state-vector form where the states $\bar{x}$ are the modal amplitudes and rates. The output equation $\bar{y} = C\bar{x}$ represents the states to be decoupled. In the decoupling control law $\bar{v}$ is the input command vector and F and G are the feedback and feedforward gain matrices, respectively. The output is related to the input through the transfer function H(s). The decoupling procedure determines the F and G matrices in a manner such that the transfer function is diagonal and nonsingular, thus providing independent control for each of the decoupled (output) variables.

SYSTEM $\Sigma(A,B,C)$

$$\dot{\bar{x}} = A\bar{x} + B\bar{f} \quad , \quad \bar{y} = C\bar{x}$$

DECOUPLING CONTROL LAW

$$\bar{f} = F\bar{x} + G\bar{v}$$

LAPLACE TRANSFORM SOLUTION

$$\hat{\bar{y}}(s) = H(s)\,\hat{\bar{v}}(s)$$

where $H(s) = C(sI - A - BF)^{-1}BG$ is the m x m transfer function.

For decoupling, H(s) is diagonal and nonsingular.

Figure 2

EXAMPLE EQUATIONS

Figure 3 presents example equations for a four-mode model (pitch plus three flexible modes) with four control actuators. The numbers in the A matrix are the frequencies squared of the various modes. The damping terms have been omitted because they are not required in the solution for decoupled control. The control-influence matrix B depends on the location of the control actuators and the modal shape functions.

$$\dot{\bar{x}} = A\bar{x} + B\bar{f}$$

$$\begin{pmatrix} \dot{\theta} \\ \dot{A}_1 \\ \dot{A}_2 \\ \dot{A}_3 \\ \ddot{\theta} \\ \ddot{A}_1 \\ \ddot{A}_2 \\ \ddot{A}_3 \end{pmatrix} = \begin{bmatrix} 0 & 0 & 0 & 0 & 1 & 0 & 0 & 0 \\ 0 & 0 & 0 & 0 & 0 & 1 & 0 & 0 \\ 0 & 0 & 0 & 0 & 0 & 0 & 1 & 0 \\ 0 & 0 & 0 & 0 & 0 & 0 & 0 & 1 \\ -3 & 0 & 0 & 0 & 0 & 0 & 0 & 0 \\ 0 & -.0032 & 0 & 0 & 0 & 0 & 0 & 0 \\ 0 & 0 & -.0288 & 0 & 0 & 0 & 0 & 0 \\ 0 & 0 & 0 & -.0931 & 0 & 0 & 0 & 0 \end{bmatrix} \begin{pmatrix} \theta \\ A_1 \\ A_2 \\ A_3 \\ \dot{\theta} \\ \dot{A}_1 \\ \dot{A}_2 \\ \dot{A}_3 \end{pmatrix}$$

$$+ \begin{bmatrix} 0 & 0 & 0 & 0 \\ 0 & 0 & 0 & 0 \\ 0 & 0 & 0 & 0 \\ 0 & 0 & 0 & 0 \\ T_1 & T_2 & T_3 & T_4 \\ \Phi_{1,1} & \Phi_{1,2} & \Phi_{1,3} & \Phi_{1,4} \\ \Phi_{2,1} & \Phi_{2,2} & \Phi_{2,3} & \Phi_{2,4} \\ \Phi_{3,1} & \Phi_{3,2} & \Phi_{3,3} & \Phi_{3,4} \end{bmatrix} \begin{pmatrix} f_1 \\ f_2 \\ f_3 \\ f_4 \end{pmatrix}$$

Figure 3

DERIVATION OF DECOUPLING CONTROL LAW

Figure 4 is an example of a derivation of the decoupling control law for the model of the previous figure. Inasmuch as the number of control actuators equals the number of modes, complete decoupling is obtained. That is, each of the modes can be independently controlled. Obviously, if the number of actuators is reduced, some of the modes will remain uncontrolled. These uncontrolled modes will be influenced by effects because of control of the decoupled modes. Subsequent results will illustrate several methods for reducing or eliminating these undesired effects.

For pitch control only, let

$$y_1 = \theta \quad , \quad \dot{y}_1 = \dot{\theta} \quad , \quad \ddot{y}_1 = \ddot{\theta}$$

$$\therefore \ddot{y}_1 = (-3 \times 10^{-6})\theta + T_1 f_1 + T_2 f_2 + T_3 f_3 + T_4 f_4$$

To obtain desired second-order response dynamics,

$$\ddot{y}_1 + 2\zeta_\theta \omega_\theta \dot{y}_1 + \omega_\theta^2 y_1 = (\omega_\theta^2 - 3 \times 10^{-6})\theta + 2\zeta_\theta \omega_\theta \dot{\theta} +$$

$$T_1 f_1 + \ldots\ldots + T_4 f_4 = V_1$$

Similar equations are determined for the modal amplitude controls. The four equations can be collected to form:

$$V_1 = (\omega_\theta^2 - 3 \times 10^{-6})\theta + 2\zeta_\theta \omega_\theta \dot{\theta} + T_1 f_1 + \ldots\ldots + T_4 f_4$$

$$V_2 = (\omega_1^2 - .0032) A_1 + 2\zeta_1 \omega_1 \dot{A}_1 + \phi_{1,1} f_1 + \ldots\ldots + \phi_{1,4} f_4$$

$$V_3 = (\omega_2^2 - .0288) A_2 + 2\zeta_2 \omega_2 \dot{A}_2 + \phi_{2,1} f_1 + \ldots\ldots + \phi_{2,4} f_4$$

$$V_4 = (\omega_3^2 - .0931) A_3 + 2\zeta_3 \omega_3 \dot{A}_3 + \phi_{3,1} f_1 + \ldots\ldots + \phi_{3,4} f_4$$

Figure 4

EQUATIONS IN MATRIX FORM

Figure 5 shows the equations for the control law in matrix form. Note that the feedforward matrix G is merely the inverse of the control-influence matrix. Each column of G can be multiplied by a constant to change the output sensitivity. Note that the matrix M is composed of the modal frequencies ω and the damping ratios ζ. These are closed-loop quantities and their values can be selected to provide feedback gains for desired dynamic-response characteristics. Note that the feedback gain matrix can be separated into two parts, that part F' which deletes the unaugmented dynamics and F'' which incorporates the dynamics selected for the closed-loop system.

$$\bar{v} = M\bar{x} + N\bar{f}$$

or $$\bar{f} = -N^{-1}M\bar{x} + N^{-1}\bar{v}$$

Providing N is not singular, then

$$\bar{f} \triangleq F\bar{x} + G\bar{v}$$

where

$$F = -N^{-1}M = F' + F''$$

$$G = N^{-1}$$

are the required feedback and feedforward matrices for the decoupling control law.

Figure 5

PITCH COMMAND FOR COMPLETELY DECOUPLED MODEL

Figure 6 is an example of an instantaneous pitch command to change the pitch attitude θ by 0.01 rad. The quantities A_1, A_2, and A_3 are the modal amplitudes; f_1 and f_2 are the actuator forces in newtons. As shown, the system is completely controlled in that the flexible modes are not affected. The results apply to the condition that complete feedback of all modal amplitude magnitudes and rates is required. Also, the effect of unmodeled modes, not included in the computer simulation, is not considered.

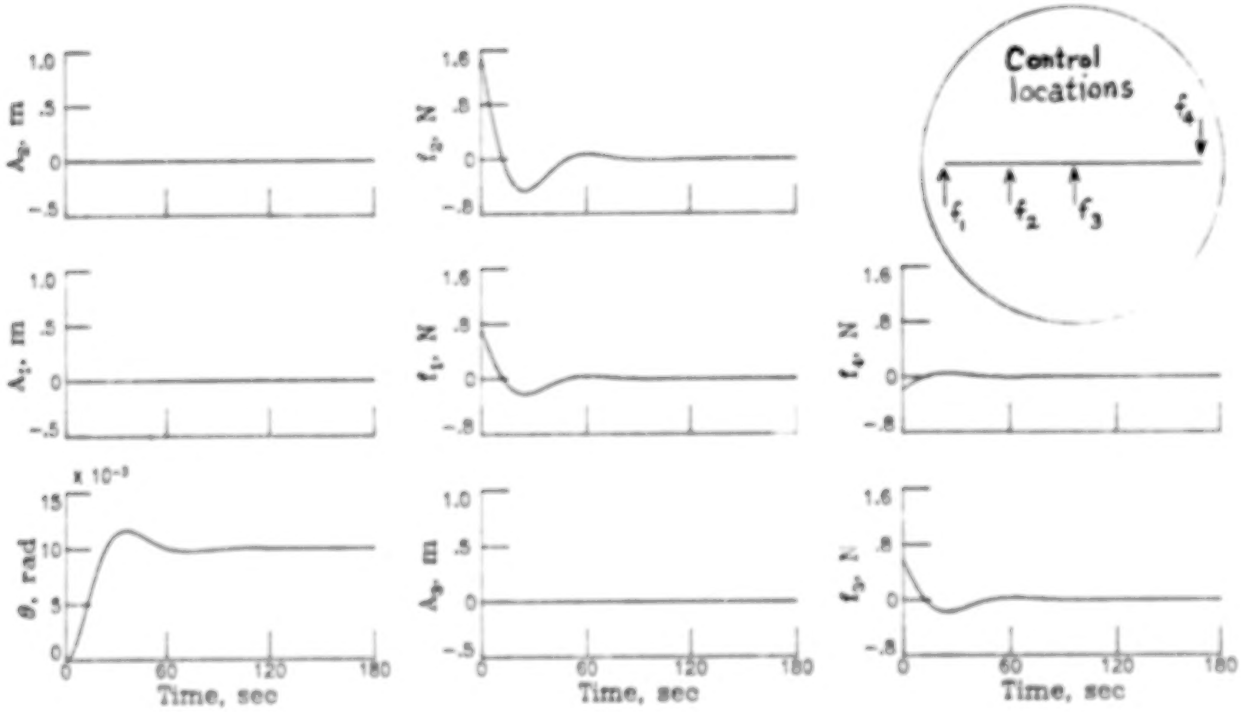

Figure 6

ZERO COMMAND FOR COMPLETELY DECOUPLED MODEL

Figure 7 is an example of an instantaneous zero command to null initial disturbances of 0.01 rad in pitch and 0.01 m in the modal amplitudes. The values selected for the closed-loop dynamics of each mode were $\omega = 0.1$ rad/sec and $\zeta = 0.5$. This gives similar responses in all modes leading to equilibrium in about 60 sec.

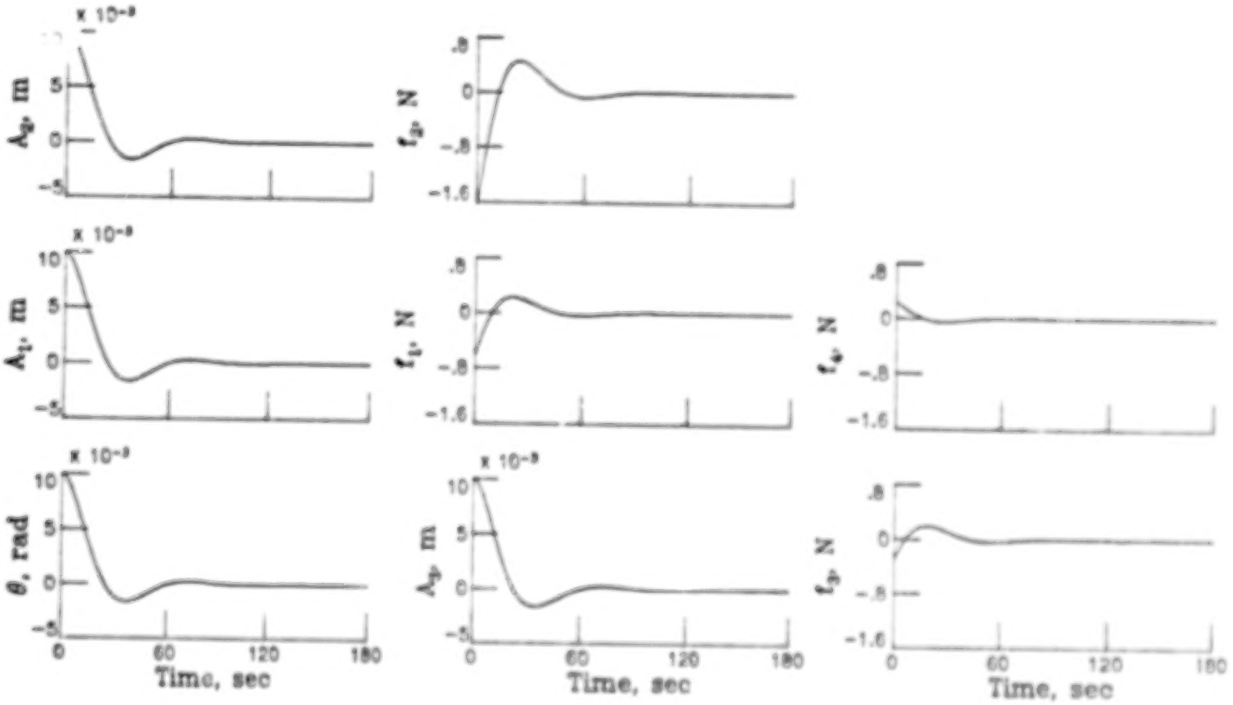

Figure 7

ONE CONTROL ELIMINATED

Figure 8(a) is an example of a pitch command where the f_3 control (actuator) was eliminated from the completely decoupled system. The same F gains derived for the completely-decoupled model were used, except that the gains for the f_3 control were deleted. As shown, this condition leads to uncontrolled first and third flexible modes which are caused by oscillations in the f_1 and f_4 actuators.

Figure 8(b) shows how overall control of the previous case can be obtained by a simple gain adjustment. The example is for a zero command and shows that the initial disturbances are controlled (nulled) after about 100 sec. The gain adjustment required in this case was a change in $F_{1,8}$ (element in first row, eighth column of the feedback matrix) by a factor of ten.

More than one control can be eliminated from the completely decoupled system; however, as more controls are eliminated, a larger number of adjustments in the feedback gain matrix are required (involving many trial and error attempts).

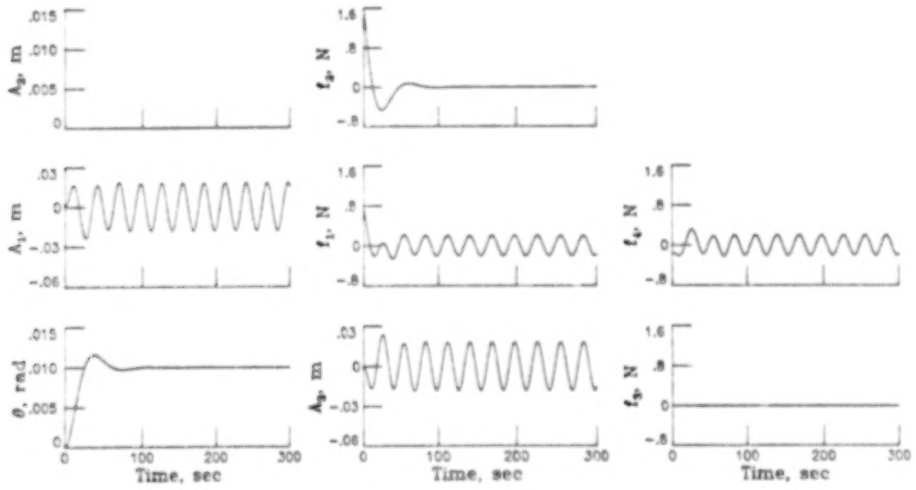

(a) Feedback not adjusted.

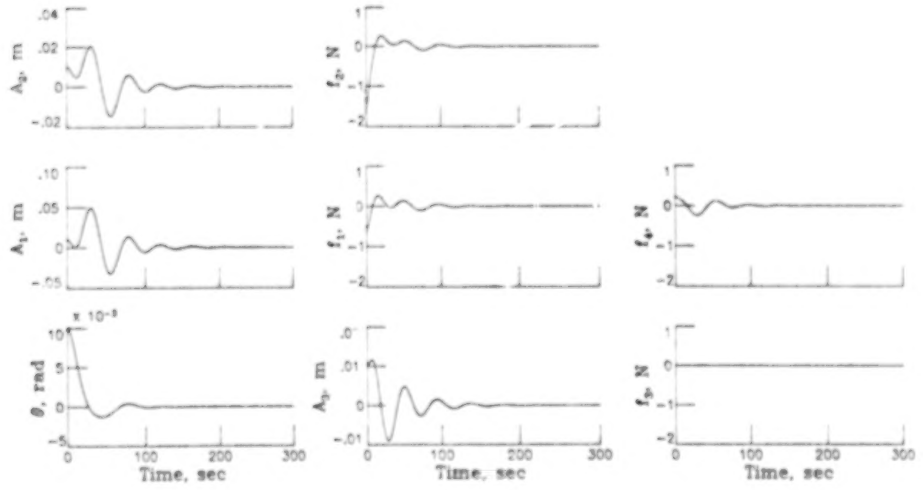

(b) Feedback adjusted.

Figure 8

ZERO COMMAND WITH TWO ACTUATORS

Figure 9 presents an example of a zero command where the pitch mode and first flexible mode are decoupled with two control actuators. This leads to incomplete decoupling, due to the reduced numbers of controls. However, as shown, except for some initial effects in the modal responses, overall control of the system is maintained. This is a special case inasmuch as the actuators are exactly at each end of the beam. Gain information derived from this special case can be useful for adjusting gains for other control arrangements which lead to uncontrolled modes.

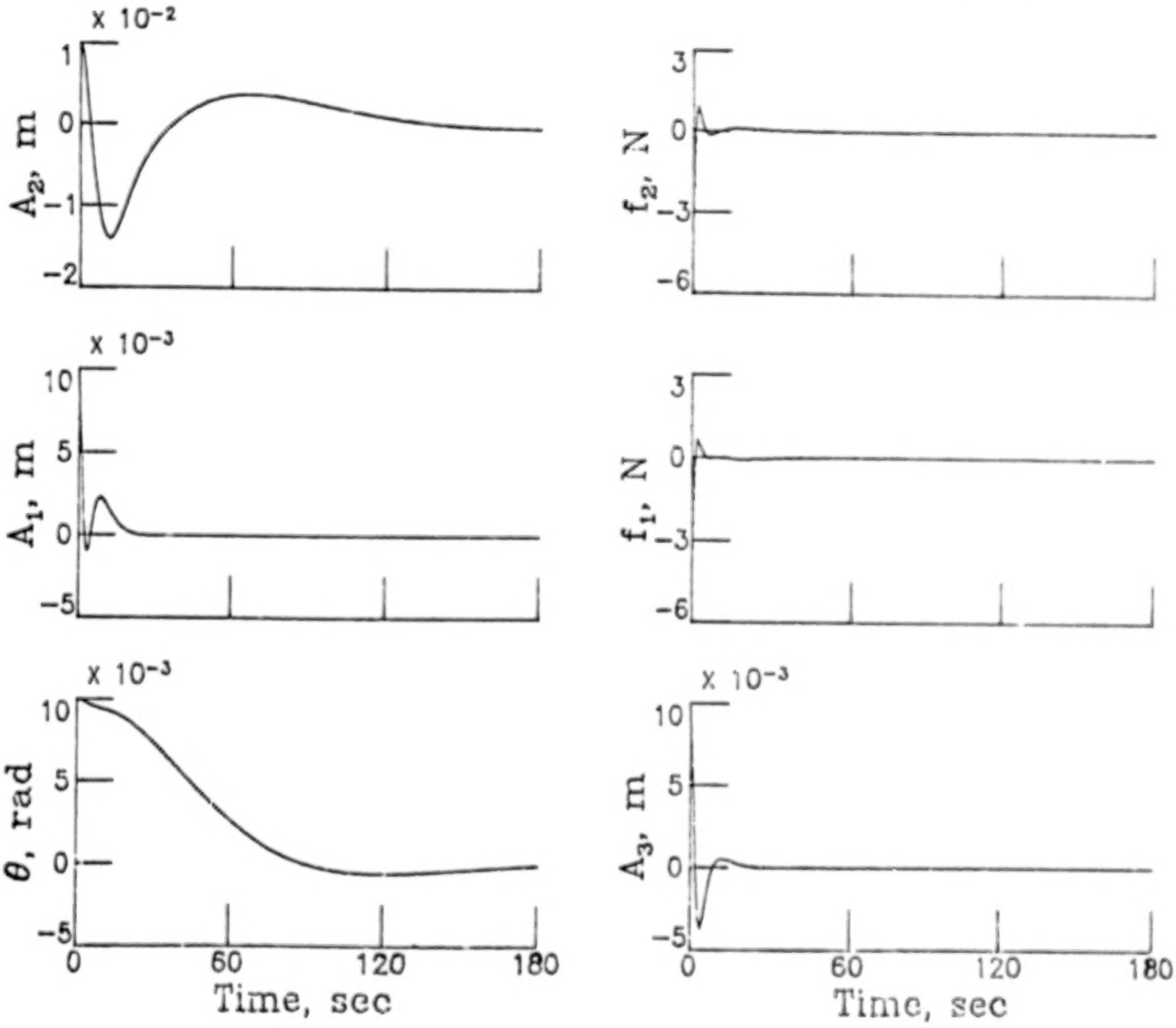

Figure 9

CONTROL-FORCE REQUIREMENTS

Figure 10 illustrates the control-force requirements for the two-control model. The values shown apply to a pitch command of 0.10 rad. It is important to note the high dependence of control force on the value selected for the closed-loop pitch frequency. At the larger values of ω_θ the forces become prohibitive. The forces for the higher-mode models are somewhat lower because the F matrices require higher-order dynamics to calculate the gain values for these models.

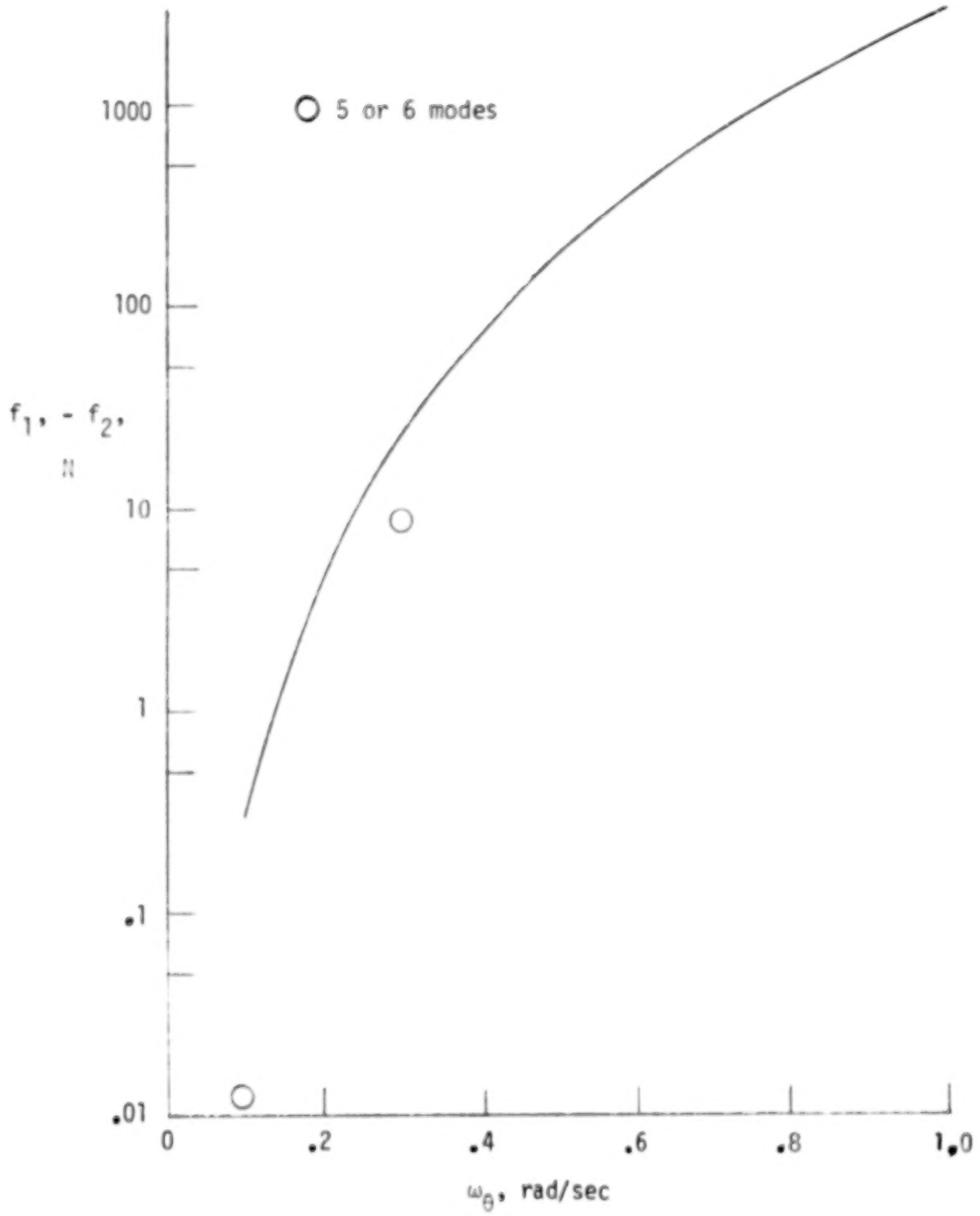

Figure 10

EFFECT OF PARAMETER UNCERTAINTY

Figure 11 shows the negligible effect of parameter uncertainty on a pitch command; the solid curves represent the no-error case. The dashed curves represent a typical result from a number of cases where random errors of ±10 and ±20 percent were incorporated into the control-influence matrix B. For these cases, the feedback gains calculated for the original B matrix were used. The uncertainty in beam model parameters was also found to have no appreciable effect on the decoupling process. These uncertainties included errors of 20 percent in the modal frequencies and large changes in the modal damping factors (up to 500 percent of the nominal values).

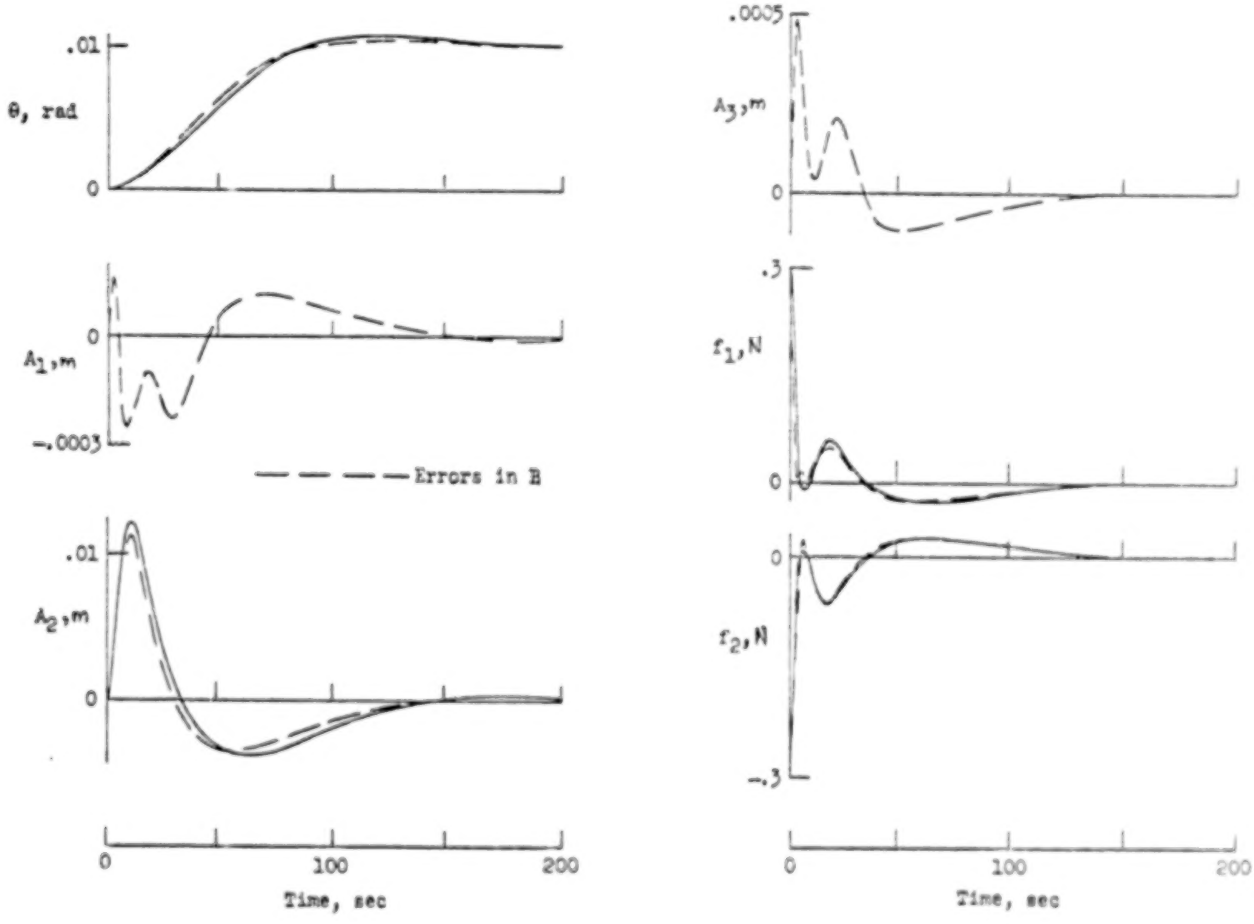

Figure 11

PITCH COMMAND WITH TWO ACTUATORS OFFSET

Figure 12 shows an example of a pitch command where the pitch mode and first flexible mode are decoupled with two control actuators. This incomplete-decoupling case differs from the previous case in that one of the actuators is not exactly at the end of the beam. As shown for this offset case (which is the general case), the required decoupling is achieved for θ and A_1; however, the other two flexible modes remain uncontrolled. This result is described in the next figure.

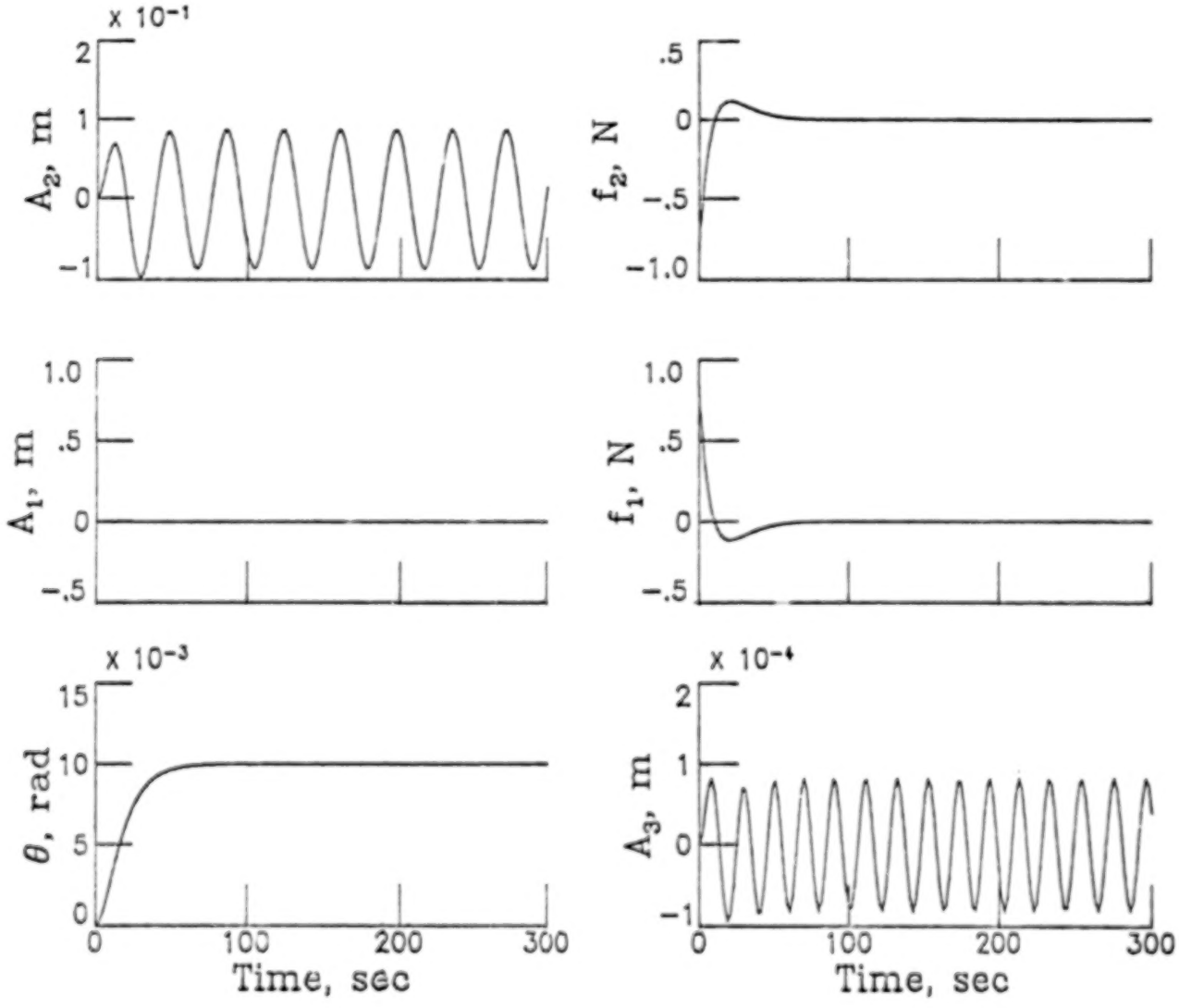

Figure 12

FEEDBACK GAINS REQUIRED TO CHANGE DYNAMICS

Figure 13 shows the feedback gain matrices derived for the two cases, one for offset actuators and one for actuators exactly at each end of the beam. Only the first four columns are shown for F''_{exact}, inasmuch as the last four repeat by replacing S with R and Q with P. As shown for this matrix, fourth-order dynamics are required to calculate the gains. The constants P, Q, R, and S depend on the closed-loop values selected for ω and ζ. The zero columns in F''_{offset}, which provide no control for the second and third flexible modes, result from B-matrix columns of unequal magnitudes. The F''_{exact} matrix is full order in that no zero columns exist. This condition occurs only when the values in the columns of the B-matrix have exactly the same magnitude. The ratios between the columns in F''_{exact} can be used to adjust the feedback gains for the zero columns of the offset case. In applying the ratio method, the third column of F''_{offset} is adjusted so that its ratio with the first column in F''_{offset} is the same as the respective columns in F''_{exact}. The same procedure is used with respect to the fourth and second columns, the seventh and fifth columns, and the eighth and sixth columns. A result of this gain-adjustment procedure is shown in the next figure.

$$F''_{exact} = \left[\begin{array}{cc} 8400 & 250 \\ -8400 & 250 \end{array}\right]\left[\begin{array}{c|c|c|c} \dfrac{S_\theta - Q_\theta \omega_{\theta u}}{\omega_{2u} - \omega_{\theta u}} & 0 & 0 & 0 \\ 0 & \dfrac{S_1 - Q_1 \omega_{1u}}{\omega_{3u} - \omega_{1u}} & 0 & 0 \end{array}\right] +$$

$$\left[\begin{array}{cc} 250 & 250 \\ -250 & 250 \end{array}\right]\left[\begin{array}{c|c|c|c} 0 & 0 & \dfrac{-S_\theta + Q_\theta \omega_{2u}}{\omega_{2u} - \omega_{\theta u}} & 0 \\ 0 & 0 & 0 & \dfrac{-S_1 + Q_1 \omega_{3u}}{\omega_{3u} - \omega_{1u}} \end{array}\right]$$

$$(s^2 + 2\zeta\omega s + \omega^2)^2 = s^4 + 4\zeta\omega s^3 + 2\omega^2(1+2\zeta^2)s^2 + 4\zeta\omega^3 s + \omega^4$$
$$= s^4 + Ps^3 + Qs^2 + Rs + S$$

$$F''_{offset} = \left[\begin{array}{cc} 8400 & 250 \\ -8400 & 250 \end{array}\right]\left[\begin{array}{cccccccc} E_\theta & 0 & 0 & 0 & D_\theta & 0 & 0 & 0 \\ 0 & E_1 & 0 & 0 & 0 & D_1 & 0 & 0 \end{array}\right]$$

$$s^2 + 2\zeta\omega s + \omega^2 = s^2 + Ds + E$$

Figure 13

ZERO COMMAND WITH TWO ACTUATORS OFFSET

(FEEDBACK ADJUSTED BY RATIO METHOD)

Figure 14 shows an example of a zero command where the feedback gains were adjusted by the ratio method previously described. As shown, the adjusted gains provide sufficient control for all modes. There are small initial effects, but they damp out after about 200 sec.

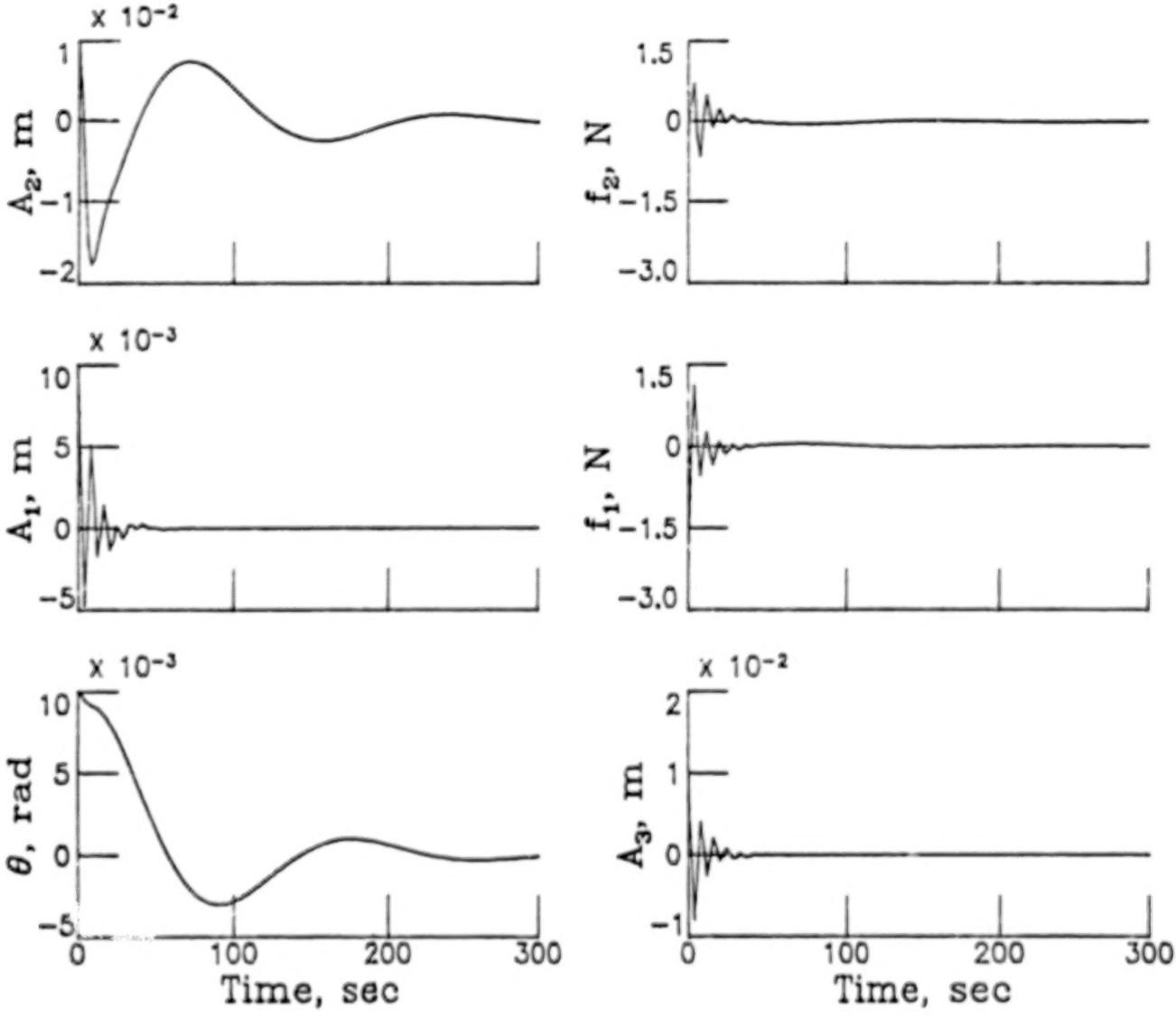

Figure 14

UNCONTROLLED MOTIONS FOR FOUR-MODE MODEL

Figures 15(a) and 15(b) illustrate the use of Kalman regulator theory in estimating the modal amplitudes. Similar results are obtained for the amplitude rates. These estimates are required for the feedback control inasmuch as the actual modal values cannot be measured directly. The first plot shows the uncontrolled motions resulting from small initial distrubances. The second plot shows how well these motions can be estimated with measurements from one pitch-attitude (star tracker) sensor located at a point one quarter the distance from the end of the beam. This plot shows that perfect estimates are established at a time of about 60 sec, where the magnitudes of the oscillations are equal to those of the first plot. (Oscillations are actually present in the estimates of $\hat{A}_1$, but are not discernible due to the large scale.) In this one-sensor case, if the control actuators are turned on before good estimates are obtained, excessive control forces would be required.

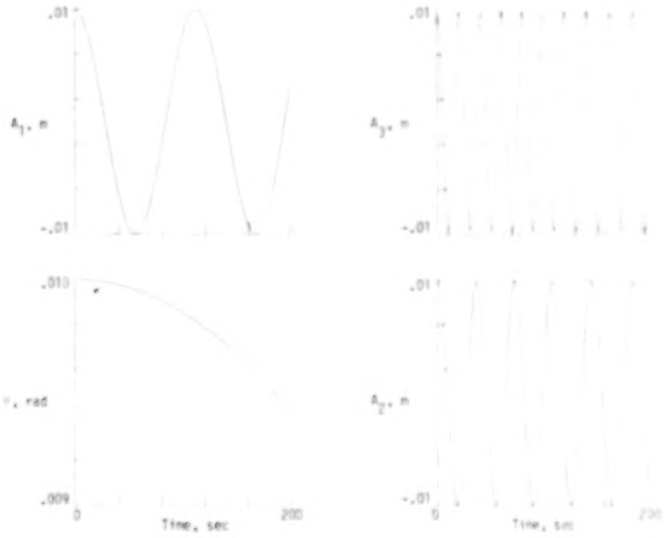

(a) Small initial disturbances.

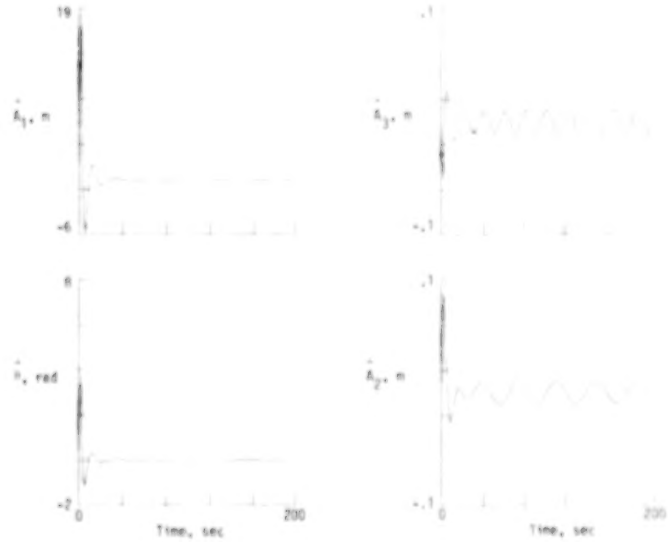

(b) One sensor.

Figure 15

ZERO COMMAND WITH THREE SENSORS

Figures 16(a) to 16(c) show zero-command results for a three-sensor case. The sensors were located at the middle and quarter points of the beam and the control actuators were at each end of the beam. In this case, the initial estimates were adequate so that the actuators could be turned on at $t = 0$ without requiring excessive forces, as seen in the last plot. These forces were about six times those required for the case with perfect initial estimates. With only two sensors employed, the forces increased substantially (to about 65 N), which would require turning off the actuators until good estimates are produced.

These Kalman-regulator results apply to the case where unmodeled modes are not considered in the computer simulations. In any practical application, unmodeled modes cause observation and control spillover effects which can lead to instability. Additional analysis is required to include these effects in determining the overall stability and control of the system.

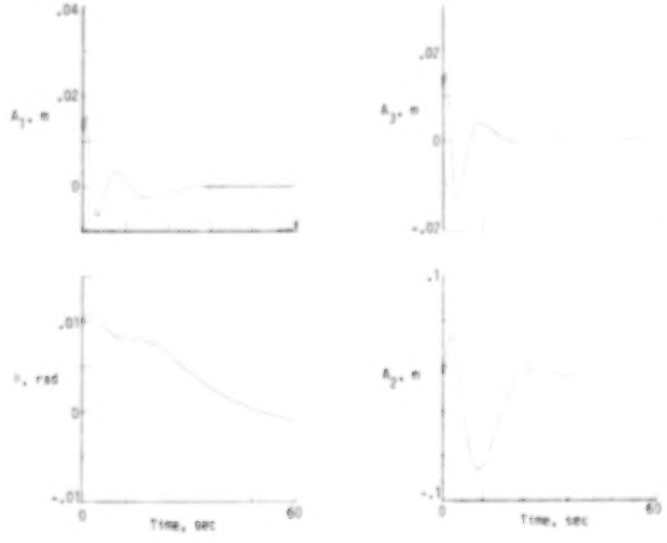

Figure 16

(a) Two actuators.

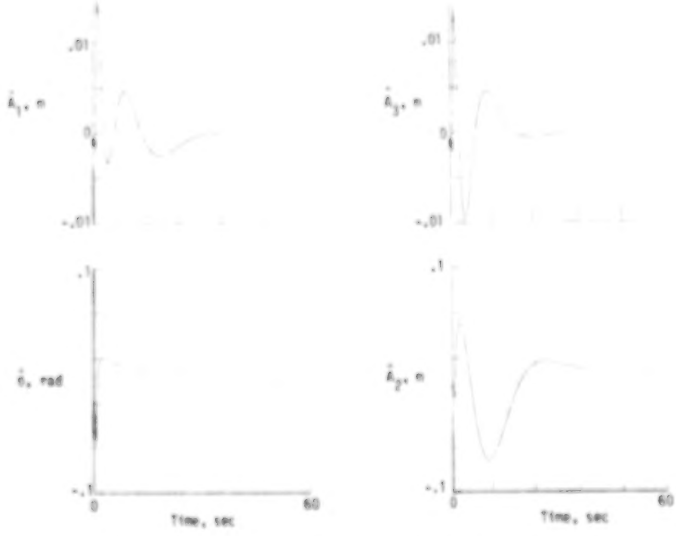

(b) Estimates of controlled motion.

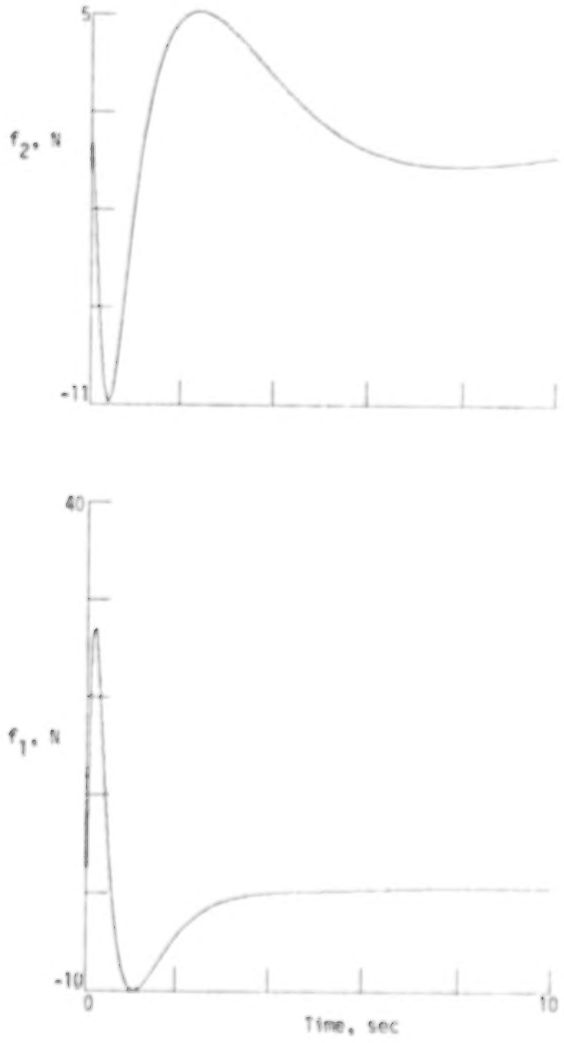

(c) Actuator forces.

Figure 16.- Concluded.

BLANK PAGE

INVESTIGATIONS OF ALGORITHMS FOR LARGE SPACE STRUCTURES

E. D. Denman
Department of Electrical Engineering
University of Houston

Workshop on the Structural Dynamics and
Control of Large Space Structures

October 30-31, 1980

1. Introduction

The feasibility of constructing large space structures such as the solar power system, the SEP (solar electric power) array, or numerous other space structures currently under study will undoubtedly be realized in the future. The existence of such structures will depend to a great extent on the ability to analyze and control large scale structures. The dynamic behavior will require algorithms that are efficient for handling thousands of differential equations. These types of problems have been included in disucssions on weather prediction by Bellman where tens and hundreds of thousand partial differential equations are required for local weather phenomena.

Currently available algorithms will most likely be unable to handle large scale systems because of storage requirements, execution time, or numerical accuracy. The investigation of algorithms for large scale problems is part of the research being carried out by this investigation. The primary objective of the research is to obtain an efficient algorithm for decoupling a large set of differential equations into subsets of differential equations that can be numerically integrated. The solution of the large set is then constructed from the subset solutions.

Problems Under Consideration

1. Spectral factorization
2. Decoupling of a large number of differential equations
3. Eigenvalue-eigenvector subroutines
4. Matrix polynomials
5. System identification

2. Sign Algorithm

The sign algorithm was first introduced by Roberts as an algorithm to compute the solution to the algebraic matrix Riccati equation given in equation (2.1). It is not difficult to show that the matrix given in equation (2.2) can always be associated with the matrix Riccati equation. The two solutions to equation (2.1) are given in equation (2.3) where Φ_{ij} are partitioned blocks of the eigenvector matrix of A as given in equation (2.4). The sign algorithm given by Roberts is a Newton procedure where S_i in equation (2.5) will converge to the sign of A.

Let A be $2n \times 2n$ with n eigenvalues having $Re(\lambda_i) > 0$ and n with $Re(\lambda_i) < 0$. If J is as defined in equation (2.6) then sign (A) is as given in equation (2.7). It can be shown that the inverse of $S + J$ contains the two solutions to the algebraic matrix Riccati equation (see eq. (2.8)) and is related to the eigenvector matrix of A as given in equation (2.9).

The T matrix will block diagonalize A when applied to A as a similarity transformation. The resultant of the operation is shown in equation (2.10). The

spectrum of A_{B1} will contain only eigenvalues with $Re(\lambda_i) > 0$, whereas that of A_{B2} will have $Re(\lambda_i) < 0$. The transformation on A is a spectral decomposition and is useful in solving a system of differential equations. Let x(t) be a 2nxl vector satisfying the state equation (2.11). If z(t) is as defined in equation (2.12), then equations (2.13) and (2.14) hold where $z_1(t)$ and $z_2(t)$ are nxl vectors which are partitions of the 2nxl z(t) vector. The system response vector x(t) can be recovered by using equation (2.15) or (2.16). The procedure can obviously be extended to more than two diagonal blocks.

Knowledge of the sign matrix of A is sufficient to define a set of eigenprojectors P_1 and P_2 for a simple spectral decomposition. If P_1 and P_2 are as defined in equation (2.17), then A_1 and A_2, as given in equation (2.18), will have spectrums $\rho(A_1) \geq 0$ and $\rho(A_2) \leq 0$. The eigenprojectors P_1 and P_2 will also decompose x(t) into two 2nxl vectors $x^+(t)$ and $x^-(t)$. The vector $x^+(t)$ will be a function of $\exp(\lambda_i t)$ with λ_i having $Re(\lambda_i) \geq 0$ and $x^-(t)$ will contain modes with $Re(\lambda_i) \leq 0$.

The eigenprojectors introduced in the previous paragraph were computed from the sign function computed on the basis of splitting the spectrum along the $j\omega$ axis. The bilinear transformation of equation (2.20) will permit a spectral decomposition with respect to circles of radius ρ chosen as to split the spectrum by eigenvalue magnitudes. The previous analyses still hold and, as before, several transformations may be used to decompose the spectrum into more than two domains.

The above decoupling procedure has several disadvantages. The first of these is the requirement for inverting 2nx2n matrices which is costly and inaccurate when n is large. In addition, several large matrices must be stored. An alternate approach is to use a standard eigenvalue-eigenvector routine to compute S. There is very little to gain in this approach, since the time domain solution can then be determined without the use of the decoupling.

(2.1) $$A_{12} + A_{11}R - RA_{22} - RA_{21}R = 0$$

(2.2) $$A = \begin{bmatrix} A_{11} & A_{12} \\ A_{21} & A_{22} \end{bmatrix} \qquad A_{ij} \text{ are nxn}$$

(2.3) $$R_1 = \phi_{12}\,\phi_{22}^{-1} \qquad R_2 = \phi_{11}\,\phi_{21}^{-1} \qquad R_i \text{ are nxn}$$

(2.4) $$\phi = \begin{bmatrix} \phi_{11} & \phi_{12} \\ \phi_{21} & \phi_{22} \end{bmatrix} \qquad \phi_{ij} \text{ are nxn}$$

(2.5) $$S_{i+1} = \frac{1}{2}\left[S_i + S_i^{-1}\right] \qquad S_0 = A$$

(2.6) $$J = \text{diag}[I \; -I]$$ I is nxn identify matrix

(2.7) $$S = \Phi J \Phi^{-1}$$ S is 2nx2n

(2.8) $$T = (S + J)^{-1} = \frac{1}{2}\begin{bmatrix} I & -R_1 \\ R_2^{-1} & -I \end{bmatrix}$$ T is 2nx2n

(2.9) $$T = \frac{1}{2}\begin{bmatrix} I & -\Phi_{12}\Phi_{22}^{-1} \\ \Phi_{21}\Phi_{11}^{-1} & -I \end{bmatrix}$$

(2.10) $$A_B = T^{-1}AT = \begin{bmatrix} A_{11} + A_{12}R_2^{-1} & 0 \\ 0 & A_{22} + A_{21}R_1 \end{bmatrix} = \begin{bmatrix} A_{B1} & 0 \\ 0 & A_{B2} \end{bmatrix}$$

$\rho(A_{B1})$ is in right half plane $\rho(A_{B2})$ is in left half plane

(2.11) $$\dot{x}(t) = Ax(t) + Bu(t)$$

(2.12) $$z(t) = T^{-1}x(t)$$

(2.13) $$\dot{z}(t) = T^{-1}AT\, z(t) + T^{-1}Bu(t)$$
$$= \begin{bmatrix} A_{B1} & 0 \\ 0 & A_{B2} \end{bmatrix} z(t) + \begin{bmatrix} B_1 \\ B_2 \end{bmatrix} u(t)$$

(2.14) $$\dot{z}_1(t) = A_{B1} z_1(t) + B_1 u(t)$$

$$\dot{z}_2(t) = A_{B2} z_2(t) + B_2 u(t)$$

(2.15) $$x(t) = T\, z(t)$$

(2.16) $$x_1(t) = \frac{1}{2}[z_1(t) - R_1 z_2(t)]$$

$$x_2(t) = \frac{1}{2}[R_2^{-1} z_1(t) - z_2(t)]$$

(2.17) $$P_1 = \frac{1}{2}(I + S) \qquad P_2 = \frac{1}{2}(I - S) \qquad P_1 + P_2 = I$$

(2.18) $$AP_1 = A_1 \qquad AP_2 = A_2 \qquad A_1 + A_2 = A$$

(2.19) $$P_1 x(t) = x^+(t) \qquad P_2 x(t) = x^-(t) \qquad x^+(t) + x^-(t) = x(t)$$

(2.20) $$A_0 = (A - \rho I)(A + \rho I)^{-1} \qquad \rho < |\lambda_j|$$

3. Matrix Polynomials

The difficulties encountered in the previous section are less severe if the A matrix is in or can be transformed into the block companion form and certain algorithms can be developed. As an example, assume that A has the form given in equation (2.2) which can be transformed into the second order companion form of equation (3.1) by a Krylov transformation given in equation (3.2). A typical Krylov matrix is given in equation (3.3) where it is assumed that A_{12} is invertible. The matrix polynomial of equation (3.4) will have $2n$ latent roots λ_i and $2n$ latent vectors y_i where the latent roots λ_i are the eigenvalues of A and A_c. The latent vectors y_i are the $2n$ vectors of Φ_1 and Φ_2 where Φ is the eigenvector matrix of A_c. Since $A(\lambda)$ is of the form of the differential equation for a finite element model, the second order matrix polynomial is usually of interest in structural problems. The coefficients of the matrix polynomial, the latent roots, and the latent vectors of $A(\lambda)$ require less storage than that required for storing A_c, the eigenvalues and the eigenvectors. This approach is therefore of interest because of storage requirements. The disadvantages of formulating the problem in terms of matrix polynomials is that efficient algorithms for computing the latent roots and the latent vectors of $A(\lambda)$ do not exist. This is an area that is currently under investigation.

A substantial decrease in storage requirements can be obtained by transforming $A(\lambda)$ into a higher order polynomial with matrix coefficients of lower order. Assume that $A(\lambda)$ is nxn and that A is $2n$x$2n$. If $2n$ is divisible by m in an integer sense, then an mth order polynomial can be found when $A(\lambda)$ has distinct latent roots. The matrix coefficients of $A(\lambda)$, as given in equation (3.6), will now be $(2n/m)$ x $(2n/m)$ matrices. The latent roots of $A(\lambda)$ and the latent vectors are sufficient to define the eigenvalues and eigenvectors of A where A is $2n$x$2n$ as given in equation (3.7).

The computation of the eigenvalues and eigenvectors of A_c or the latent roots and latent vectors of $A(\lambda)$ is not necessary if the time domain solution to the system differential equation is sought.

The Krylov type transformation required to construct the higher order polynomial is also used to transform $x(t)$ to a new vector $z(t)$, as given in equation (3.10), where $z(t)$ will be partitioned as in equation (3.11). It can be shown that $z_1(\lambda)$ will be defined by equations (3.12) and (3.13) with $z_1(t)$ given by equation (3.14). $x(t)$ can then be constructed from the $z_i(t)$ with $x(t) = K^{-1}z(t)$.

A second method of analysis is to use block matrices throughout. Let ϕ_i be solutions to the mth order polynomial, then $A(\lambda)$ can be factored as in equation (3.15). Thus, $z_1(t)$ can be found from equations (3.16) and (3.17). The $z_i(t)$ required for constructing $x(t)$ are found in a similar manner with the proper modifications in the matrix coefficients of equation (3.17).

The procedure given has several associated problems which must be solved prior to implementing the above algorithms. The first of these is that there does not exist an efficient algorithm for the Krylov transformation to construct the mth order polynomial from a lower order polynomial. Secondly, there does not exist at this time an efficient algorithm to compute the latent roots of $A(\lambda)$ or the latent vectors. The factorization procedure expressed in equation (3.15) is also an area for development of an efficient algorithm. The development of these algorithm is presently under study.

$$A_c = \begin{bmatrix} 0 & I \\ -A_2 & -A_1 \end{bmatrix} \tag{3.1}$$

$$A_c = K\,A\,K^{-1} \tag{3.2}$$

$$K = \begin{bmatrix} I & 0 \\ A_{11} & A_{12} \end{bmatrix} \tag{3.3}$$

$$A(\lambda) = I\lambda^2 + A_1\lambda + A_2 \tag{3.4}$$

$$\Phi_c = \begin{bmatrix} \Phi_1 & \Phi_2 \\ \Phi_1\Lambda_1 & \Phi_2\Lambda_2 \end{bmatrix} \tag{3.5}$$

$$A(\lambda) = I\lambda^m + A_1\lambda^{m-1} + \ldots + A_m \tag{3.6}$$

$$A = \begin{bmatrix} 0 & I & 0 & \ldots & 0 \\ 0 & 0 & I & \ldots & 0 \\ . & . & . & \ldots & . \\ 0 & 0 & 0 & \ldots & I \\ -A_m & -A_{m-1} & -A_{m-2} & & -A_1 \end{bmatrix} \tag{3.7}$$

$$\Phi = \begin{bmatrix} \Phi_1 & \Phi_2 & \ldots & \Phi_m \\ \Phi_1\Lambda_1 & \Phi_2\Lambda_2 & \ldots & \Phi_m\Lambda_m \\ . & . & \ldots & . \\ . & . & \ldots & . \\ \Phi_1\Lambda_1^{m-1} & \Phi_2\Lambda_2^{m-1} & \ldots & \Phi_m\Lambda_m^{m-1} \end{bmatrix} \tag{3.8}$$

(3.9) $$\left[\tilde{x}(t)\right]^T = \left[x^T(t)\ \dot{x}^T(t)\right]$$

(3.10) $$z(t) = K\,x(t)$$

(3.11) $$z^T(t) = \left[z_1(t)\ z_2(t)\ \ldots\ z_m(t)\right] \qquad z_i(t) \text{ is } 2n/m \times 1$$

(3.12) $$A(\lambda)\ z_1(\lambda) = B(\lambda)\ U(\lambda) \qquad A(\lambda) \text{ is } 2n/m \times 2n/m$$

(3.13) $$z_1(\lambda) = [A(\lambda)]^{-1}B(\lambda)\ u(\lambda) = \sum_{i=1}^{2n} \frac{\hat{P}_{i0}}{(\lambda - \lambda_i)} B(\lambda_i)\ u(\lambda)$$

(3.14) $$z_1(t) = \sum_{i=1}^{2n} \hat{P}_{i0}\, B(\lambda_i) \int_0^t \exp\left[\lambda_i(t - \tau)\right] u(\tau)\, d\tau$$

(3.15) $$A(\lambda) = (I\lambda - Q_1)(I\lambda - Q_2)\ \ldots\ (I\lambda - Q_m)$$

(3.16) $$[A(\lambda)]^{-1}B(\lambda) = \sum_{i=1}^{m} \frac{B(\phi_i)}{\prod_{\substack{i=1 \\ i \neq j}}^{m} (\phi_i - \phi_j)} = \sum_{i=1}^{m} \tilde{P}_{i0}$$

(3.17) $$z_1(t) = \sum_{i=1}^{m} \tilde{P}_{i0} \exp\left[Q_i(t - \tau)\right] u(\tau) d\tau$$

4. System Identification

Numerous algorithms have been written for the identification of a system and for parameter estimation. The method of least squares solution of a set of overdetermined equations appears to be the most widely used algorithm, although there are other methods that are acceptable. The least square algorithm basicly takes the discrete time data from the system response with a known input to define an overdetermined set of equations. As an example, free response is given in equation (4.1) for a time invariant system having a typical set of equations for a system with no input. The matrix θ is the state transition matrix which will be invariant for all t. Equations (4.2 to (4.5) can then be established.

The unknown parameters in θ are then computed by a least squares algorithm such as given in equations (4.6) and (4.7). This approach is not recommended but is

given only to illustrate the simplest procedure. The singular value decomposition would be preferred for determining the vectors 0_i.

The complete set of row vectors 0_i would be identified and Φ would then be known. Since Φ is discrete, the state transition matrix will have the form given in equation (4.8). The eigenvalues and eigenvectors of Φ could then be identified. It has been assumed that all computations were made with no error although this is an ideal situation. It must also be assumed that the sampling frequency of the system response has been sufficiently high to satisfy the sampling theorem.

The numerical problems encountered in the decoupling algorithm will be present in the identification procedure. The storage requirements of the algorithm dictate that a large machine be available, and the algorithm will probably require multiple precision. The execution time for a system with 1000 eigenvalues on a typical machine may be an hour.

The research has concentrated on the decoupling algorithm, eigenvalue and eigenvector algorithms, matrix polynomials, and identification procedures. The decoupling algorithm as presently used requires inversion of large matrices which is inefficient. Experience with applying the algorithm to a free-free beam indicates that numerical errors are severe when the beam has several hundred nodes due to the condition number of the matrix or the range of the elements in the matrix.

Numerical errors have also been apparent in the use of the eigenvalue-eigenvector subroutines from EISPACK on relatively small matrices, 30 × 30. The free-free beam problem with twenty-one nodes has been decoupled with the algorithm discussed in the next section, and it has been necessary to use an eigenvalue-eigenvector subroutine with all computations in double precision on a 30-bit machine.

Research on matrix polynomials has been underway, and some of the results were presented in Section 3 of this report. This mathematical development of algorithms for analyzing matrix polynomials has not received the attention that seems to be warranted. Some aspects of the use by matrix polynomials will be covered.

System identification of large scale systems has not received much attention in the past, since most practical systems are of order 100 or less. Identification of a system with 200 or more parameters is not a commonly occurring computational task.

The use of a matrix polynomial in identification has received very little, if any, attention in the past. The identification algorithm by quadrature methods uses scalar functions for determination of the parameters. The question arises as to whether matrix functions can be utilized rather than the scalar functions. This question and many other remain unanswered.

(4.1) $x(k + 1) = \Phi x(k)$ $\quad T$ = sampling time; $k = t/T$

$$x_1(1) = \theta_{11}x_1(0) + \theta_{12}x_2(0) + \ldots + \theta_{1n}x_n(0)$$

$$x_1(2) = \theta_{11}x_1(1) + \theta_{12}x_2(1) + \ldots + \theta_{1n}x_n(1)$$

(4.2) $\quad . \qquad . \qquad . \qquad \ldots \qquad .$

$\quad . \qquad . \qquad . \qquad \ldots \qquad .$

$$x_1(m) = \theta_{11}x_1(m-1) + \theta_{12}x_2(m-1) + \ldots + \theta_{1n}x_n(m-1)$$

(4.3) $$x^T(k) = [x_1(k) \; x_2(k) \; \ldots \; x_n(k)]^T$$

(4.4) $$\begin{bmatrix} x_1(1) \\ x_1(2) \\ . \\ . \\ x_1(m) \end{bmatrix} = \begin{bmatrix} x_1(0) & x_2(0) & \ldots & x_n(0) \\ x_1(1) & x_2(1) & \ldots & x_n(1) \\ . & . & \ldots & . \\ . & . & \ldots & . \\ x_1(m-1) & x_2(m-1) & \ldots & x_n(m-1) \end{bmatrix} \begin{bmatrix} \theta_{11} \\ \theta_{12} \\ . \\ . \\ \theta_{1n} \end{bmatrix}$$

(4.5) $$\theta = \begin{bmatrix} \theta_1 \\ \theta_2 \\ \theta_n \end{bmatrix}$$

(4.6) $$Y = R\,\theta_1$$

(4.7) $$\theta_1 = (R^TR)^{-1}R^TY$$

(4.8) $$\theta = \Phi e^{\Lambda T}\Phi^{-1}$$

(4.9) $$e^{\Lambda T} = \text{diag}\,[e^{\lambda_1 T} \; e^{\lambda_2 T} \; \ldots \; e^{\lambda_n T}]$$

IDENTIFICATION AND CONTROL

FOR FLEXIBLE VEHICLES

Christopher S. Greene
Honeywell Systems and Research Center

Workshop on the Structural Dynamics
and Control of Large Space Structures

October 30-31, 1980

INTRODUCTION

Controlling large, flexible objects in space is currently a "hot" topic in the research community. Many "solutions" have been proposed, most of which have either not worked in practice or have flaws which come to light when one considers implementation. At Honeywell, we have done extensive research on implementable control designs, which has served to guide the research to be performed. One of the critical problems we see is in obtaining and then properly using accurate information about the structure to be controlled.

By way of motivation, I will first give a brief review of our view of LSS control, describing the problem and what's new. Following this, the results of applying a new identification measure to a sample LSS will be presented. These results indicate the promise/problems of on-orbit identification. I will conclude by summarizing the line of research we are pursuing.

- MOTIVATION
- IDENTIFICATION
- OUR PROGRAM
- EXPECTED RESULTS

Figure 1

THE CONVENTIONAL PROBLEM

In the past, spacecraft flexibility has been handled by requiring the flexible modes of the spacecraft to occur well outside the bandwidth of the control system. Where this did not occur naturally, system modifications were made to ensure that it did happen. By then "rolling-off" the control system, interactions with the flexible dynamics were avoided.

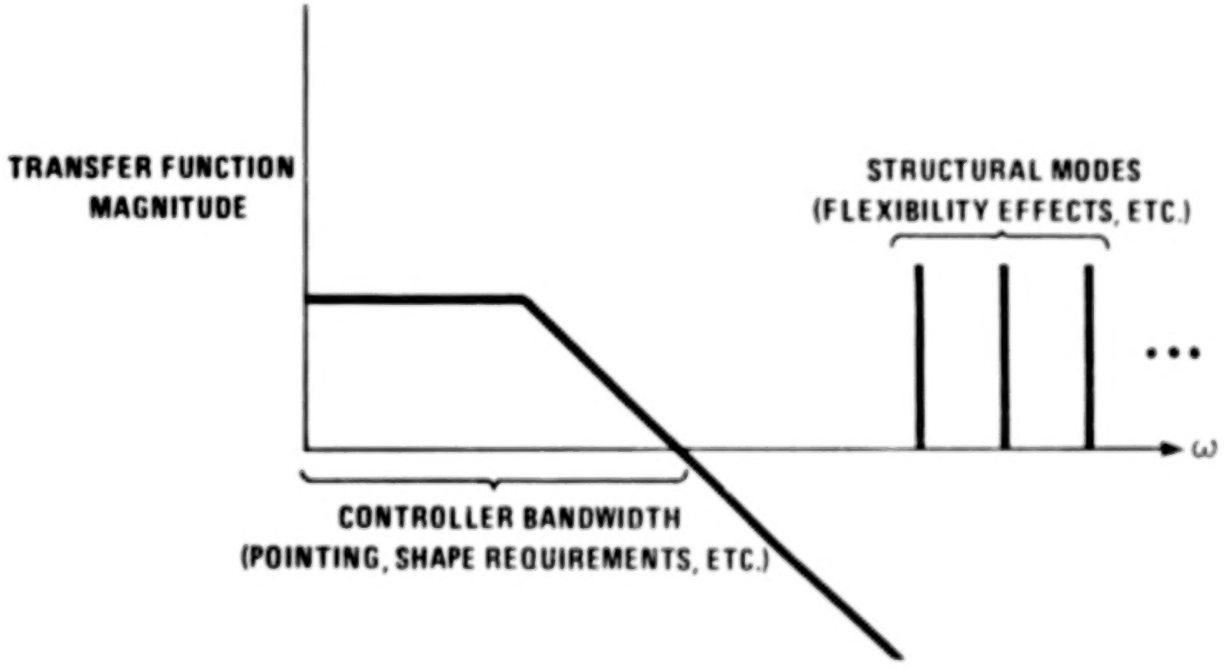

SOLUTION: "ROLL OFF" CONTROLLER TO AVOID EXCITING HIGH FREQUENCY MODES.

Figure 2

THE PROJECTED PROBLEM

As spacecraft grow and become more flexible and as control bandwidth increases due to increasingly stringent control requirements, the solution of forced separation is becoming intolerable. Talk is heard of hundreds of flexible modes within the bandwidth. This overlap characterizes what we call "the LSS control problem."

The solution is then clear: one must "actively control" the modes in the pass band of the controller and roll-off (while maintaining stability) the higher frequency modes.

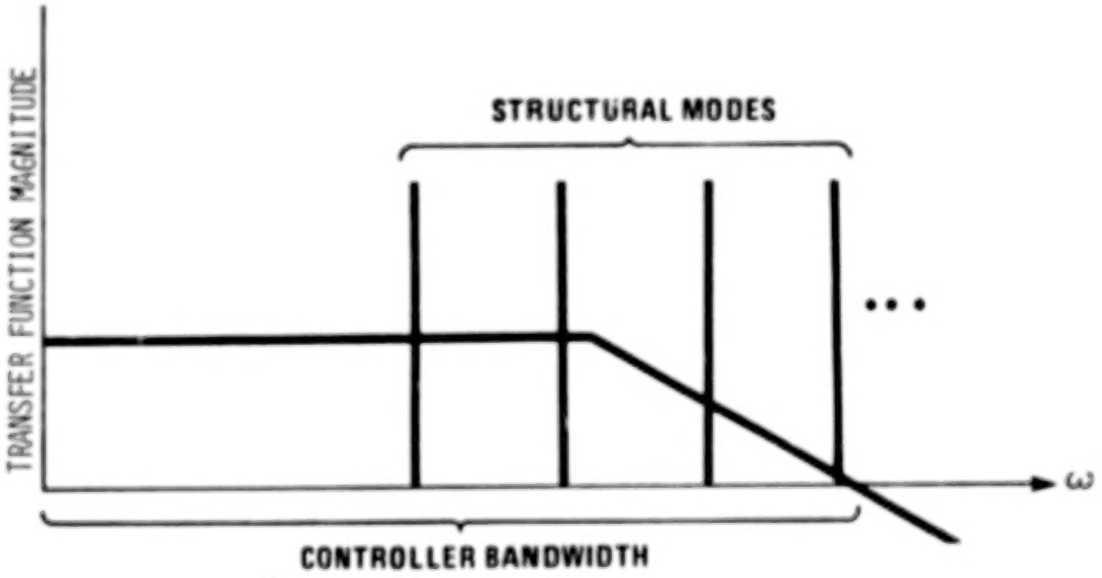

SOLUTION: 1) **ACTIVE STRUCTURAL CONTROL OF MODES WITHIN CONTROLLER BANDWIDTH.**

2) **"ROLL OFF" CONTROLLERS TO AVOID EXCITING STRUCTURAL MODES BEYOND CONTROLLER BANDWIDTH.**

Figure 3

INFORMATION TRADE-OFF

There are two basic approaches to achieving these. The first is a robust controller based on colocated actuators and sensors using rate feedback. This approach is extremely insensitive to model information requiring only crude mode shape and frequency information and only a limit to damping. However, the amount of modal damping achievable this way is limited and relatively high bandwidth actuators, sensors, etc., are required.

In contrast, many methods have been proposed which achieve better damping and require less bandwidth from components. However, invariably, these require accurate model data.

- **Robust Control**
  - Insensitive to Model Information
  - Achieved Damping Limited
  - Requires High Bandwidth Intelligence

- **High Performance Control**
  - Achieves High Damping
  - Requires Less Bandwidth
  - Very Sensitive to Model Data

Figure 4

WHY IDENTIFY

In general, pre-launch data is not accurate enough to permit design of high performance controllers. Thus, if the benefits of these are to be realized, system identification must be performed.

- WANT BENEFITS OF HIGH PERFORMANCE CONTROL
- PRE-LAUNCH DATA POOR
- ONLY TWO OPTIONS
  - ADAPTIVE
  - IDENTIFY AND RECONFIGURE
- EITHER REQUIRES IDENTIFICATION

Figure 5

IDENTIFICATION

Two basic methods of system identification are currently popular in the aerospace community: those based on Maximum Likelihood Estimation (MLE) and those based on the frequency domain (FFT). Some recent advances in the MLE analysis are very useful for our type of problem. We have applied these to a sample problem, the results of which I would like to present.

- MAXIMUM LIKELIHOOD ESTIMATION (MLE) BASED
- FREQUENCY DOMAIN BASED

Figure 6

The MLE method is based on finding which model from a (possibly infinite) set of models comes closest to the true system. Closest, for the MLE method, is defined as minimizing the negative log likelihood function which can be computed from the Kalman filter based on a model M_α.

Of course, LSS are infinite dimensional and therefore no finite dimensional model can ever perfectly match the true system. This mismatch has caused problems in the past and until recently no method of analysis was available.

$$x(\kappa+1) = A_\bullet x(\tau) + B_\bullet u(\tau) + L_\bullet \zeta(\tau)$$
$$Z(\tau) = C_\bullet x(\tau) + \Theta(\tau)$$

TRUTH: $M_\bullet = \{A_\bullet, B_\bullet, C_\bullet, L_\bullet, \Xi_\bullet, \Theta_\bullet\}$

MODEL: $M_\alpha = \{A_\alpha, B_\alpha, C_\alpha, L_\alpha, \Xi_\alpha, \Theta_\alpha\}$

GOAL: FIND MODEL M_α "CLOSEST" TO $M_\bullet$.

CLOSEST = MINIMIZE THE NEGATIVE LOG LIKELIHOOD FUNCTION (COMPUTED FROM KBF FOR M_α)

Figure 7

DISTANCE MEASURE

Based on recent work by Baram, extended by Yared (Ph.D. thesis, MIT, 1979), a distance measure relating the information favoring one model over another can now be computed. Using this, the distance from a model to the true system can be computed.

Note that this assumes the true system to be known. It is, however, useful for analysis purposes for predicting the behavior of the MLE method under various model order, initial condition, and noise conditions.

$I_a^\bullet$ = EXPECTED VALUE OF THE CONDITIONAL LIKELIHOOD FUNCTION WITH RESPECT TO THE TRUE SYSTEM.

$I(a_1, a_2) = I_{a2}^\bullet - I_{a1}^\bullet$ = DISTANCE MEASURE

INFORMATION FAVORING MODEL a_1 OVER a_2.

$I(\bullet, a)$ = DISTANCE FROM TRUE SYSTEM TO MODEL a.

Figure 8

SAMPLE TETRAHEDRAL TRUSS STRUCTURE

We have applied this technique to a sample structure used in the ACOSS program known as the tetrahedral truss. Test signals (forces) and displacement measurements were assumed in one leg of the truss. Noise sources were included as shown.

Tests were then conducted to determine the distance between the assumed true system and a model. For all tests, the model used for identification contained a single mode while the number of modes used to represent the true system was either one or nine. In all tests, only one parameter was assumed unknown.

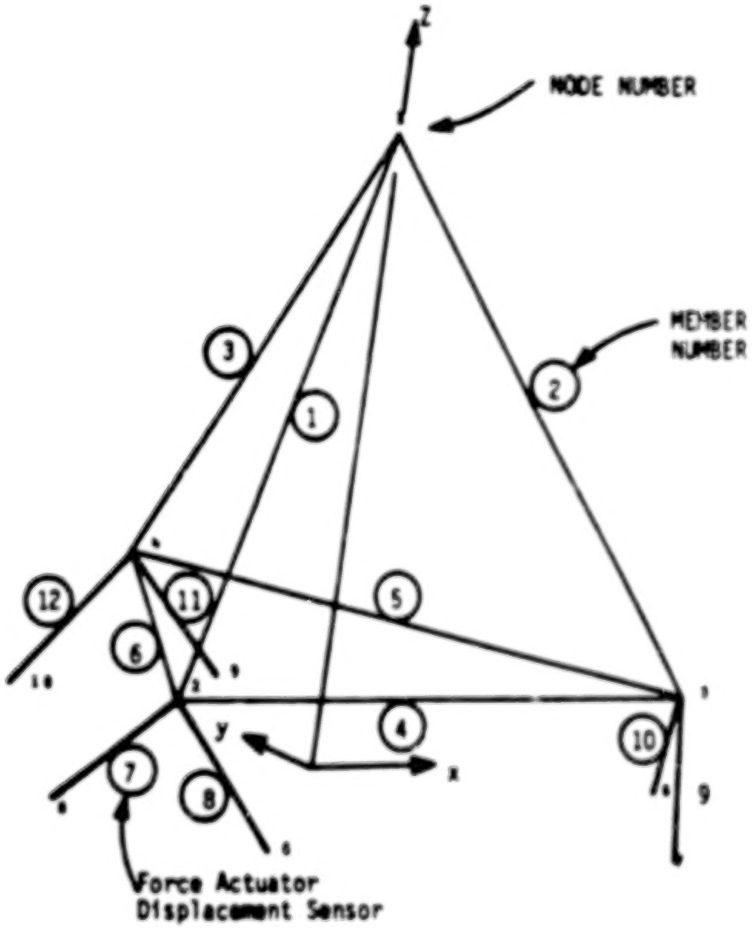

Notes:

Plant Disturbance	.005 rms (produces .001 at sensor)
Sensor Noise	.001 rms
Test Input	.05 rms (produces .01 at sensor)
Damping Ratio	.5%

Figure 9

DISTANCE FROM ONE MODEL TRUTH FOR ω ID

In the first experiments, the objective was to identify the frequency of a model assuming the damping to be known. If the true system and identification model match in order, the distance is as below.

Note that the distance is zero at the true value of the parameter. Also, the valley is very steep, indicating good local convergence but requiring good initial guesses.

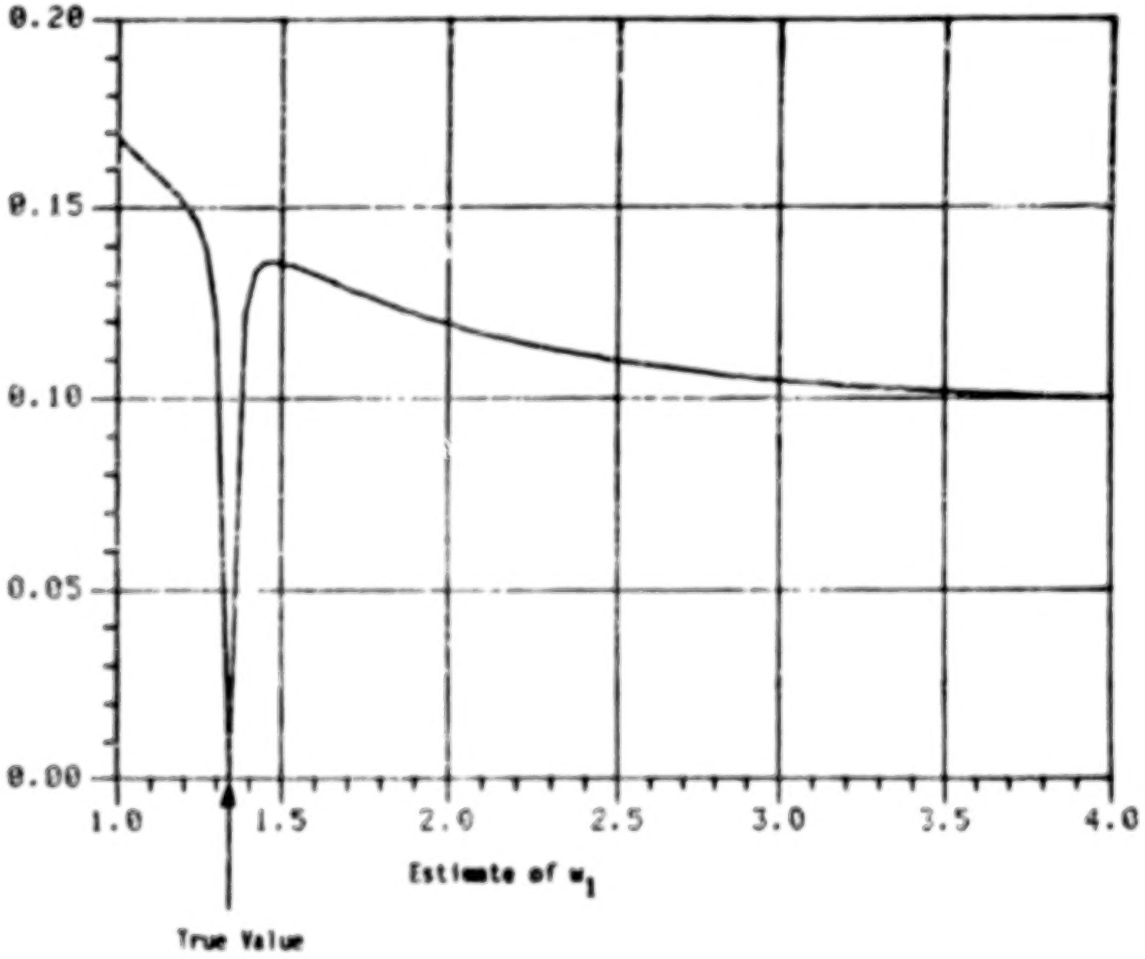

Figure 10

DISTANCE FROM 9 MODE TRUTH FOR ω ID

If the true system is larger, the distance becomes large and no value of ω_1 reduces the distance to zero. In addition, multiple minima occur.

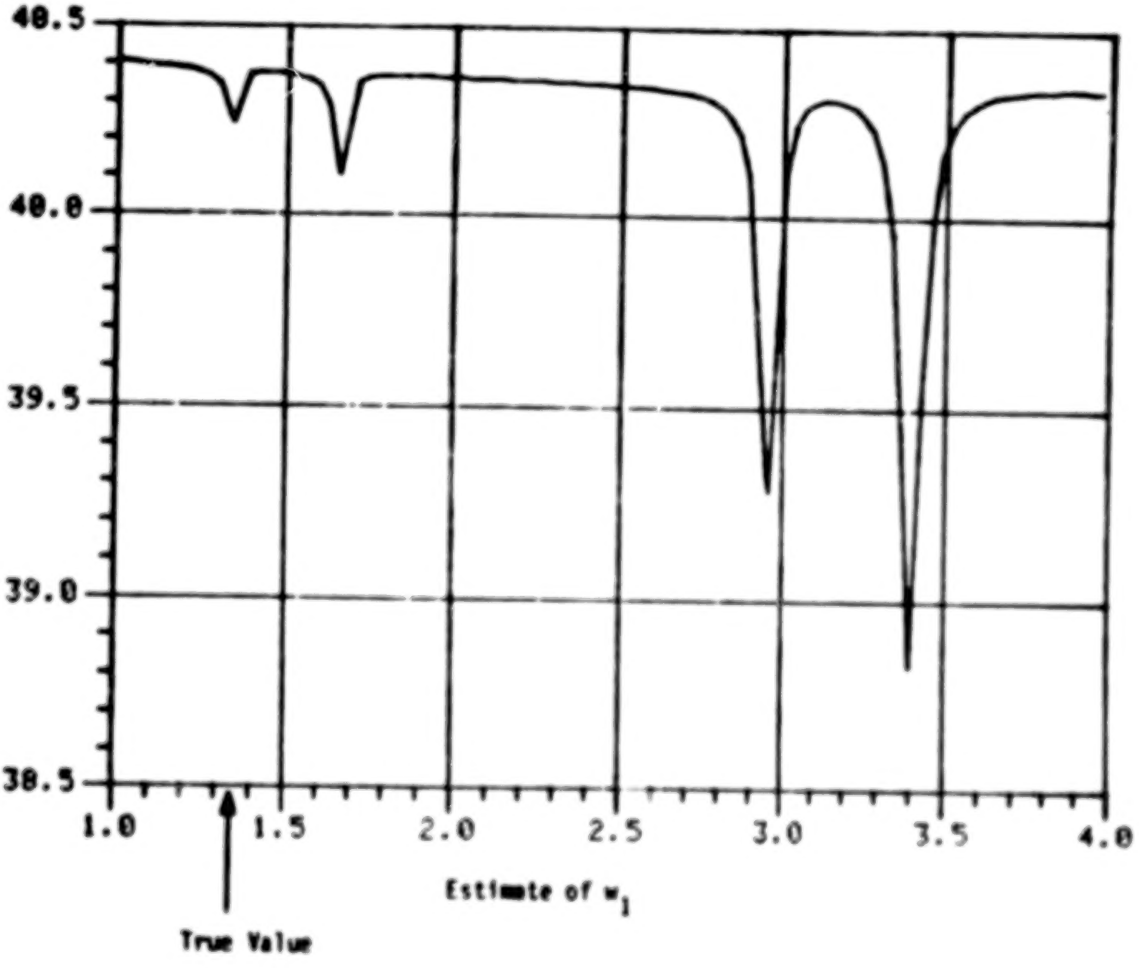

Figure 11

DISTANCE FROM ONE MODE TRUTH FOR DAMPING ID

If damping is assumed unknown (but first mode frequency is known), the distance measure curve becomes quite broad and well shaped. If the true system and the model agree in order, this measure reduces to zero at the true value. However, the lack of significance of distance measure indicates that the convergence of the MLE method will be poor and susceptible to noise.

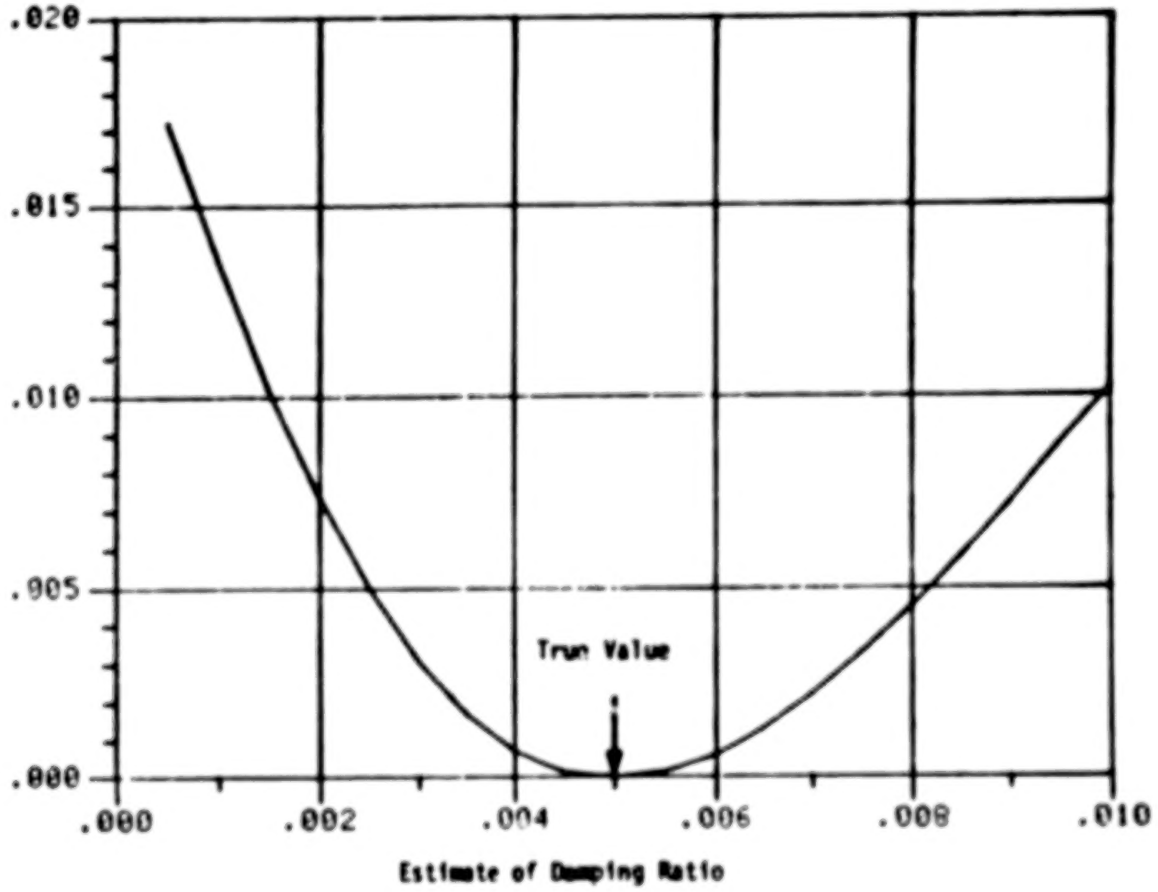

Figure 12

DISTANCE FROM 9 MODE TRUTH FOR DAMPING ID

This conclusion remains if the true system is assumed larger than the model. In addition, a bias can be seen between the minimum distance damping ratio (the value the MLE method will converge to) and the true value. This bias is caused by the order mismatch and it is important to analyze this bias as it limits MLE performance. In addition, tradeoffs can now be performed to determine how large the identification model is required to be to keep the bias "small enough".

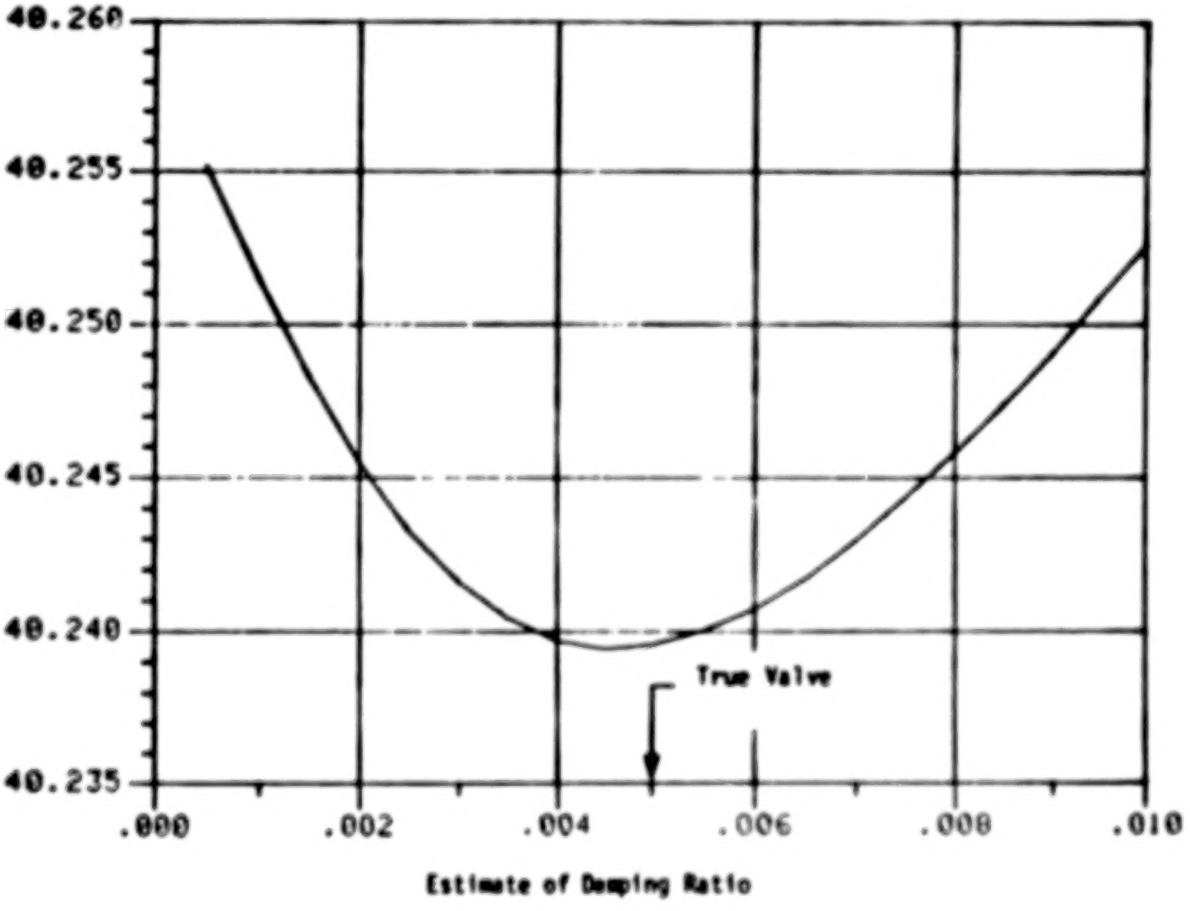

Figure 13

CONCLUSIONS TO DATE

We now have a tool which can be used to analyze these biases and other effects of system mismatch.

The next step is to enlarge the study to include a more realistic situation.

- TOOL FOR ASSESSING MISMATCH
- MISMATCH CAN RESULT IN BIASED ESTIMATE
- FREQUENCY ESTIMATE WILL NEED GOOD INITIAL GUESS
- DAMPING HARD TO ESTIMATE
- MORE STUDY NEEDED

Figure 14

OUR PROGRAM

We will be doing this by starting with a realistic strawman -- the space shuttle with a payload on the end of the remote manipulator system (RMS) arm. In addition, we will be supporting and guiding the beam experiment as needed and will be guided by those results.

Our first step is to determine representative parameters for sensor noises, actuator uncertainties, and other disturbances. This will help insure that our results are of more than academic interest. We will then be performing extensive identifiability studies to determine how accurately the parameters of the model can be identified.

Finally, a controller will be designed which is compatible with the expected residual uncertainty and the performance compared to that obtained using a robust controller.

- USE THE SHUTTLE/RMS/PAYLOAD AS STRAWMAN.
  - ALSO BEAM EXPERIMENT
- DETERMINE REPRESENTATIVE ENVIRONMENTAL PARAMETERS.
- INVESTIGATE IDENTIFIABILITY OF PARAMETERS.
- DESIGN A CONTROLLER USING AVAILABLE PARAMETERS.
- COMPARE RESULTS WITH THOSE USING ILAS/RATE FEEDBACK.

Figure 15

EXPECTED RESULTS

In this way, we will determine the limitiations to be expected in performing on-orbit parameter identification. In addition, we will have investigated how these limitations affect the control design process and identified the achievable benefits using a high performance controller in place of a robust one.

- **LIMITATIONS ON SYSTEM IDENTIFICATION**
- **EFFECTS OF THESE LIMITATIONS ON CONTROL DESIGN.**
  - **HOW TO DESIGN WITH AVAILABLE INFORMATION**
  - **BENEFITS OVER "ROBUST CONTROL"**

Figure 16

BLANK PAGE

RELIABILITY ISSUES IN ACTIVE CONTROL OF FLEXIBLE SPACE STRUCTURES

W. E. VanderVelde
Department of Aeronautics & Astronautics
Massachusetts Institute of Technology

Workshop on the Structural Dynamics and Control
of Large Space Structures
October 30-31, 1980

EXPECTED NUMBER OF COMPONENT FAILURES IN A YEAR

Why do we need to consider component unreliability? A large, lightweight structure in space will display many vibratory modes which may have to be actively damped to assure mission success. Effective control of these many modes will require use of a large number of sensors and actuators - possibly hundreds of them. Even if these control systems are serviced in orbit, one would like the service interval to be long - at least 1 year. With component mean time between failures which can reasonably be anticipated, one must expect many of the control system components to fail in the course of a year. Figure 1 presents the expected number of component failures per year versus component mean time between failures.

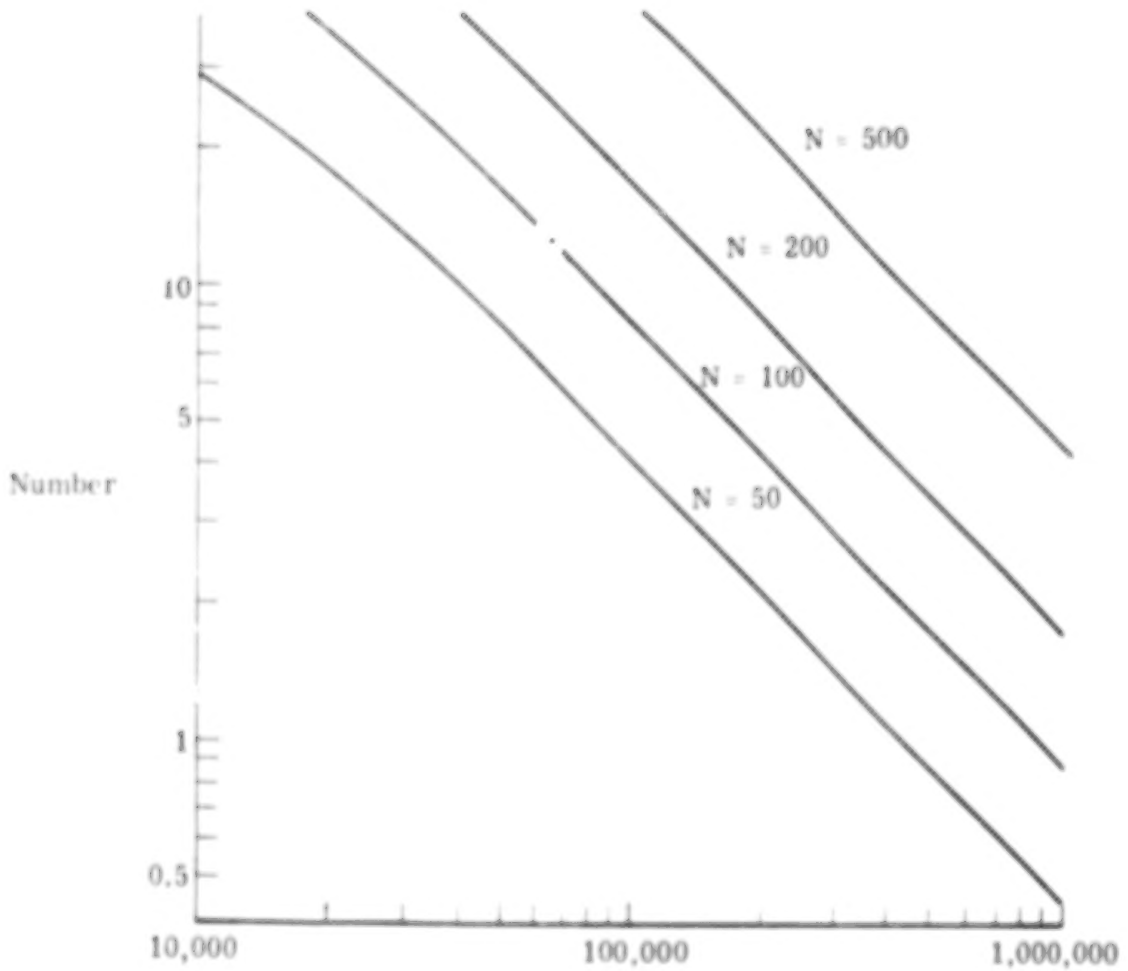

Figure 1

PROBABILITY OF ADDITIONAL FAILURES WITHIN 24 HOURS

OF A COMPONENT FAILURE

Will it be necessary to accommodate more than one component failure at a time? Following a component failure which is detected and identified, the system will be reconfigured to function with the remaining components. This reconfiguration should be accomplished in a relatively short time - perhaps on the order of 1 day. With the component mean time between failures which must be achieved to restrict the expected number of failures in a year to a reasonable value, the probability of one or more additional failures in 1 day following a single failure is small. (See fig. 2.) To reduce this probability further, it may be possible to reconfigure the failure detection and identification system more quickly than the complete control system.

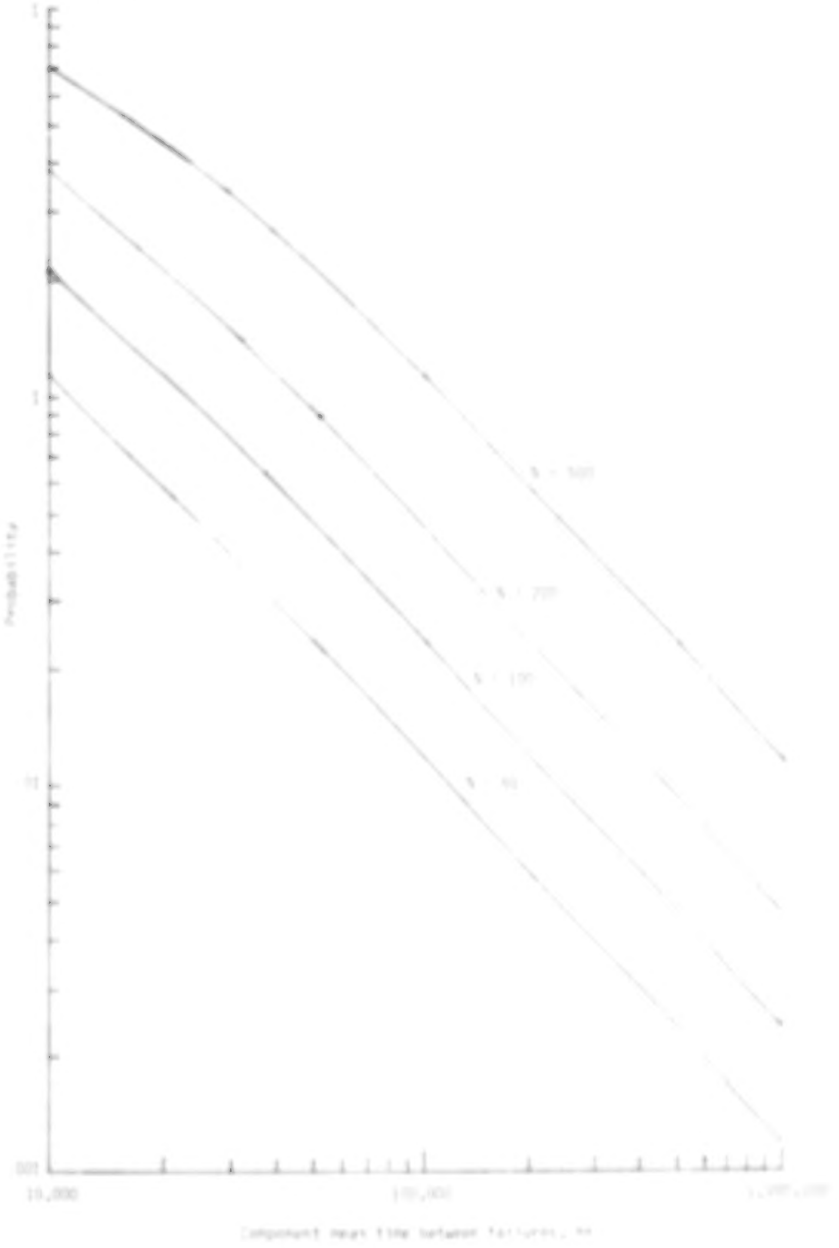

Figure 2

SYSTEM OPERATIONAL APPROACH

Figure 3 outlines the system operational approach.

- IMPLEMENT A QUICK-REACTION STANDBY MODE OF CONTROL FOLLOWING INDICATION OF A COMPONENT FAILURE.
- COMPLETE FDI SYSTEM RECONFIGURATION QUICKLY—PERHAPS WITHIN A FEW HOURS.
- COMPLETE CONTROL SYSTEM RECONFIGURATION AS SOON AS POSSIBLE—PERHAPS WITHIN A DAY.

Figure 3

SYSTEM DESIGN APPROACH

Figure 4 outlines the system design approach.

- UTILIZE FAULT-TOLERANT COMPUTERS AS DATA PROCESSORS FOR THE CONTROLLER AND FDI FUNCTIONS.
- INCORPORATE DIAGNOSTIC AND/OR BITE INFORMATION TO GIVE DIRECT INDICATION OF COMPONENT FAILURES WHERE POSSIBLE.
- IMPLEMENT AN FDI SYSTEM TO DETECT AND IDENTIFY SINGLE ADDITIONAL CONTROL SYSTEM COMPONENT FAILURES—SENSORS AND ACTUATORS.
- ANALYZE SPECIFIC SYSTEM IMPLEMENTATIONS TO CHECK FOR COMPLETE FDI COVERAGE INCLUDING OTHER COMPONENTS SUCH AS POWER SUPPLIES, DATA CONVERTERS, DATA TRANSMISSION LINES, ETC.

Figure 4

FAILURE DETECTION AND IDENTIFICATION

Figure 5 outlines failure detection and identification.

- MANY APPROACHES TO FDI HAVE BEEN SUGGESTED.
- WILL NOT CONSIDER METHODS WHICH REQUIRE SPECIFICATION OF THE MODE OF FAILURE.
- WILL CONCENTRATE ON METHODS WHICH ARE APPLICABLE TO BOTH SENSOR AND ACTUATOR FAILURES.
- TWO CANDIDATE TECHNIQUES FOR INITIAL CONSIDERATION:

  AN OPEN LOOP METHOD: GENERALIZED PARITY RELATIONS

  A CLOSED LOOP METHOD: FAILURE DETECTION FILTER

Figure 5

GENERALIZED PARITY RELATIONS

The usual concept of parity relations in FDI applies to redundant measurements such that a linear combination of the measurements can be set to zero.

The generalized concept of parity relations utilizes measurements at more than one time, which introduces actuator input signals as well as sensor output signals.

Discrete system model:

$$\underline{x}_{k+1} = A\,\underline{x}_k + B\,\underline{u}_k + \underline{n}_k$$

$$\underline{y}_k = C\,\underline{x}_k + D\,\underline{u}_k + \underline{v}_k$$

$$\underline{y}_k = C\,\underline{x}_k + D\,\underline{u}_k + \underline{v}_k$$

$$\underline{y}_{k+1} = CA\,\underline{x}_k + CB\,\underline{u}_k + D\,\underline{u}_{k+1} + C\,\underline{n}_k + \underline{v}_{k+1}$$

$$\underline{y}_{k+2} = CA^2\,\underline{x}_k + CAB\,\underline{u}_k + CB\,\underline{u}_{k+1} + D\,\underline{u}_{k+2} + CA\,\underline{n}_k + C\,\underline{n}_{k+1} + \underline{v}_{k+2}$$

etc.

Example:

$$A = \begin{bmatrix} 1 & 0.3 & 0.1 \\ 0 & 1 & 0.4 \\ 0 & 0.2 & 0.5 \end{bmatrix} \quad B = \begin{bmatrix} 0 \\ 0.1 \\ 0.6 \end{bmatrix} \quad C = \begin{bmatrix} 1 & 0 & 0 \\ 0 & 1 & 0 \end{bmatrix} \quad D = 0$$

Except for the noise terms,

$$y_{1k} = x_{1k}$$

$$y_{2k} = x_{2k}$$

$$y_{1k+1} = x_{1k} + 0.3\,x_{2k} + 0.1\,x_{3k}$$

$$y_{2k+1} = x_{2k} + 0.4\,x_{3k} + 0.1\,u_k$$

$$y_{1k+2} = x_{1k} + 0.62\,x_{2k} + 0.27\,x_{3k} + 0.09\,u_k$$

$$y_{2k+2} = 1.08\,x_{2k} + 0.60\,x_{3k} + 0.34\,u_k + 0.10\,u_{k+1}$$

One simple generalized parity relation for a group of four rate gyros at one location can be derived considering:

Measurements: $y_{ik} = \underline{c}_i^T \underline{x}_k \qquad i = 1,2,3,4$

The set of four $\underline{c}_i$ in three-dimensional space are dependent, and one can find a_i such that

$$\sum_{i=1}^{4} a_i \underline{c}_i = 0$$

Thus

$$r_k = \sum_{i=1}^{4} a_i y_{ik}$$

equals zero except for noise. A significantly nonzero r_k indicates a failure among the four gyros.

More generalized parity relations are formed from dependent rows of C, CA, CA^2, etc. This eliminates the unknown state $\underline{x}_k$ from the parity relations.

An appropriate set of parity relations must be used, each depending on different subsets of sensors and actuators, so that from the set of residuals one can identify the failed component.

One possible set of parity relations is for the example:

$$r_{1k} = 1.9\, y_{1k} - 0.01\, y_{2k} - 0.9\, y_{1k+1} + 0.9\, y_{2k+1} - y_{1k+2}$$

$$r_{2k} = -0.42\, y_{2k} + 1.5\, y_{2k+1} - y_{2k+2} + 0.19\, u_k + 0.1\, u_{k+1}$$

$$r_{3k} = 4\, y_{1k} + 0.2\, y_{2k} - 4\, y_{1k+1} + y_{2k+1} - 0.1\, u_k$$

Sensor 1 failure $\longrightarrow$ r_1 , not r_2 , r_3

Sensor 2 failure $\longrightarrow$ r_1 , r_2 , r_3

Actuator failure $\longrightarrow$ not r_1 , r_2 , r_3

FAILURE DETECTION FILTER

The failure detection filter (fig. 6) incorporates a model of the system being monitored. The difference between the filter output and the measured outputs of the system are fed back through the matrix D to cause the model to track the system. If the system is performing nominally, the output errors, after initial transients have subsided, are due only to unmodelled noises and disturbances and to model mismatch.

When a component fails, the model no longer matches the behavior of the system and a significant output error develops. The filter gain matrix D is designed so that the output error due to each monitored failure is restricted to a single direction, and that direction is different for each component the filter is designed to monitor. Thus the presence of a significant output error - larger than that due to noise - indicates a component failure, and the direction of that error identifies the component that failed.

It is possible to use detection filters to monitor sensor failures, actuator failures, and to indicate significant mismatches in system parameters.

Reference: Beard, R. V.: Failure Accommodation in Linear Systems Through Self-Reorganization. NASA CR-118314, 1971.

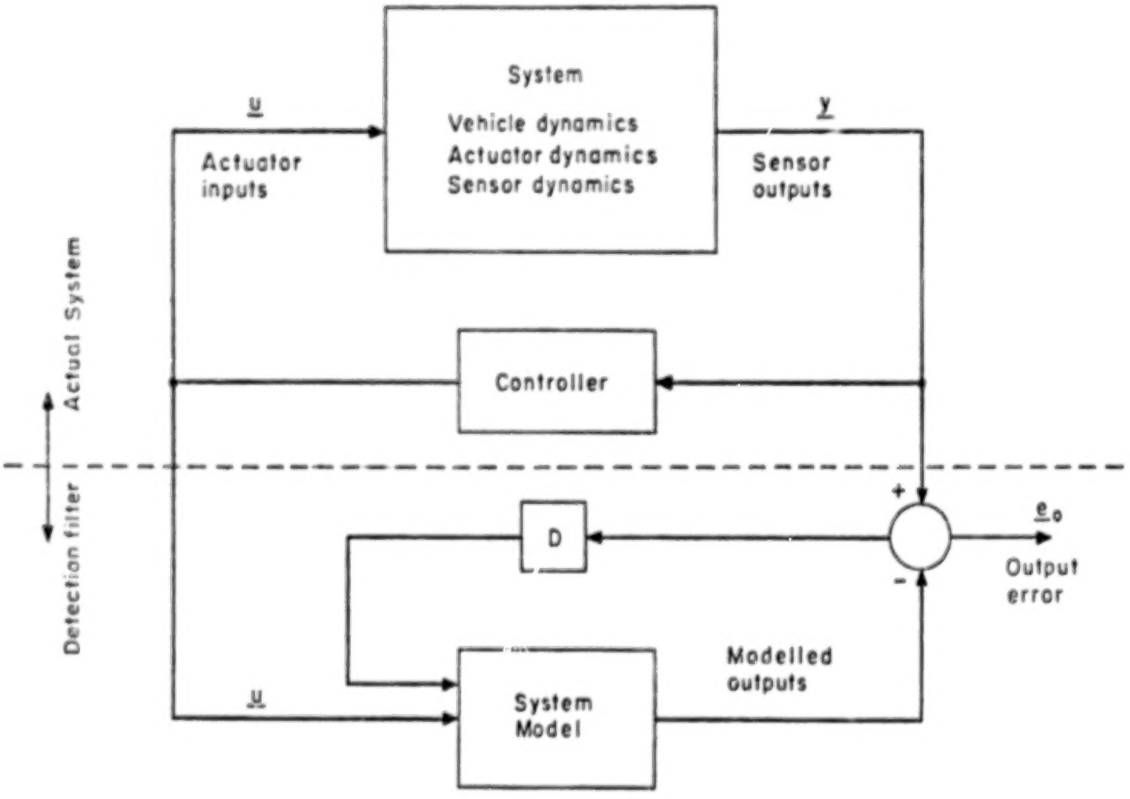

Figure 6

QUICK-REACTION STANDBY CONTROL MODE FOLLOWING A FAILURE

Figure 7 presents the quick-reaction standby control mode following a failure.

- A SIMPLE CONTROL SYSTEM WHICH MAINTAINS STABILITY AND RESTRICTS RESPONSE TO DISTURBANCES IN SPITE OF LOSS OF AN ARBITRARY COMPONENT.
- NORMAL PERFORMANCE REQUIREMENTS MAY BE SUSPENDED DURING STANDBY OPERATION.
- ONE CANDIDATE IS A CONTROL SYSTEM WHICH ONLY FEEDS BACK RATE INFORMATION TO COLOCATED ACTUATORS.

Figure 7

SYSTEM RECONFIGURATION

An outline of the system reconfiguration is given in figure 8.

- USE OF THE INTERIM STANDBY MODE ALLOWS SOME TIME IN WHICH TO RECONFIGURE THE CONTROL SYSTEM; A DAY SEEMS REASONABLE.
- WITH THE CONTROLLERS IMPLEMENTED AS DIGITAL DATA PROCESSORS, RECONFIGURATION AMOUNTS TO REVISING THE PROGRAMS WHICH THESE PROCESSORS EXECUTE.
- THIS COULD BE AS DIFFICULT AS DESIGNING THE SYSTEM IN THE FIRST PLACE—BUT USING FEWER SENSORS AND/OR ACTUATORS.
- IT IS ASSUMED THAT MOST MISSION SITUATIONS WILL PERMIT GROUND-BASED SUPPORT OF THE RECONFIGURATION FUNCTION WITH THE RESULTS UP-LINKED TO THE SPACE SYSTEM.
- LOOK FOR WAYS TO SIMPLIFY THE RECONFIGURATION PROCESS—PERHAPS USING INFORMATION GENERATED DURING THE ORIGINAL DESIGN OF THE SYSTEM.

Figure 8

RESEARCH TASK 1

Research Task 1 calls for development of a preliminary capability for the detection and identification of failures in the sensors and actuators of the laboratory experiment at Langley Research Center.

1a. Obtain from LaRC a dynamic model characterizing the laboratory apparatus and design a simple control system of some standard form to control the experimental plant.

1b. Choose one or more of the currently available FDI techniques to apply to this problem.

1c. Design the FDI processor for this application, including determination of all parameter values such as threshold settings, and check it out through simulation.

1d. Prepare and deliver a FORTRAN program which can be compiled and executed on the 175 CYBER system at LaRC to demonstrate real-time FDI on the laboratory experiment system.

RESEARCH TASK 2

Research Task 2 investigates the possible advantages which may accrue from integrating into one information processor the functions of state estimation, sensor and actuator FDI, and parameter mismatch indication.

2a. In the context of space structure control, separate the sensor and actuator FDI problem into two parts: one processor which monitors at least some of the sensors without use of system modeling, and one processor which monitors actuators and perhaps some sensors by a technique which depends on a model of the system dynamics.

2b. Determine whether it would be efficient and convenient to extend the second FDI processor defined in Task 2a to monitor significant deviations in plant parameters from the modeled values.

2c. Determine whether an additional price in computational capacity must be paid to derive an estimate of the system state from this combined processor.

2d. If the results of the above tasks have been favorable to the concept of the integrated processor, summarize the form that such a processor would likely take in a space structure control application and specify the logic which would be used to derive the best estimate of state under nominal and failure conditions.

RESEARCH TASK 3

Research Task 3 studies the problem of efficient reconfiguration of a space structure control system, including its FDI processor, following a component failure.

3a. Inquire into simple methods of reconfiguring the state estimator(s) following a sensor failure. Consider both the case of systems with highly redundant sets of sensors and the case of more sparse sensor sets.

3b. Inquire into simple methods of reconfiguring the controller(s) following an actuator failure in the case of systems utilizing only linear control devices. Consider both the case of systems with highly redundant sets of actuators and the case of more sparse actuator sets.

3c. Inquire into simple methods of reconfiguring the controller(s) following an actuator failure in the case of systems utilizing on-off jets. Consider both the case of systems with highly redundant sets of jets and the case of a more sparse complement of jets.

3d. Inquire into simple methods of reconfiguring the FDI processor following a sensor or actuator failure.

RESEARCH TASK 4

Research Task 4 investigates design techniques for multidimensional systems utilizing on-off control devices.

4a. Determine the nature of optimal trajectories for the problem stated in the Technical discussion in the case of a single-input system.

4b. Define the nature of the cost function $J(\underline{x})$ for the single-input system for initial conditions near the origin and far from the origin. Try to characterize this function on the basis of analytic arguments and check the results with computed optimal trajectories.

4c. Synthesize the controller which minimizes the Hamiltonian function with the costate variable identified with the gradient of an approximate cost function. Compare the performance of the resulting feedback control system with optimal performance.

4d. Attempt to generalize the above steps to multidimensional systems with an arbitrary number of on-off actuators.

BLANK PAGE

HARDWARE DEMONSTRATION

OF

FLEXIBLE BEAM CONTROL

David B. Schaechter

NASA Jet Propulsion Laboratory

Pasadena, California

Workshop on the Structural Dynamics and Control
of Large Space Structures

October 30-31, 1980

INTRODUCTION

The Jet Propulsion Laboratory flexible beam facility was designed to be sufficiently general to demonstrate a variety of flexible body control concepts. Some of these concepts include static shape control, vibration control, multi-input/multi-output control, noncolocated sensors and actuators, adaptive control, and distributed control. The facility consists of a 3.8-m by 15.2-cm by 0.08-cm (12½-ft by 6-in by 1/32-in) pinned-free flexible stainless-steel beam hanging in the Earth's gravity. Four eddy-current position sensors and three brushless dc motors provide position information and force capability. A 6502 microprocessor with developed software completes the control loop through twelve bit D/A and A/D interfaces.

- DEMONSTRATE LSS CONTROL IDEAS
- DEVELOP FACILITY WITH GENERAL APPLICABILITY
- STUDY HARDWARE LIMITATIONS

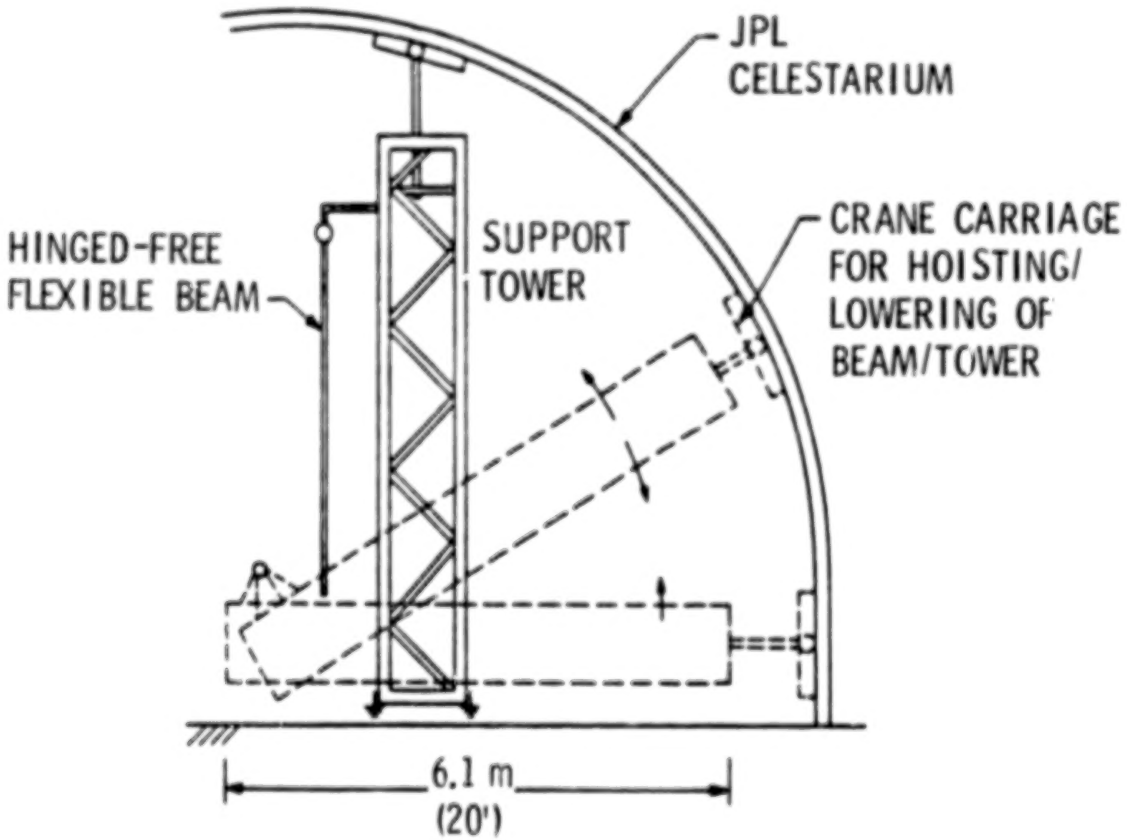

Figure 1

BEAM DYNAMICS - STRING OR ELASTIC BEAM?

The hanging beam is in tension due to gravity, and because of the very small bending stiffness, low-frequency modes appear string-like, while the higher frequency modes appear beam-like. Dynamic mode shapes are computed using string or beam partial differential equations of motion, and the results are then combined to produce accurate system mode frequencies.

$$\ddot{y} + g\,\frac{\partial}{\partial x}\left(x\,\frac{\partial y}{\partial x}\right) = 0 \qquad\qquad \rho\ddot{y} + EI\,\frac{\partial^4 y}{\partial x^4} = 0$$

$y(0) = 0$

$y(L) = \text{FINITE}$

$y(0) = 0$

$y''(0) = 0$

$y''(L) = 0$

$y'''(L) = 0$

SHAPE	BESSEL FUNCTIONS	HYPERBOLIC FUNCTIONS
FREQUENCY	$\omega^2 = \frac{g}{2L}(k-1/4)^2\pi^2$	$\omega^2 = \frac{EI}{\rho L^4}\left[(4k+1)\frac{\pi}{4}\right]^4$ $\quad k = 0, 1, \ldots$

Figure 2

MODES

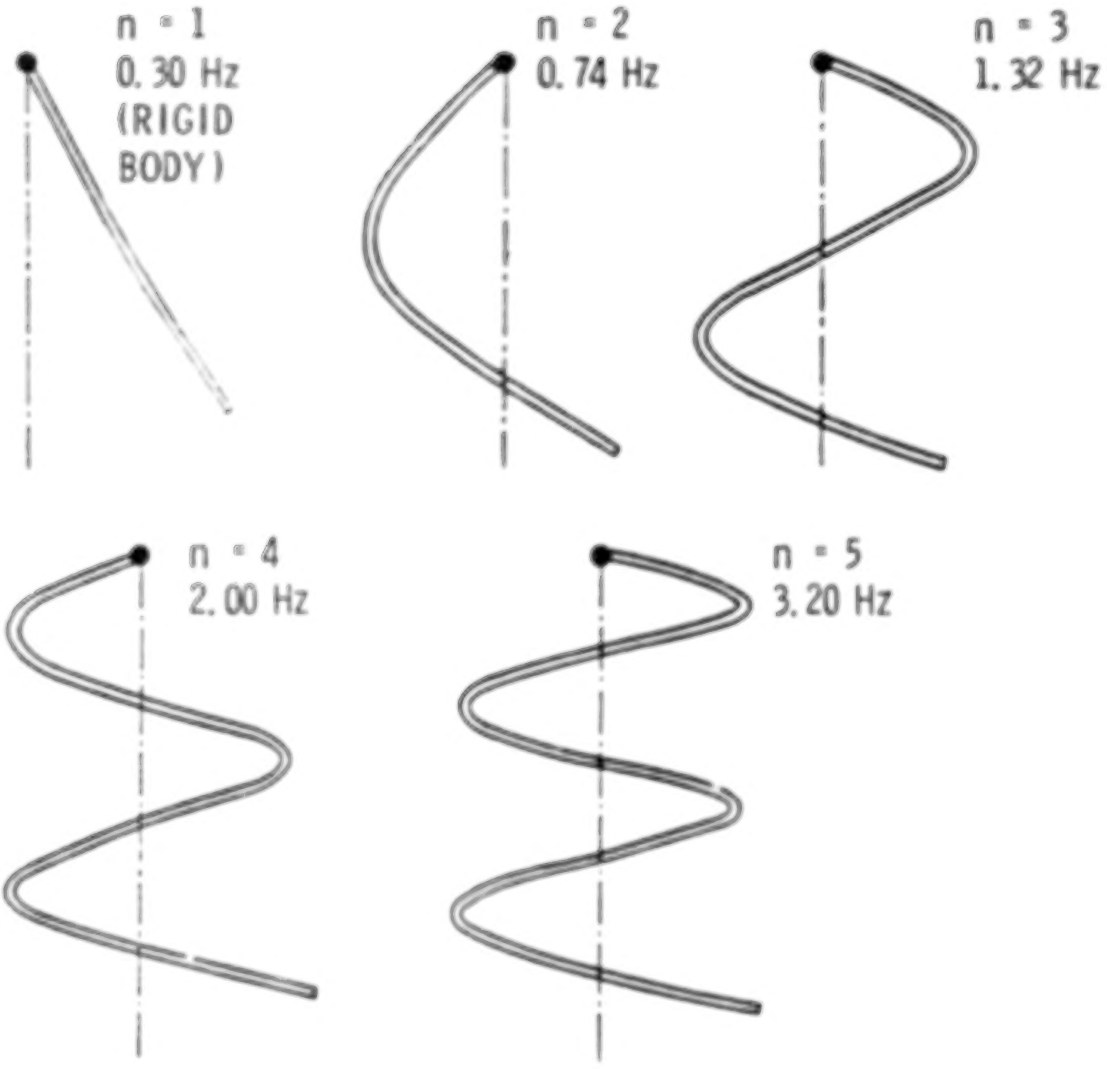

Figure 3

SYSTEM NONLINEARITIES

The effects of all major system nonlinearities are analyzed using an open-loop perturbation analysis to determine the frequency shift or damping ratio shift due to the perturbing force. The largest effect is due to aerodynamic drag with the result being the addition of 1% of critical damping. The remaining list of nonlinearities were constrained to have a negligible impact on the beam dynamics from the beginning of the design process using the perturbation analysis to predict the resulting magnitudes of the various nonlinearities.

- AERODYNAMIC DRAG — $\epsilon\, \dot{q}\,|\dot{q}|$
- FINITE TRANSDUCER SIZE — $\int y(x)\, dx$
- ANGLE DEPENDENT TORQUE — $T = T_c\,(1 - \epsilon q)$
- NON LINEAR TORQUE — $T = \epsilon \theta^3$
- NON LINEAR DAMPING — $T = \epsilon \dot{\theta}^3$
- ADDITIONAL MASS/STIFFNESS — $\rho(x)/EI(x)$

OPEN-LOOP PERTURBATION ANALYSIS

$$\ddot{q} + \omega^2 q = \epsilon\, f(q, \dot{q})$$

Figure 4

For the initial studies into the problem of vibration control, optimal control theory was used to produce estimators and control laws. All results were obtained using discrete time design techniques.

LINEAR QUADRATIC ESTIMATOR AND REGULATOR

$$x(k+1) = \Phi\, x(k) + G\, u(k) + \Gamma\, w(k)$$

$$z(k) = H\, x(k) + v(k)$$

CONTROL MIN $\sum x^T Ax + u^T Bu$ s.t. $x(k+1) = \Phi x(k) + Gu(k)$

ESTIMATOR MIN $\sum w^T Q^{-1} w + v^T R^{-1} v$ s.t. $\hat{x}(k+1) = \Phi \hat{x}(k) + Gu(k)$

RESULTS (DOPTSYS) $u = C\,\hat{x}$

$$\hat{x} \leftarrow \Phi \hat{x} + Gu + K(z - H\hat{x})$$

Figure 5

MICROPROCESSOR IMPLEMENTATION

Software for a 6502 microprocessor was developed to implement any linear, time invariant estimator and controller, and was placed into 1K of ROM. 1K of RAM is used to store the particular control system matrices and the scratch space for the ROM software. The software samples the sensor vector, updates the state-vector estimate, and outputs the control vector. The loop time is dependent on the dimensions of these vectors with a six-state controller using 1 sensor and 1 actuator requiring 50 msec per update. Twelve-bit resolution is retained in the D/A and A/D processes, while sixteen bits are used for internal computation. Fixed-point double-precision arithmetic is performed entirely in software.

$$u = C\hat{x}$$

$$\hat{x} \leftarrow \Phi\hat{x} + Kz \qquad \Phi = \Phi' + GC - KH$$

CONTROLLER FLOWCHART

BITS			
12	SAMPLE SENSORS	p	A-D's
16	FORM Kz	nxp	x
16	FORM $\Phi\hat{x}$	nxn	x
16	FORM $\Phi\hat{x} + Kz$	n	+
16	FORM $u = C\hat{x}$	nxm	x
12	OUTPUT u	m	D-A's

- FIXED POINT MULTIPLY
- MATRIX MULTIPLY
- D-A HARDWARE
- A-D SOFTWARE
- LOOP TIME T FROM OPERATION COUNT

Figure 4

CONTENTS

PREFACE	iii	1/A4
1. LANGLEY RESEARCH CENTER FLEXIBLE BEAM EXPERIMENT Raymond C. Montgomery	1	1/A8
2. STRUCTURAL DYNAMICS RESEARCH IN ACTUATOR/SENSOR LOCATIONS G. C. Horner	5	1/A12
3. REDUCED ORDER ADAPTIVE REGULATION STRATEGIES FOR THE NASA BEAM CONTROL EXPERIMENT C. Richard Johnson, Jr.	13	1/B6
4. DYNAMICS AND CONTROL OF COUPLED RIGID/FLEXIBLE BODIES Elias G. Abu-Saba	21	1/B14
5. ADJUSTED FEEDBACK CONTROL FOR INCOMPLETE DECOUPLING PROCEDURES Harold A. Hamer	27	1/C6
6. INVESTIGATIONS OF ALGORITHMS FOR LARGE SPACE STRUCTURES E. D. Denman	47	1/D12
7. IDENTIFICATION AND CONTROL FOR FLEXIBLE VEHICLES Christopher S. Greene	57	1/E8
8. RELIABILITY ISSUES IN ACTIVE CONTROL OF FLEXIBLE SPACE STRUCTURES W. E. VanderVelde	73	1/F10
9. HARDWARE DEMONSTRATION OF FLEXIBLE BEAM CONTROL David B. Schaechter	85	1/G8
10. THE ADAPTIVE/LEARNING CONTROL SYSTEM APPROACH Frederick E. Thau	93	2/A4
11. SOME EARLY EXPERIMENTS WITH NONCOLOCATED CONTROLS OF FLEXIBLE SYSTEMS R. H. Cannon, Jr.	101	2/A12
12. REVIEW OF AD HOC COMMITTEE REPORT ON TECHNOLOGY OF LARGE SPACE STRUCTURES H. Ashley	107	2/B4
13. ATTITUDE CONTROL OF A FLEXIBLE TRIANGULAR TRUSS IN SPACE Bong Wie and Arthur E. Bryson, Jr.	113	2/B10
14. LARGE MOTIONS OF DEFORMABLE SPACECRAFT T. R. Kane	127	2/C10
ATTENDEES	133	2/D2

BLANK

PAGE

RESULTS

These preliminary results show the free end response of the beam to various inputs. The open-loop initial condition (IC) and impulse responses are shown. Next, low-gain closed-loop responses to both of the above inputs are shown. The controller in this case consists of a single-position sensor and a single-force actuator at the free end. Using a six-state controller, about 40 percent of critical damping is achieved. The small residual is at the frequency of the first unmodeled mode. By decreasing the cost of control in order to obtain improved performance, the first unmodeled mode is destabilized.

Shape control, distributed control, and refining of the parameters describing the beam facility are all activities planned for the future.

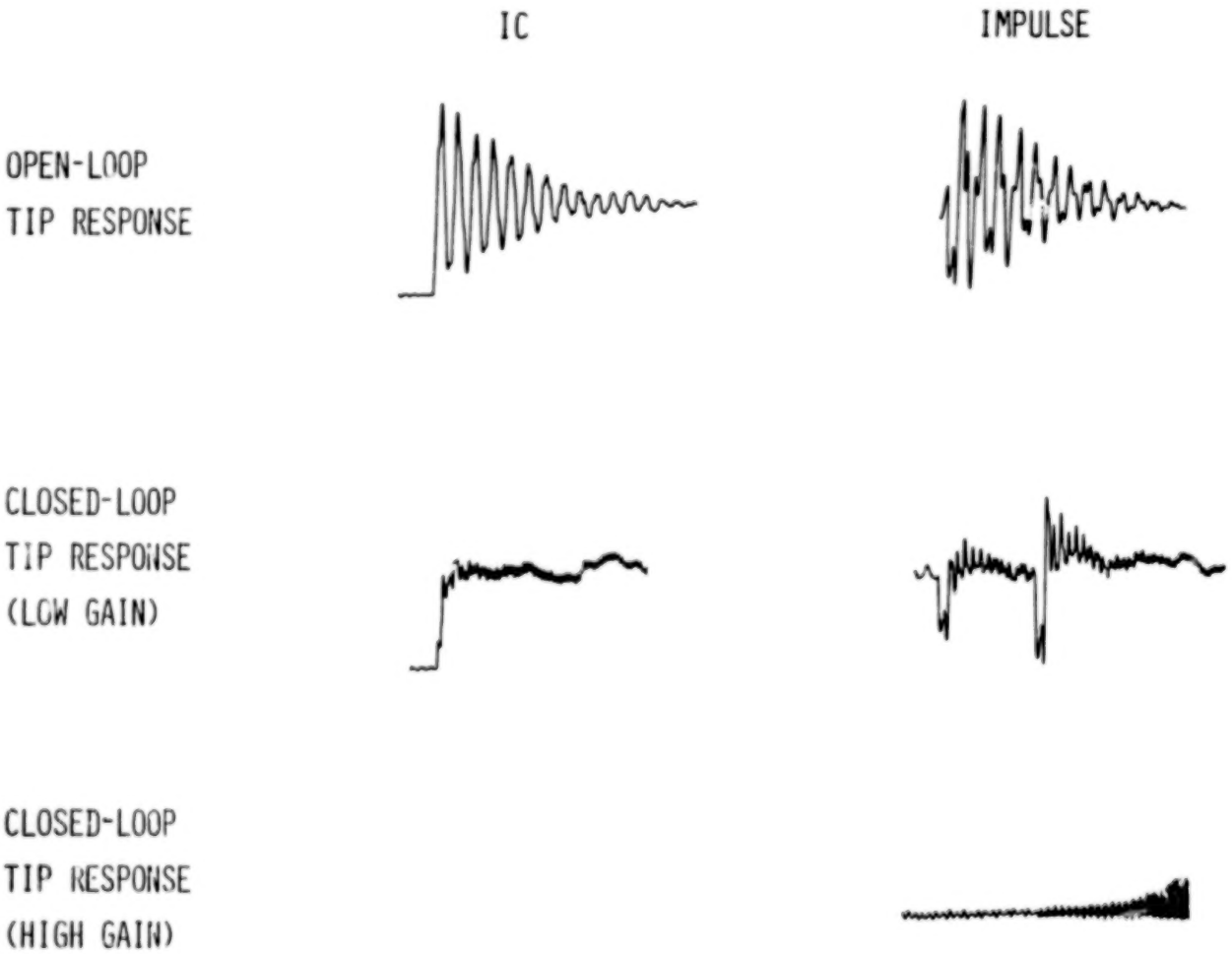

Figure 7

THE ADAPTIVE/LEARNING CONTROL SYSTEM APPROACH

Frederick E. Thau
City University of New York
New York, New York

Workshop on the Structural Dynamics and Control
of Large Space Structures
October 30-31, 1980

BASIC ELEMENTS

Parameter Identification Subsystem -

Provides "local" estimate of system model parameters at a specific operating condition.

Techniques that have been used:

Newton-Raphson parameter identification
Output-error parameter identification

Parameter Extrapolation (Learning) and Memory Subsystem -

Provides "local" extrapolation of system parameters as a function of measured configuration variables.

Technique that has been used:

Least-squares fit of functional model relating model parameters to configuration variables.

Controller -

Uses functional model stored in Memory Subsystem to generate control forces.

PARAMETER ADAPTIVE CONTROL SYSTEM

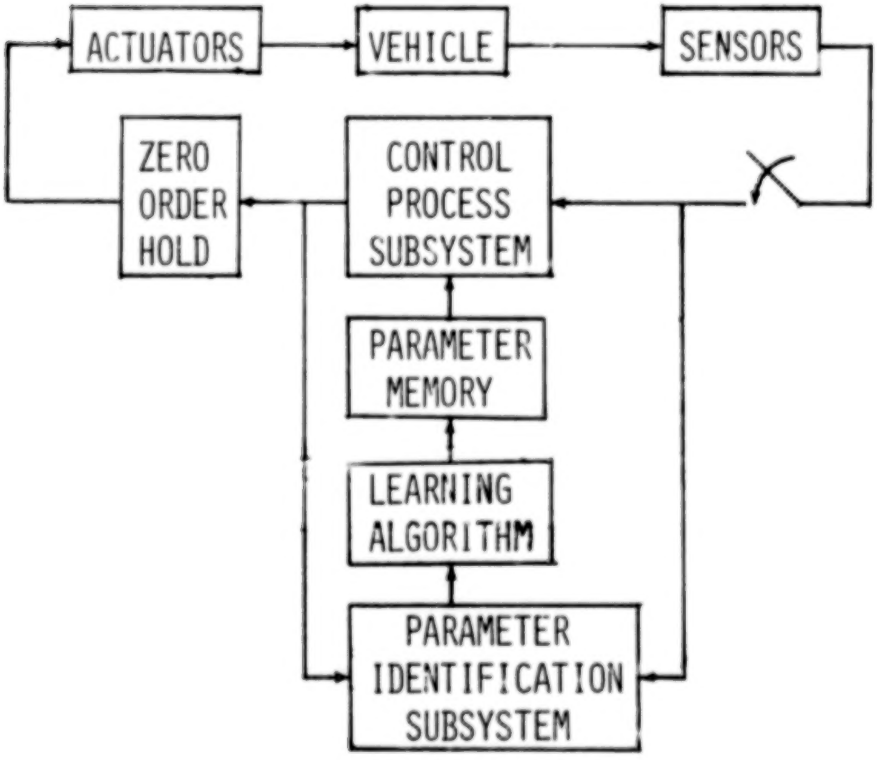

Figure 1

APPLICATION OF ADAPTIVE/LEARNING

APPROACH TO DISTRIBUTED SYSTEMS

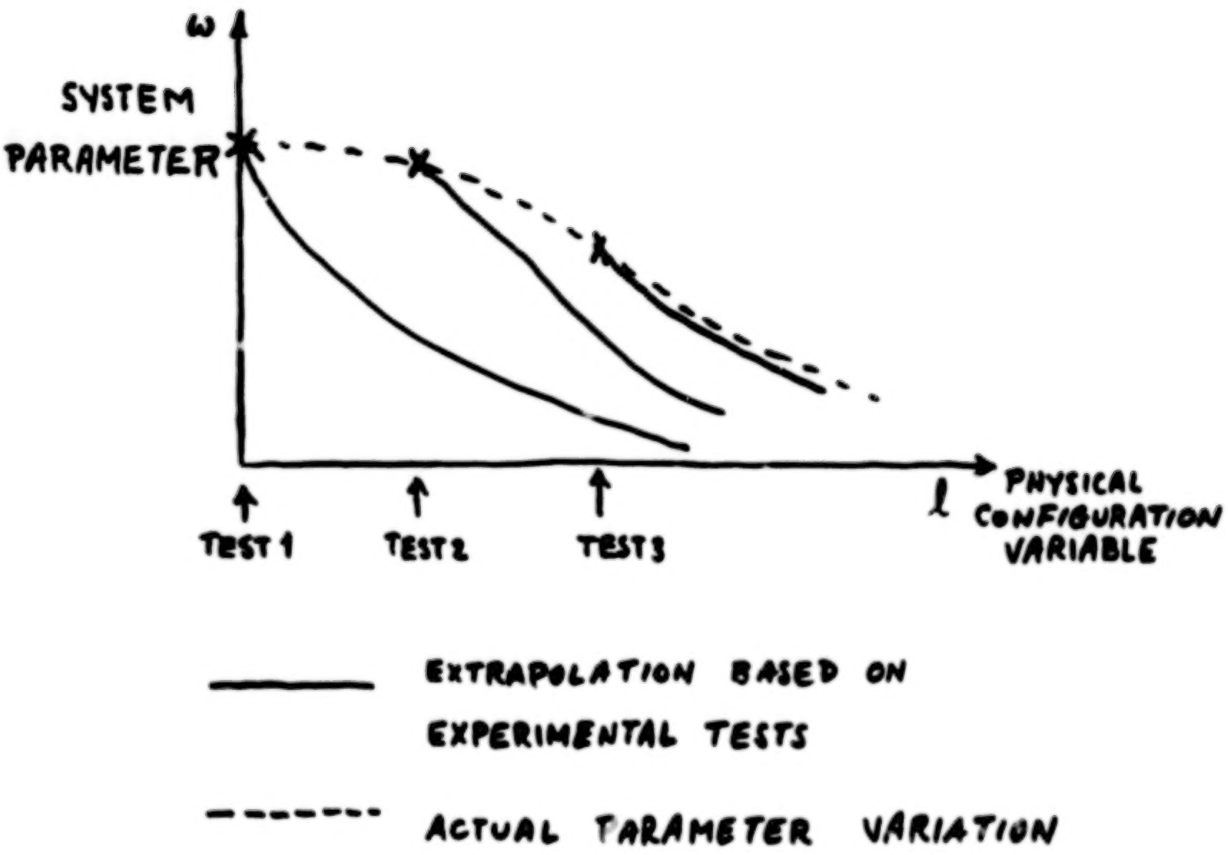

Figure 2

FEATURES OF ADAPTIVE/LEARNING APPROACH

- Approach combines advantages of a priori modeling and gain scheduling with those of on-line identification and adaptive gain computation.
- Convergence criteria may be used to monitor performance of parameter-identification and parameter-extrapolation subsystems.

APPLICATION OF ADAPTIVE/LEARNING CONTROL TO DISTRIBUTED SYSTEMS - PARAMETER IDENTIFICATION

Response Representation -

$$y(x,t,\ell) = \sum_{i=1}^{NM} \xi_i(x,\ell) w_i(t,p_i(\ell))$$

ξ_i - spatial approximation function

w_i - modal amplitude approximation

p_i - parameter vector in difference equation model for the evolution of w_i

ℓ - configuration variable

Model Parameter Identification -

Adjust p_i to obtain best fit of model data to sensor data.

$$w_i(k) = A_{1i} w_i(k-1) + A_{2i} w_i(k-2) + B_{1i} F_i(k-1) + B_{2i} F_i(k-2)$$

$$p_i = \left[A_{1i}, A_{2i}, B_{1i}, B_{2i}\right]$$

F_i - force command input

Approximation Function Tuning -

$$\xi_i(x,\ell) = \sum_{k=1}^{NB} C_{ik} \sigma_{ik}(x,\ell)$$

$\sigma_{ik}(x,\ell)$ - a set of basis functions

C_{ik} - response model spatial function tuning coefficients

STRUCTURE OF CURRENT IDENTIFICATION PROGRAM

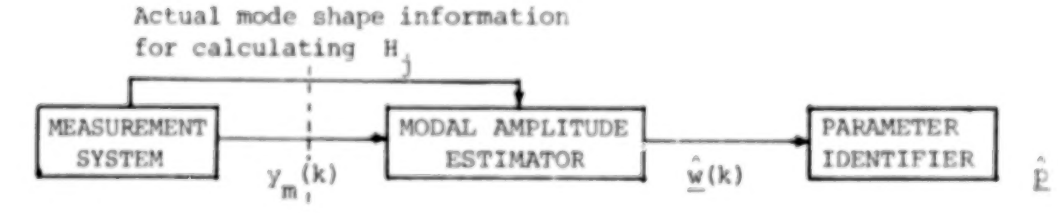

$$y_m(k) = \sum_{j=1}^{NS} H_j w_j(k) + v(k)$$

$\hat{\underline{w}}(k)$ - vector of modal amplitude estimates

$\hat{\underline{p}}$ - vector of model parameters

$y_m(k)$ - vector of displacement measurements

$v(k)$ - error vector

H_j - matrix related to assumed spatial functions ξ

SIMULATION STUDIES OF FLEXIBLE BEAM UNFORCED RESPONSE - SPATIAL VARIABLE PLOTS

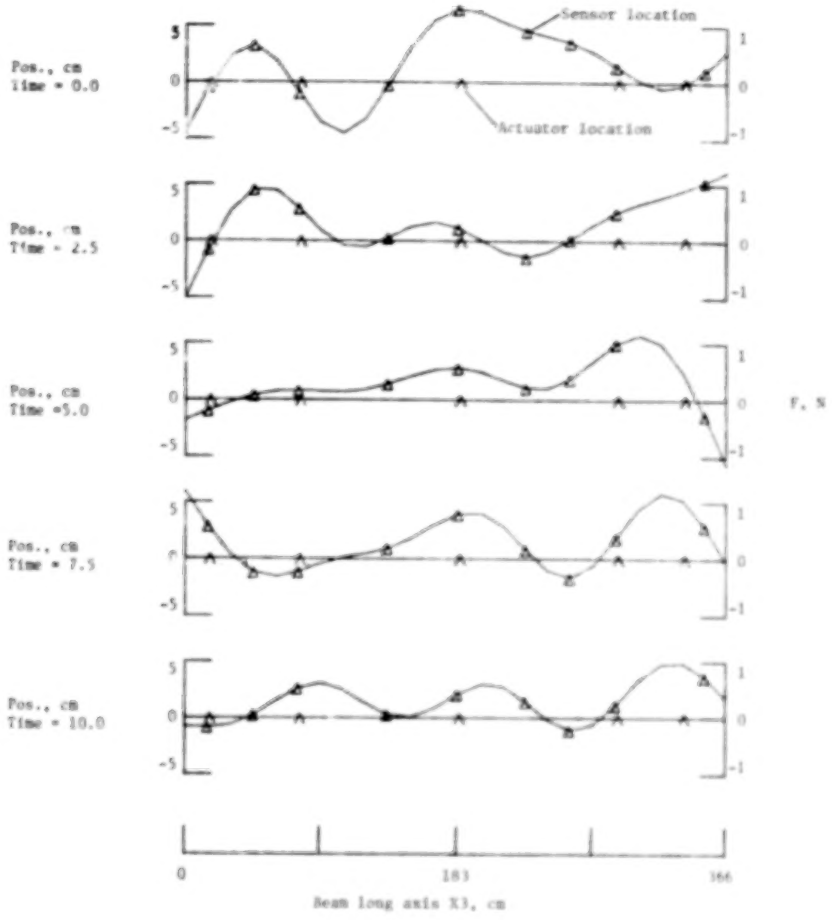

Figure 3

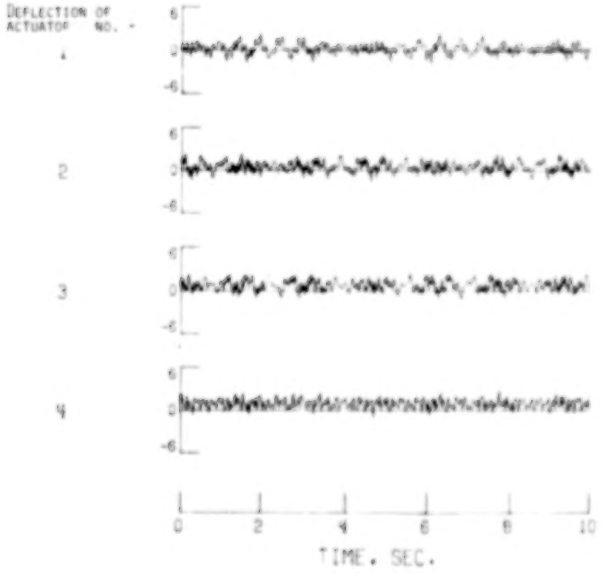

Figure 4

TIME HISTORY PLOTS, MODE 3

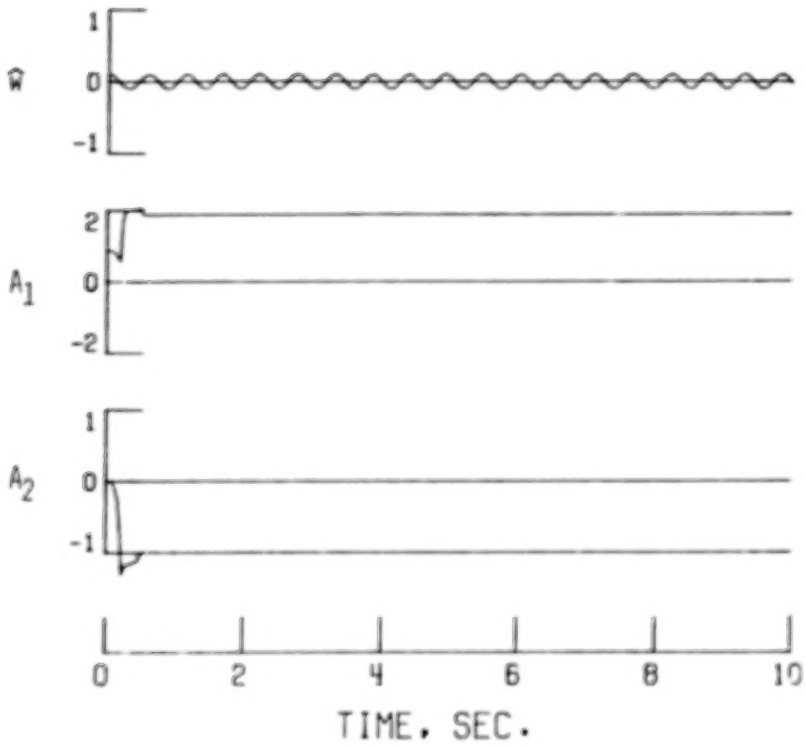

Figure 5

TIME HISTORY PLOTS, MODE 5

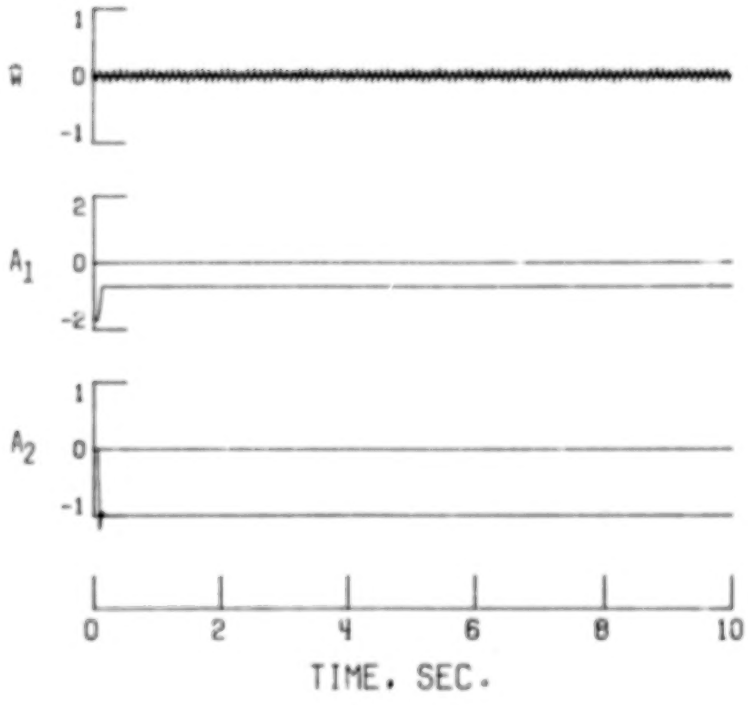

Figure 6

PROPOSED BEAM-EXPERIMENT EXTENSION TO TEST - VARIABLE-CONFIGURATION STRUCTURE

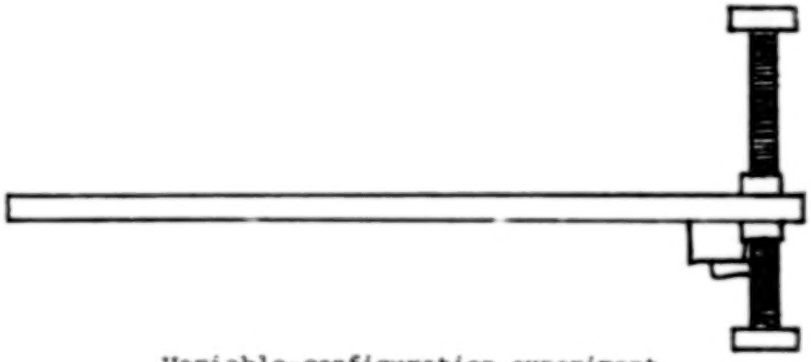

Variable-configuration experiment

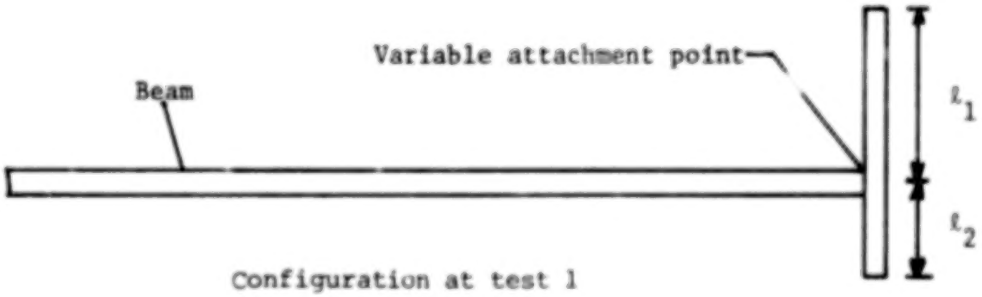

Configuration at test 1

Configuration at test 2

Figure 7

PROBLEMS FOR INVESTIGATION

1. Development of function tuning algorithm.

2. Development of test-initiation algorithm.

3. Evaluation of state-estimation and parameter-identification algorithms.

4. Development of variable-configuration experiment.

5. Performance evaluation of closed-loop adaptive/learning control system.

BIBLIOGRAPHY

1. Mekel, R. et al.: An Adaptive Learning Control System for Aircraft. 8th Asilomar Conference on Circuits, Systems, and Computers, Dec. 1974.

2. Dunn, H. J.; and Montgomery, R. C.: A Moving Window Parameter Adaptive Control System for the F8-DFBW Aircraft. IEEE Trans. on A. C., vol. AC-22, no. 5, Oct. 1977.

3. Montgomery, R. C. et al.: A Learning Flight Control for the F-8 DFBW Aircraft. AIAA Guidance and Control Conference, 1978.

4. Hall, K. R.: A Learning Control System Extension to the Modal Control of Large Flexible Rotating Spacecraft. AIAA Guidance and Control Conference, 1978.

5. Montgomery, R. C.; and Thau, F. E.: Adaptive and Learning Control of Large Space Structures. 1980 JACC and 1980 AIAA Guidance and Control Conference.

SOME EARLY EXPERIMENTS WITH NONCOLOCATED CONTROLS OF FLEXIBLE SYSTEMS

R. H. Cannon, Jr.
Stanford University
Stanford, CA

Workshop on the Structural Dynamics and Control
of Large Space Structures
October 30-31, 1980

OBJECTIVES FOR EXPERIMENTAL FACILITY

1. Very low structural damping, $\zeta < 0.001$
2. Noncolocated sensors/actuators
3. Changing (and uncertain) inertias

SKETCH OF TORQUER/ENCODER MECHANISM

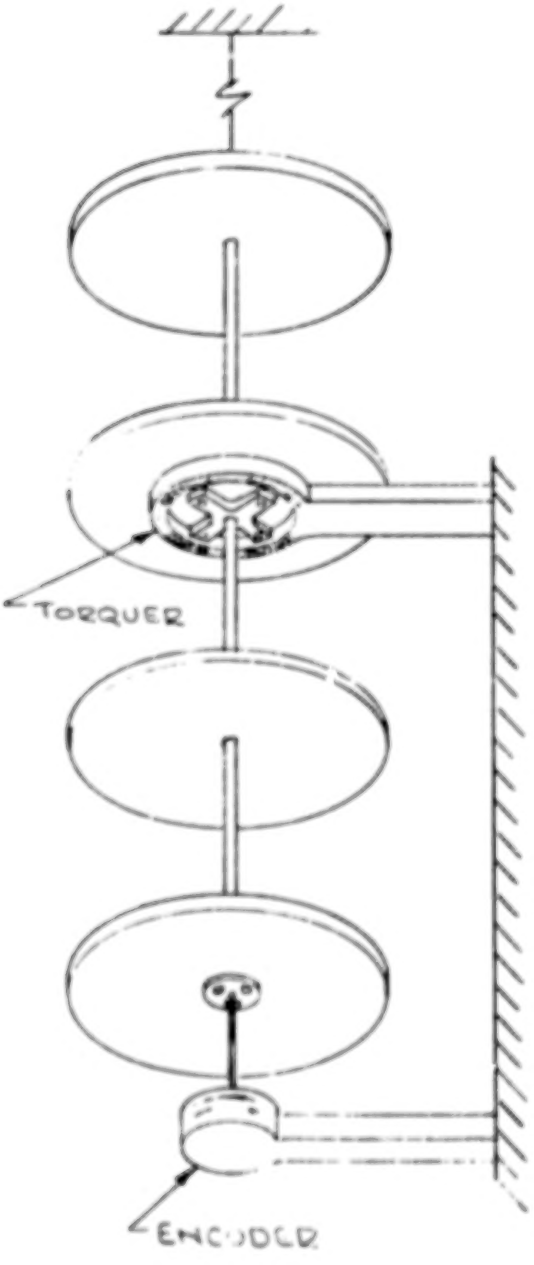

Figure 1

TRANSFER FUNCTIONS $\frac{\theta}{M}$

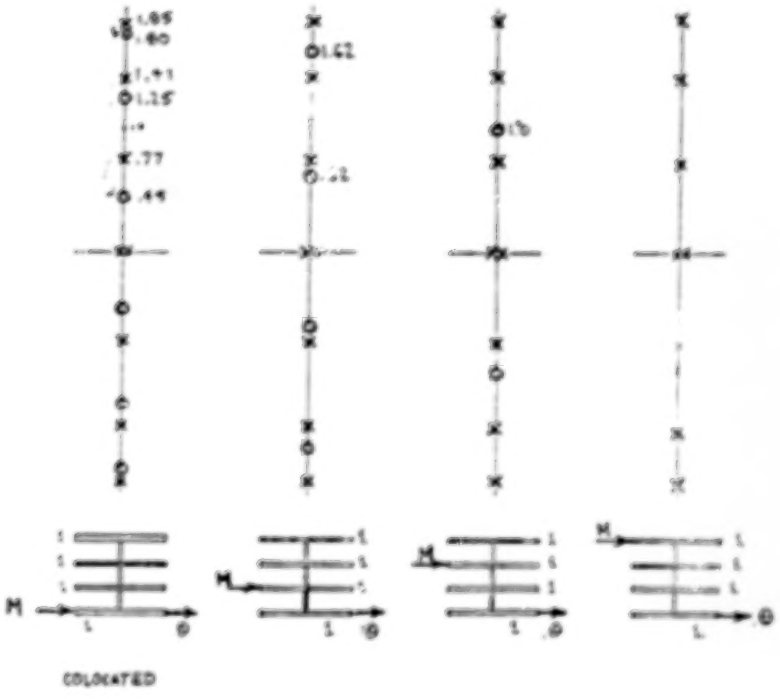

Figure 2

"ZERO FLIPPING"

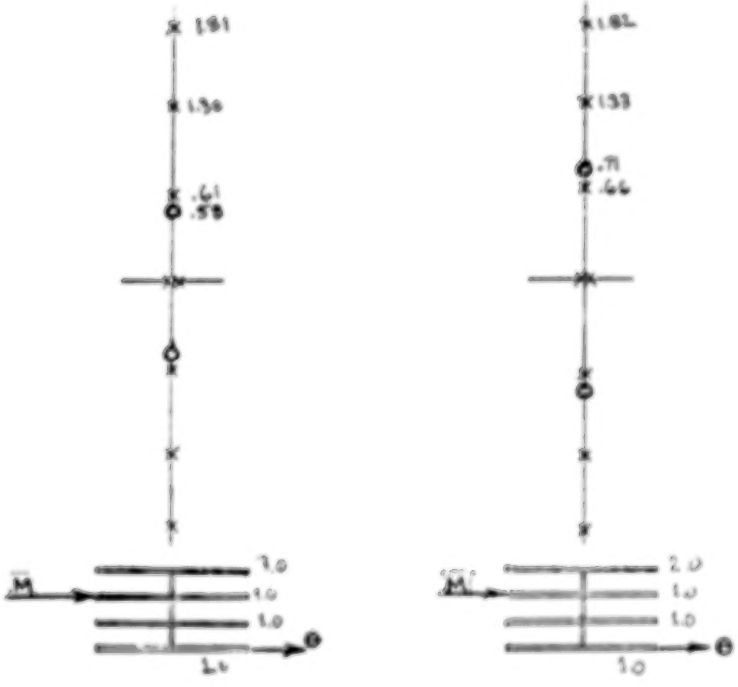

Figure 3

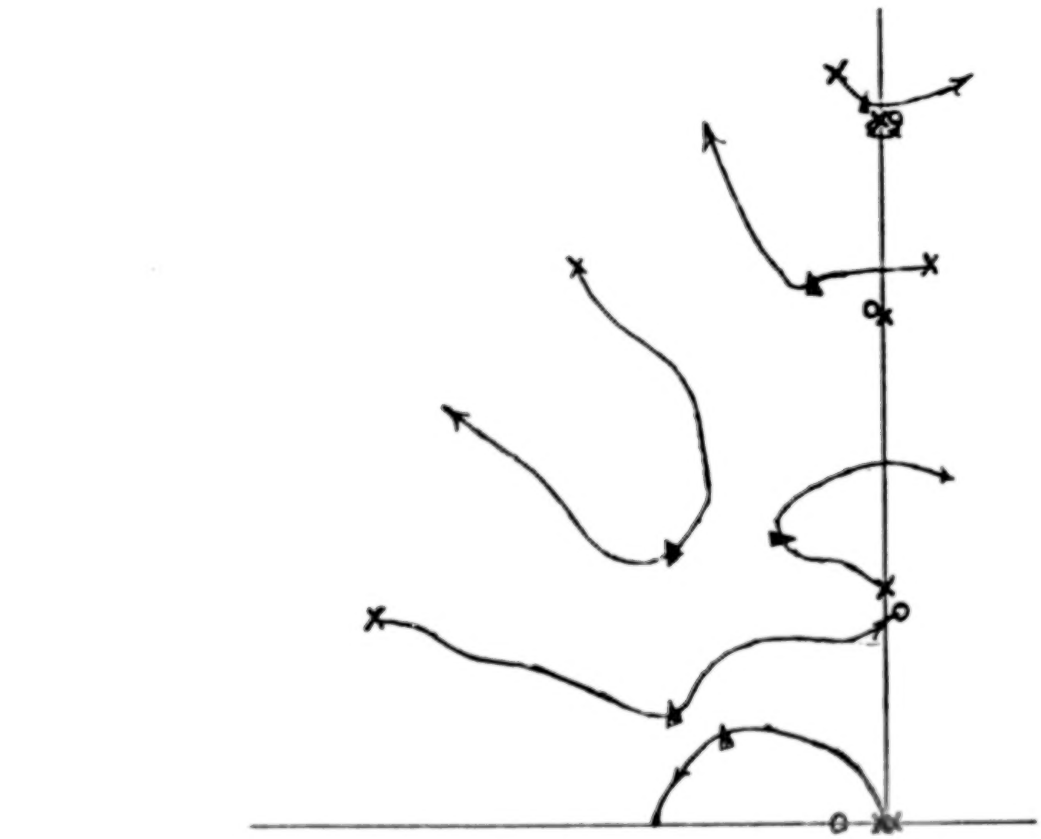

PLANT

$$\frac{\theta}{M} = \frac{1}{s^2(s^2 + 3.287)(s^2 + 1.69)(s^2 + .361)}$$

COMPENSATOR

$$\frac{M}{\theta} = \frac{16.083(s^2 + .0389s + 1.729)(s^2 - .0126s + 3.285)(s^2 + .0674s + .2919)(s + .1186)}{(s^2 + .2397s + 3.7166)(s^2 - .2470s + 2.0416)(s^2 + 1.6966s + 2.9345)(s^2 + 2.8478s + 2.3227)}$$

Figure 4

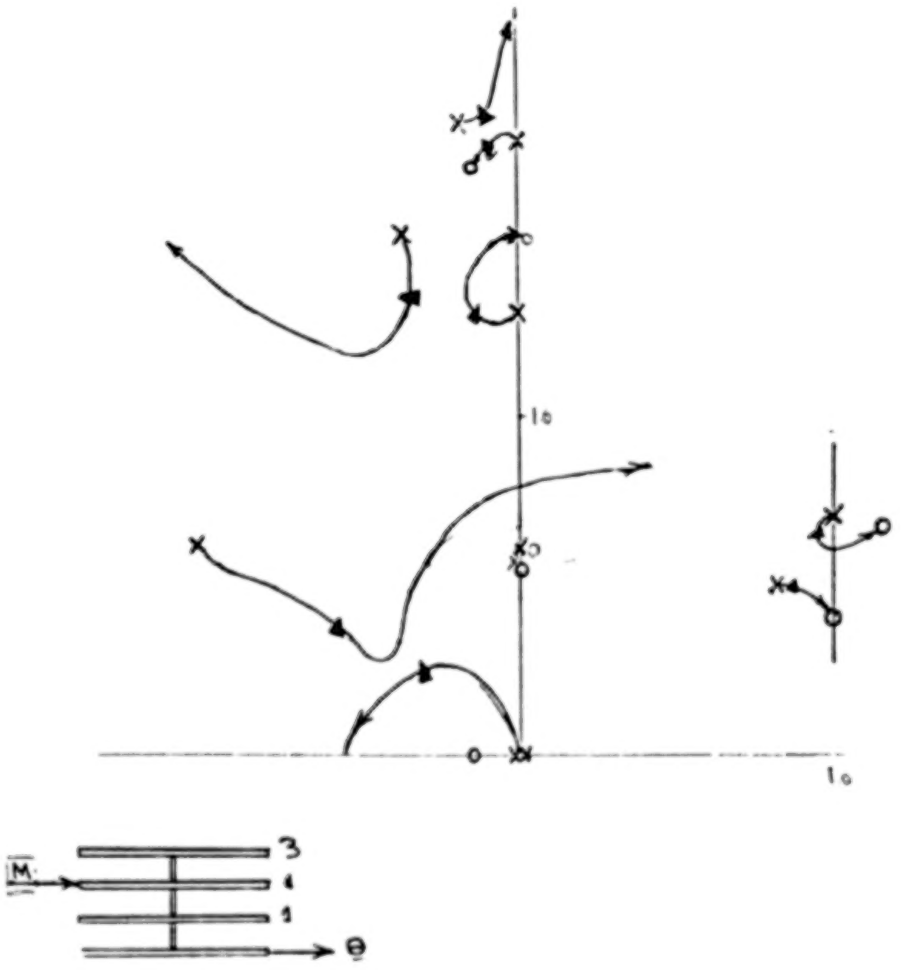

PLANT

$$\frac{\theta}{M} = \frac{(s^2 + 1/3)}{s^2(s^2 + 3.287)(s^2 + 1.69)(s^2 + .361)}$$

COMPENSATOR

$$\frac{M}{\theta} = \frac{(2.8744)(s^2 + .303s + 3.018)(s^2 - .0496s + 2.297)(s^2 - .01453s + .35719)(s + .148)}{(s^2 + .345s + 3.460)(s^2 + .724s + 2.468)(s^2 + .006s + .334)(s^2 + 1.989s + 1.369)}$$

Figure 5

BLANK PAGE

REVIEW OF AD HOC COMMITTEE REPORT

ON TECHNOLOGY OF LARGE SPACE STRUCTURES

H. Ashley
Stanford University
Stanford, CA

Workshop on the Structural Dynamics and Control
of Large Space Structures
October 30-31, 1980

STATEMENT OF TASK

At NASA's request, the Aeronautics and Space Engineering Board established an ad hoc committee to address the following tasks:

1. Evaluate and provide comments and recomendations on the objectives, approach, content, and technical balance of NASA's Large Space Systems Technology Program plan.

2. Review and recommend means to assure an effective exchange of information on technological developments in the area of large space systems between and among NASA, its contractors, and user industries and agencies.

NASA MISSIONS INVOLVING LARGE SPACE SYSTEMS

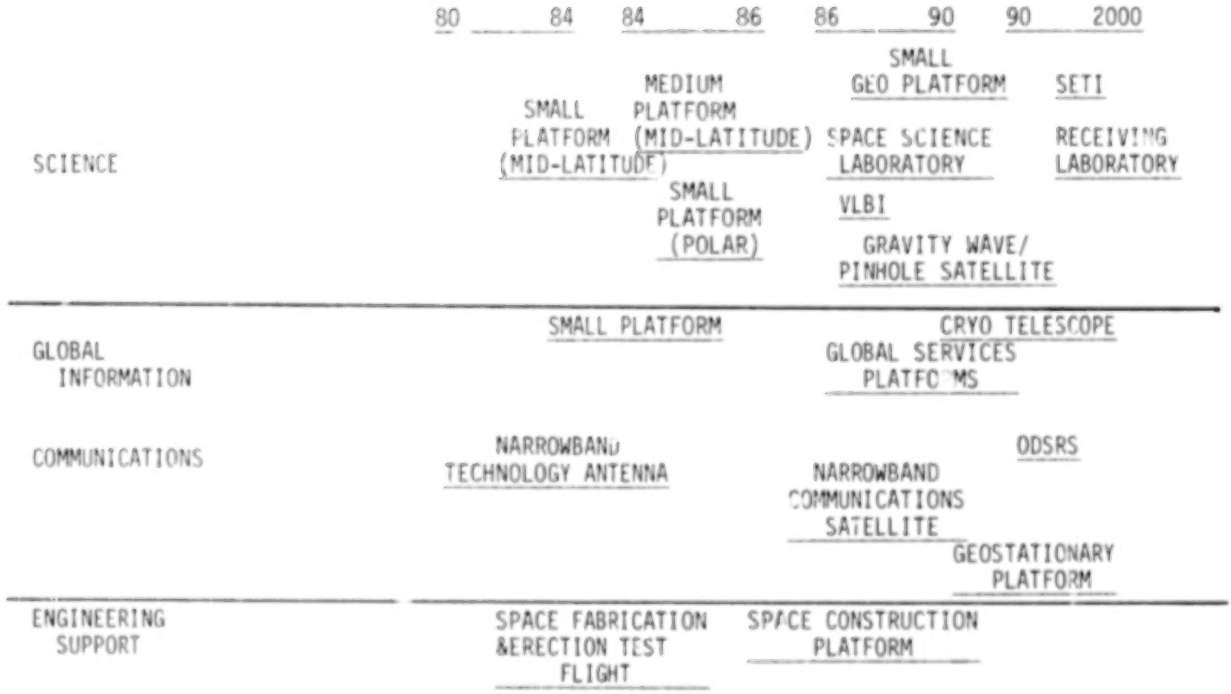

Figure 1

TRIANGULAR STRONGBACK-MEDIUM PLATFORM

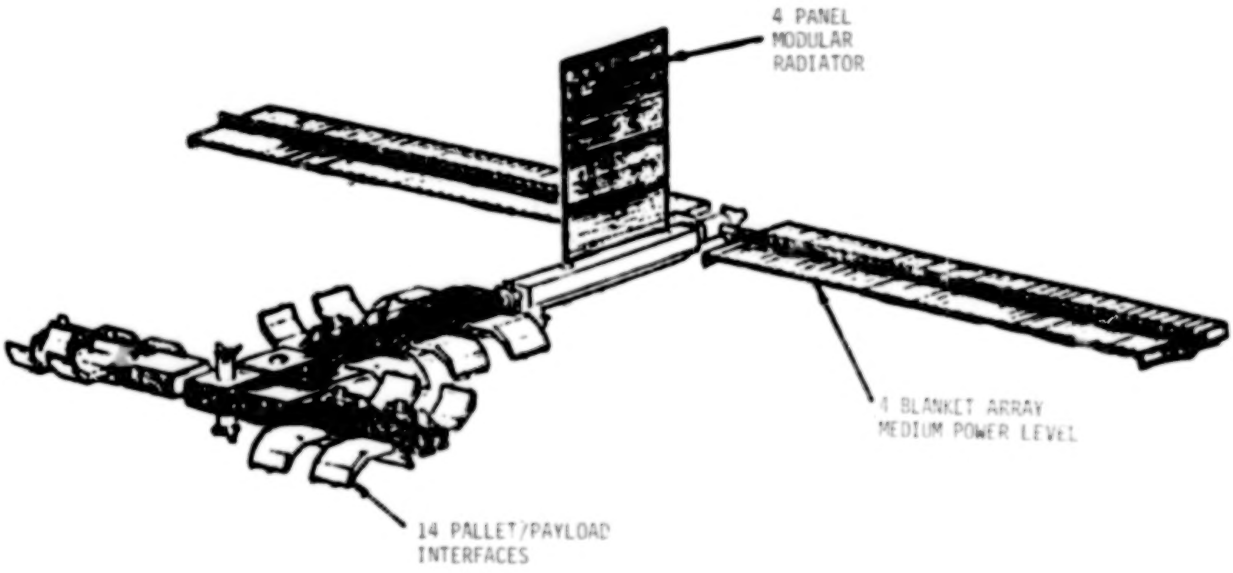

Figure 2

MEASUREMENT OF SURFACE FIGURE, LARGE DEPLOYABLE MESH ANTENNA

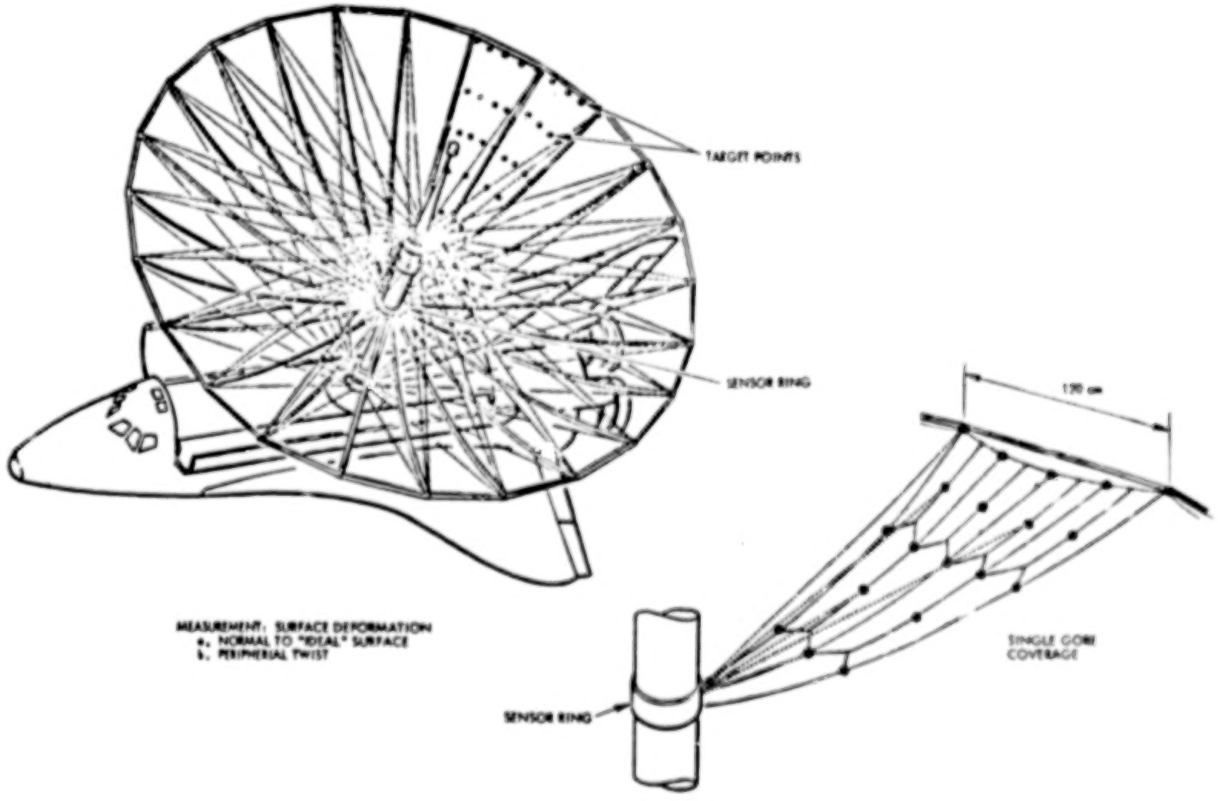

Figure 3

GENERAL CONCLUSIONS AND RECOMENDATIONS

1. LSS missions furnish solid justification for continuation of LSST program. "Current Plan" inadequate for fulfilment of needs during next 5 years.

2. LSS program should be integrated, with designated Headquarters offices as overall director.

3. Prioritization of mission model essential to focus the technology program.

4. Flight experiments during next 5 years essential to focus TLSS program.

5. "Roadmaps" needed for technological development:
   a) Total system and
   b) Local for each technology discipline.

6. Study sensitivity of system performance to relaxed requirements on technology.

7. Large platform with several experiments a particularly imaginative concept; further study needed. Can products of different users be combi:

8. Man at GEO needs to be vigorously examined. Committee not convinced benefits will outweigh costs.

9. Transfer of technology and coordination of work with other agencies (notably DOD) quite adequate and improving.

TECHNOLOGICAL CONCLUSIONS AND RECOMMENDATIONS

1. Reinforce certain areas in TLSS 5-year plan:
   a) Figure determination and control
   b) EM interference
   c) Automated vs. manual assembly
   d) Docking
   e) Rel., repair, and maintain

2. Comparative evaluation of altrnatives required.

3. Definition of orbital transfer vehicles lacking. Electric propulsion should be pursued, but capability in chemical should be preserved.

4. LSST plan tends to emphasize structures more than certain other vital areas.

5. JPL study of ODSRS should be evaluated; considered a rather unlikely candidate.

6. SEP has a significant role for orbital transfer, station-keeping, and planetary missions.

7. More attention needed to locations and systems for data processing. Needs a significant start.

8. Traffic models must be better developed to define future COMSATS.

9. Efforts applauded on low-cost ground stations. Success key is a large market.

10. Current program reasonable relative to large-platform COMSATS at GEO.

11. In structures and materials, emphasize optimization, loads determination, dynamics, damping, integrated design, and special materials for space.

12. Activity on deployment, assembly, and fabrication is effective. Time for evaluation of alternative approaches.

13. Technology of active figure sensing and control needs greater attention.

14. LSS human factors program endorsed, but specific line item should be added within LSST budget.

Figure 4

PINHOLE SATELLITE SYSTEM

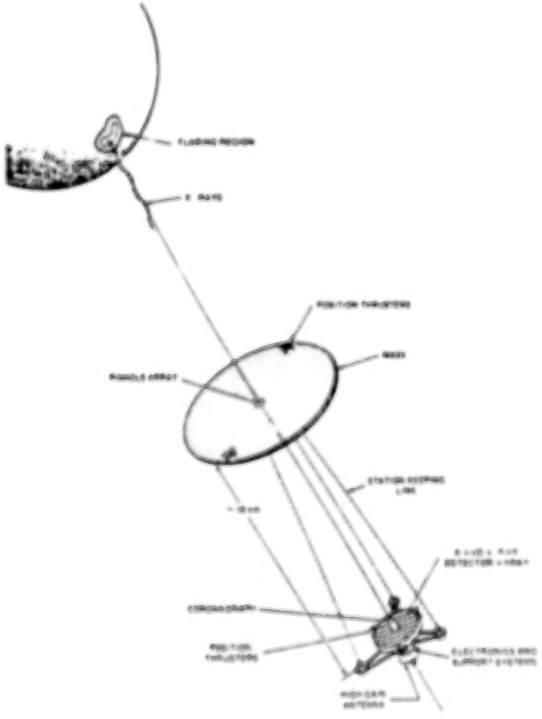

Figure 5

ATTITUDE CONTROL OF A FLEXIBLE TRIANGULAR TRUSS IN SPACE

Bong Wie and Arthur E. Bryson, Jr.
Department of Aeronautics and Astronautics
Stanford University
Stanford, CA

Workshop on the Structural Dynamics and Control
of Large Space Structures
October 30-31, 1980

OBJECTIVES

- Generic model of a planar space structure having infinite number degrees of freedom (DOF): 3 identical, simple beams joined with ball-socket connectors.
- Demonstrate roll, pitch, and yaw attitude stabilization using angle sensors and torquers at the midpoints of all 3 beams.
- Find exact transcendental transfer functions from torques to angles producing exact poles and zeros.
- Many identical natural frequencies in roll and pitch cause no control problems.
- Compare closed-loop predictions of truncated models to infinite DOF model.
- Compare finite-element approximate models with exact infinite-element model.

EXAMPLE TRIANGULAR TRUSS

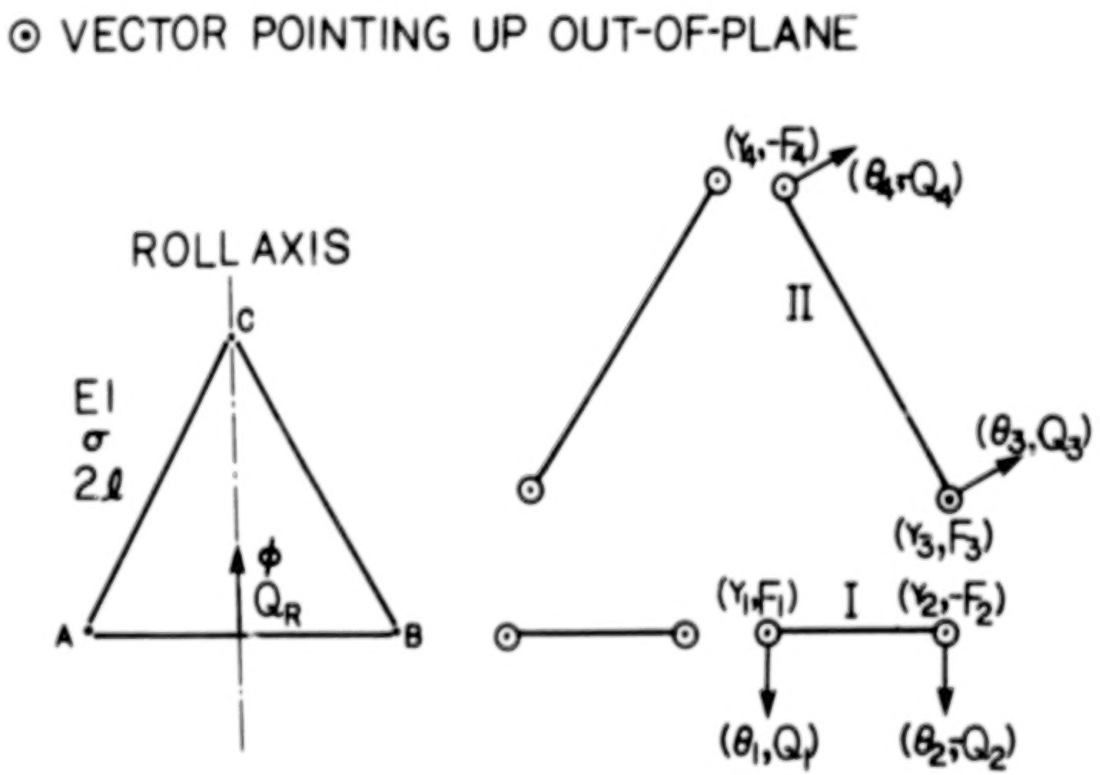

FIGURE 1. EQUILATERAL TRIANGULAR TRUSS WITH ROLL CONTROL TORQUE Q_R

NOMENCLATURE AND UNITS

σ = mass/unit length of beams

EI = bending stiffness of beams

2ℓ = length of beams

y = out-of-plane displacement

θ = out-of-plane slope

Q = in-place bending moment

F = out-of-plane shear force

$$\lambda^4 = \frac{\sigma \ell^4}{EI} s^2$$

s = Laplace transform variable

$$x = \left[y, \frac{\theta}{\lambda}, \frac{-Q}{\lambda^2}, \frac{F}{\lambda^3} \right]^T$$

Quantity	y	θ	Q	F
Units	ℓ	–	$\frac{EI}{\ell}$	$\frac{EI}{\ell^2}$

TRANSFER MATRICES

From partial differential equation of simple, we can obtain $T(\lambda)$ such that:

8 eqs.
$$\begin{cases} x_2(\lambda) = T(\lambda) x_1(\lambda) \\ x_4(\lambda) = T(2\lambda) x_3(\lambda) \end{cases}$$

where

$$T(\lambda) \triangleq \begin{bmatrix} T_1 & T_2 & T_3 & T_4 \\ T_4 & T_1 & T_2 & T_3 \\ T_3 & T_4 & T_1 & T_2 \\ T_2 & T_3 & T_4 & T_1 \end{bmatrix}$$

$$\left.\begin{matrix} T_1 \\ T_3 \end{matrix}\right\} = \frac{1}{2}(\cosh \lambda \pm \cos \lambda)$$

$$\left.\begin{matrix} T_2 \\ T_4 \end{matrix}\right\} = \frac{1}{2}(\sinh \lambda \pm \sin \lambda)$$

For roll motion:

8 boundary conditions
$$\begin{cases} 0 = y_1 = y_4 & \text{(antisymmetry)} \\ 0 = Q_2 = Q_3 = Q_4 & \text{(ball-socket joints)} \\ y_2 = y_3 & \text{(compatibility of displacements)} \\ F_2 = F_3 & \text{(transmission of shear force)} \\ Q_1 = -\frac{1}{2} Q_R & \text{(antisymmetry)} \end{cases}$$

Definition $\left\{ \theta_1 \triangleq \phi = \text{Roll angle} \right.$

ROLL TRANSFER FUNCTION

Combining 8 boundary conditions with 8 equations of two transfer matrices gives $\phi(s)/Q_R(s)$:

$$\frac{\varphi(s)}{Q_R(s)} = \frac{EI\lambda^2}{\ell}\frac{N(s)}{D(s)} \qquad \text{(dimensional)}$$

where

$$N(s) = \tfrac{1}{4}(\cosh 2\lambda \sin 2\lambda - \sinh 2\lambda \cos 2\lambda)(\cosh \lambda \sin \lambda - \sinh \lambda \cos \lambda)$$
$$-\tfrac{1}{2} \sinh 2\lambda \sin 2\lambda(1 + \cosh \lambda \cos \lambda)$$

$$D(s) = (\cosh 2\lambda \sin 2\lambda - \sinh 2\lambda \cos 2\lambda)(\sinh \lambda \sin \lambda + \sinh 2\lambda \sin 2\lambda)$$
$$+ \sinh 2\lambda \sin 2\lambda(\cosh \lambda \sin \lambda - \sinh \lambda \cos \lambda)$$

We may now write:

$$\frac{\phi(s)}{Q_R(s)} = \frac{1}{Js^2}\prod_{n=1}^{\infty}\frac{1 + s^2/Z_n^2}{1 + s^2/\omega_n^2} \qquad \text{(dimensional)}$$

where

$J = 2\sigma\ell^3$ = Roll moment inertia of rigid truss

Using a root solver code, we can find exact poles and zeros (ω_n,Z_n) from transcendental transfer function above. First 6 deformation modes and rigid-body mode are shown in figure 2. Zeros are for colocated angle sensor. (Note that poles and zeros alternate !)

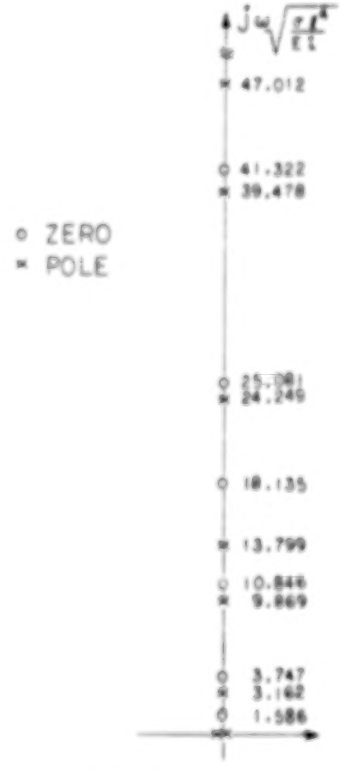

FIGURE 2. POLE-ZERO DISTRIBUTION OF ROLL TRANSFER FUNCTION $\frac{\phi(s)}{Q_R(s)}$

ROLL-MODE SHAPES

From the partial differential equation of the simple beam,

$$y(\eta) = y_1 T_1(\lambda\eta) + \theta_1 T_2(\lambda\eta) - Q_1 T_3(\lambda\eta) + F_1 T_4(\lambda\eta) \qquad \text{(Beam I, } 0 \le \eta \le 1\text{)}$$

$$y(\xi) = -y_4 T_1(\lambda\xi) - \theta_4 T_2(\lambda\xi) + Q_4 T_3(\lambda\xi) - F_4 T_4(\lambda\xi) \qquad \text{(Beam II, } 0 \le \xi \le 1\text{)}$$

For antisymmetric roll motion, $y_1 = y_4 = Q_1 = Q_4 = 0$. For each ω_n yielding λ_n, find θ_1, θ_4, F_1, F_4 from transfer matrices ("eigenvector") derived from mode shapes from above. The first 6 mode shapes are shown in figure 3.

ROLL-RATE STABILIZATION

Colocate roll-rate sensor with roll torquer. Use simple proportional feedback $Q_R = -K\dot{\phi}$. Figure 4 is part of the infinite-dimensional root locus vs. K. All modes are stabilized: Only 2 deformation modes are significant. Figure 5 is the root locus vs. K for the truncated model including only the 2 significant deformation modes. Figure 6 shows the 6th order model in more detail.

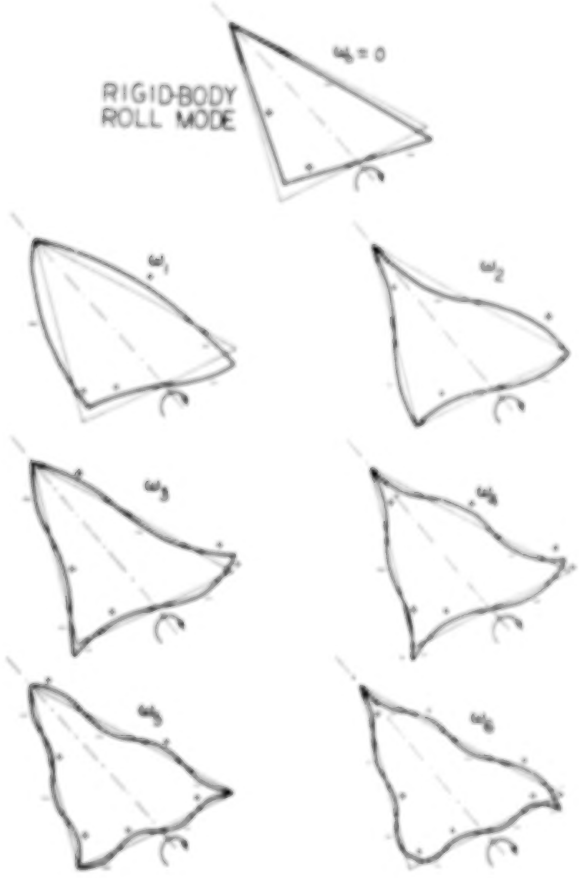

FIGURE 3. ROLL-MODE SHAPES

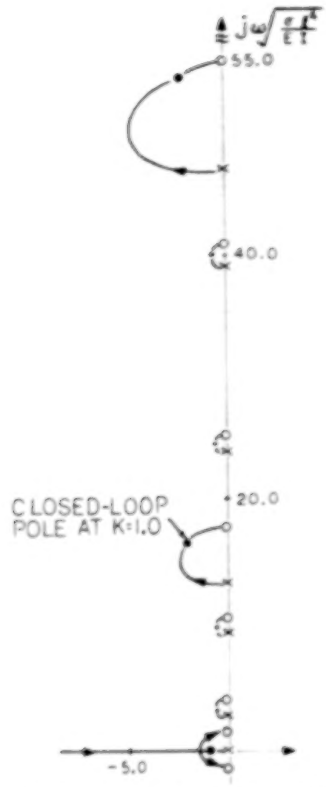

FIGURE 4. EXACT INFINITE-DIMENSIONAL ROOT LOCUS vs. K WITH RATE FEEDBACK $Q_R=-K\dot{\phi}$

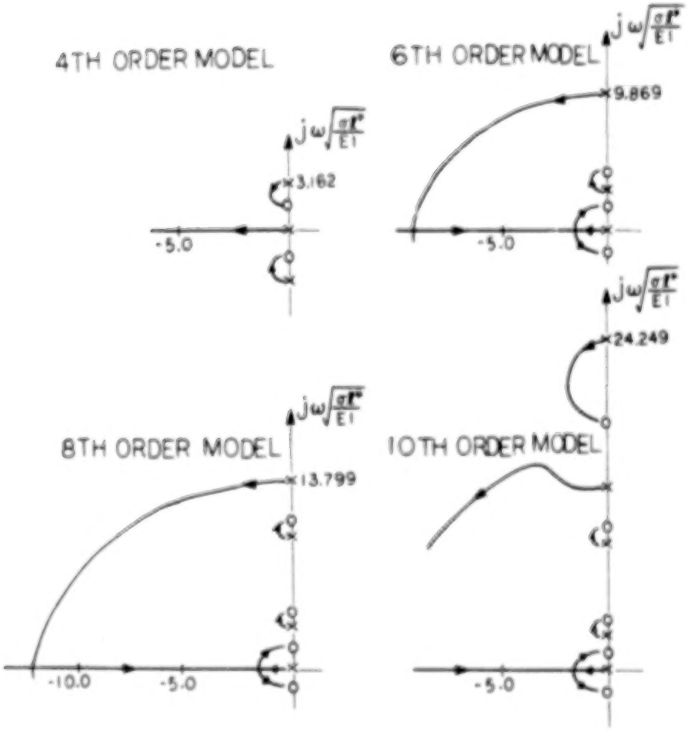

FIGURE 5-A. ROOT LOCI vs. K FOR REDUCED ORDER MODELS WITH RATE FEEDBACK $Q_R=-K\dot{\phi}$

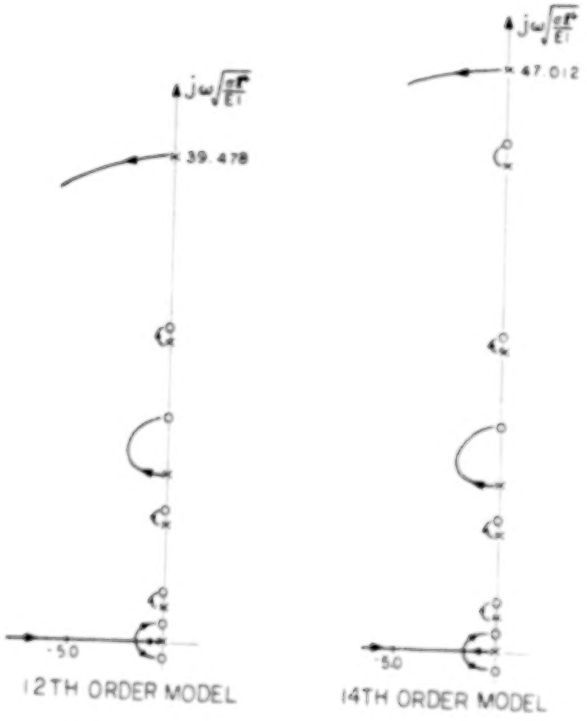

FIGURE 5-B. ROOT LOCI vs K FOR REDUCED ORDER MODELS WITH RATE FEEDBACK $Q_\phi = -K\dot{\phi}$

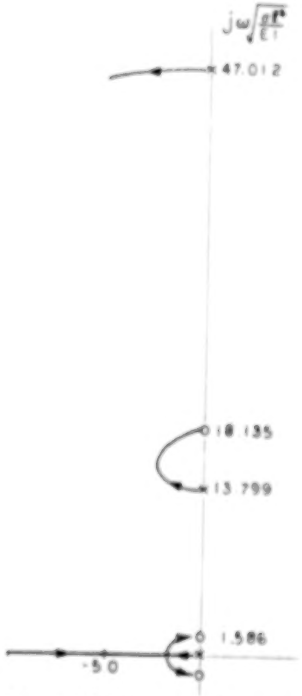

FIGURE 6. ROOT LOCUS vs K FOR 6TH ORDER MODEL WITH RATE FEEDBACK $Q_\phi = -K\dot{\phi}$ (MODES 1,2,4,5 ARE NEGLECTED)

ROLL-ATTITUDE STABILIZATION

Colocate roll-angle sensor with roll torquer. Use lead compensation

$$Q_R = -K \frac{s + 1}{s + 10} \phi(s)$$

Figure 7 is the root locus vs. K for the infinite-dimensional model.

PITCH CONTROL

Figure 8 shows the free-body diagram for analyzing pitch motions using 2 torquers Q_{P_1} and Q_{P_2}. Using the same method, we found the exact transfer function $\theta(s)/Q_p(s)$. The first few poles and zeros are shown in figure 9 for colocated sensors and torquers. Note the pole/zero cancellation plunge modes. The first few mode shapes are shown in figure 10. Some, but not all, frequencies are identical to the roll frequencies. Sensors do not pick up roll motions so there is no roll-pitch coupling.

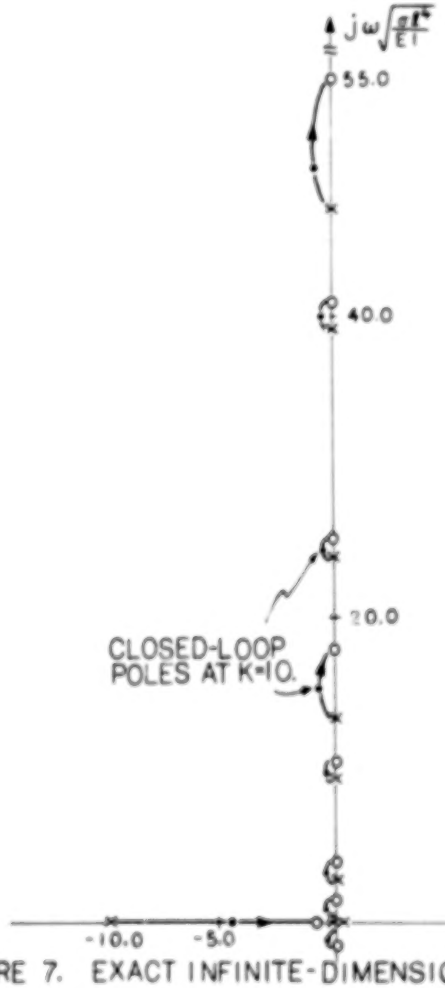

FIGURE 7. EXACT INFINITE-DIMENSIONAL ROOT LOCUS vs. K WITH LEAD COMPENSATION

$Q_R = -K \frac{S+1.0}{S+10.0} \phi$

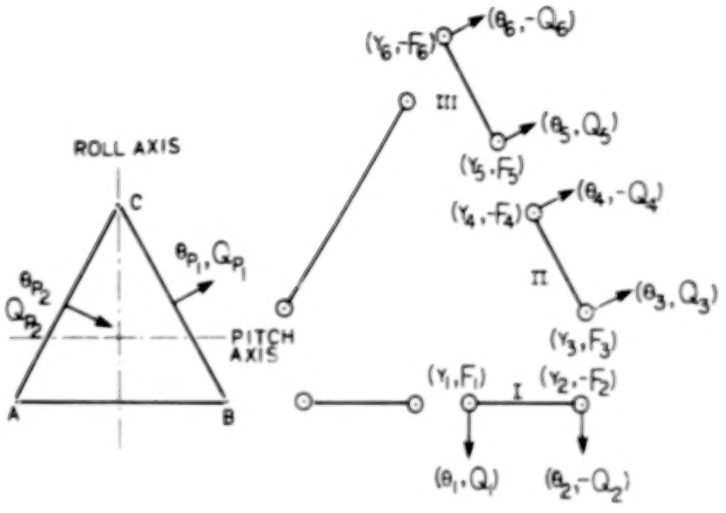

FIGURE 8. EQUILATERAL TRIANGULAR TRUSS WITH TWO IDENTICAL PITCH CONTROL TORQUES $Q_{p_1}=Q_{p_2}$

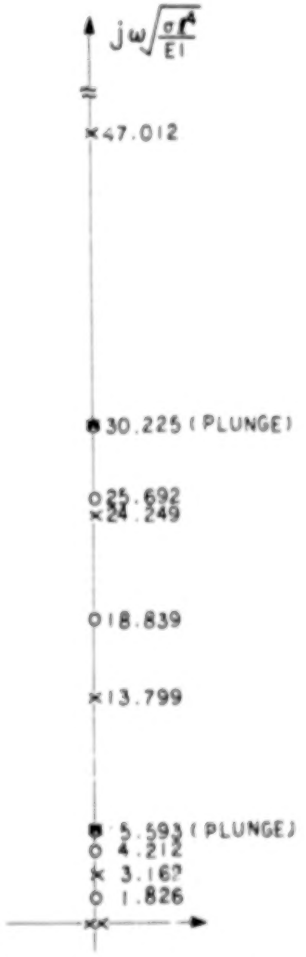

FIGURE 9. POLE-ZERO DISTRIBUTION OF PITCH TRANSFER FUNCTION $\frac{\theta(s)}{Q_p(s)}$ $(\theta \triangleq \frac{1}{2}(\theta_{p_1}+\theta_{p_2}))$

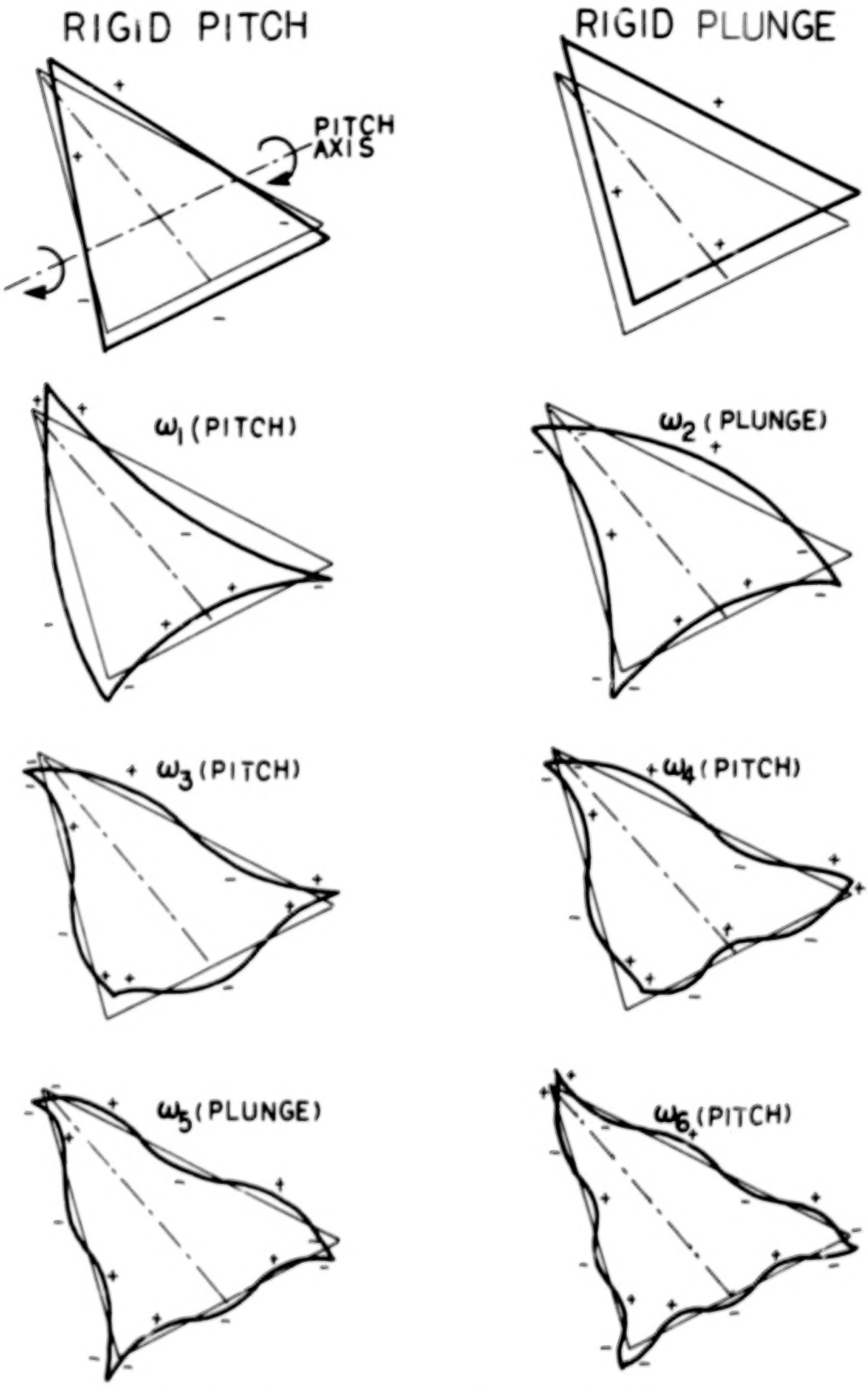

FIGURE 10. PITCH/PLUNGE MODE SHAPES (SYMMETRIC ABOUT ROLL AXIS)

Figure 11 shows the free-body diagram for analyzing yaw motions by using 3 torquers (at beam midpoints). We must now include the axial deformation of the beams since bending is in-plane. The values (x_i, G_i) are the axial displacements and axial forces at the points indicated.

Using the same methods, we found the first few exact poles and zeros for co-located sensors/torquers, shown in figure 12 for 3 different beam-slenderness ratios. The first few mode shapes are shown in figure 13.

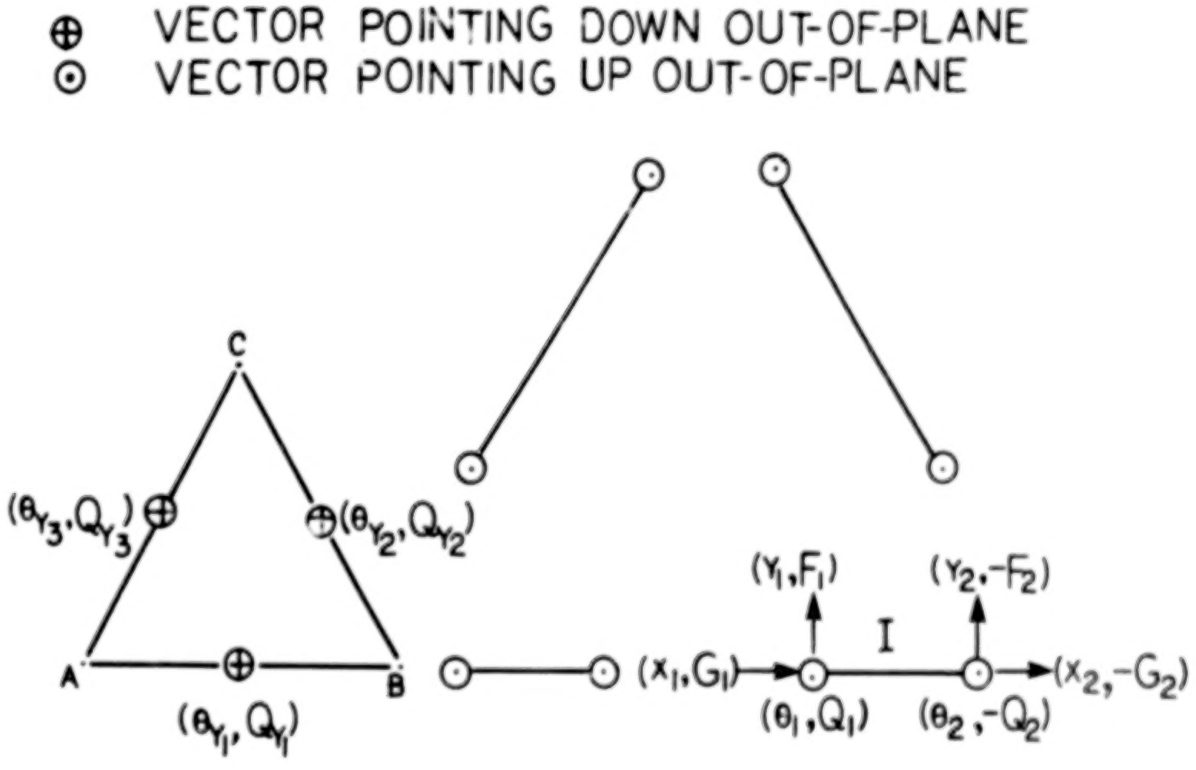

FIGURE 11. EQUILATERAL TRIANGULAR TRUSS WITH THREE IDENTICAL YAW CONTROL TORQUES

$$Q_{Y_1} = Q_{Y_2} = Q_{Y_3} \triangleq \frac{1}{3} Q_Y$$

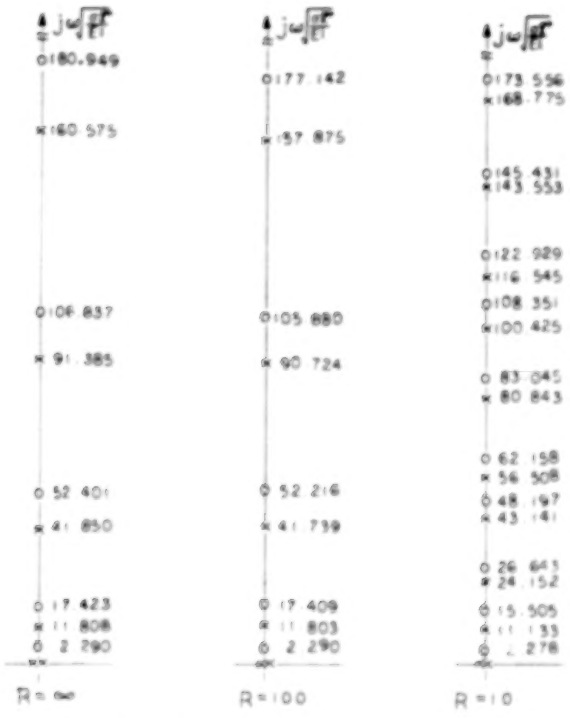

FIGURE 12 POLE-ZERO DISTRIBUTIONS OF YAW TRANSFER FUNCTION $\frac{\Psi(s)}{Q_3(s)}$
(R≙SLENDERNESS RATIO = $\frac{\ell}{r}$, $\Psi \triangleq \frac{1}{3}(\theta_1+\theta_2+\theta_3)$)

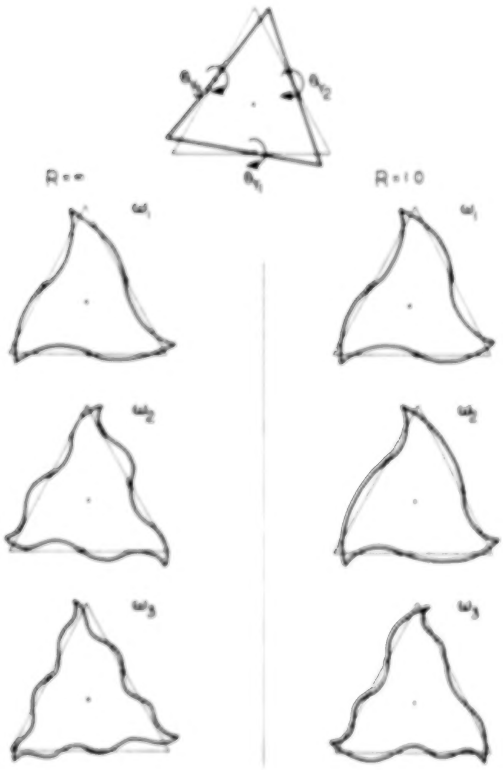

FIGURE 13 YAW MODE SHAPES WITH $\theta_1 = \theta_2 = \theta_3$

CONCLUSIONS

1. Exact infinite degree-of-freedom transfer functions can be found for truss/frame space structures using simple beam "transfer matrices".

2. By using symmetries, we can omit unexcitable modes in numerator/denominator, saving computation time.

3. Proper location of sensors and actuators avoids feedback-coupling of naturally uncoupled modes at the same resonant frequency.

4. Transfer function zeros (which depend on mode shapes) are found more accurately by this method than by the usual "finite-element" codes.

BLANK PAGE

LARGE MOTIONS OF DEFORMABLE SPACECRAFT

T. R. Kane
Stanford University
Stanford, CA

Workshop on the Structural Dynamics and Control
of Large Space Structures
October 30-31, 1980

CONSIDERATIONS FOR DYNAMIC SIMULATION OF LARGE SPACE STRUCTURES

- Large attitude changes
- Small deformations
- Arbitrary initial conditions

STRUCTURAL DYNAMIC ISSUES IN LARGE SPACE STRUCTURES

- Lump masses at nodes ?
- Treat members as linear springs ?
- Formulate the differential equations governing the coordinates of the nodal particles ?
- Solve the differential equations ?

  N nodes (N very large)
  3N second-order differential equation
  6N third-order differential equation

  The fact that only small deformations are of interest is not exploited.

- Small motions can be described in terms of principal modes - and only a few modes suffice. Can one use the same approach to describe large motions ? (See fig. 1.)

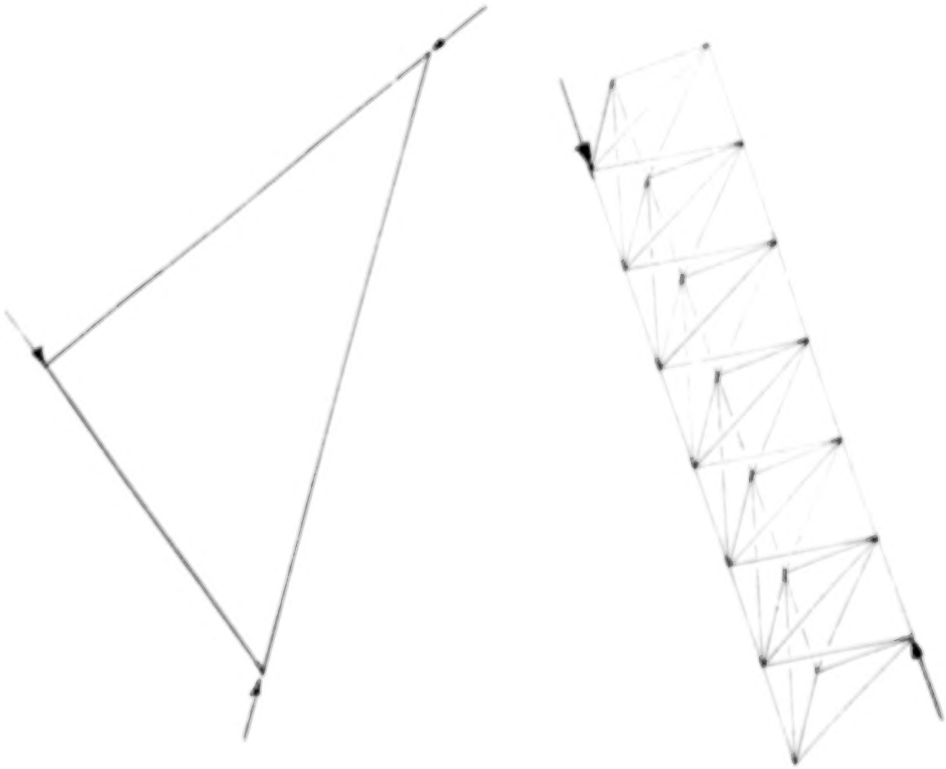

Figure 1

SIMULATION CONFIGURATION

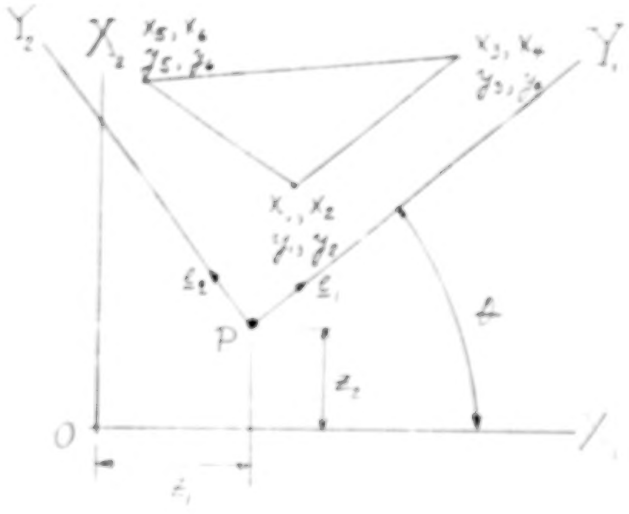

Figure 2

Configuration Variables

$x_1, \ldots, x_6$

or

$y_1, \ldots, y_6 ; z_1, z_2 ; \theta$

Modal Coordinates

$q_1, \ldots, q_v$

$$y_j = \bar{x}_j + \sum_{k=1}^{v} A_{jk} q_k$$

Generalized Speeds

$u_1 = \dot{\theta}$, $u_2 = \underline{v}^P \underline{e}_1$, $u_3 = \underline{v}^P \underline{e}_2$, $u_{3+k} = \dot{q}_k$ $(k = 1, \ldots, v)$

EQUATIONS OF MOTION

Kinematical

$$\dot{\theta} = u_1$$

$$\dot{z}_1 = u_2 \cos\theta - u_3 \sin\theta$$

$$\dot{z}_2 = u_2 \sin\theta + u_3 \cos\theta$$

$$\dot{q}_k = u_{3+k} \qquad (k = 1, \ldots, v)$$

Dynamical

$$I\dot{u}_1 - w_2\dot{u}_2 + w_3\dot{u}_3 + \sum_{j=1}^{v}\sum_{i=1}^{3} m_i(y_{2i-1}A_{2ij} - y_{2i}A_{2i-j})\dot{u}_{3+j}$$

$$= \sum_{i=1}^{3}\left[(Q_{2i} - m_i a_{i2})y_{2i-1} - (Q_{2i-1} - m_i a_{i1})y_{2i}\right] - w_2\dot{u}_1 + \bar{m}\dot{u}_2$$

$$= \sum_{i=1}^{3}(Q_{2i-1} - m_i a_{i1})w_1\dot{u}_1 + \bar{m}\dot{u}_3 = \sum_{i=3}^{3}(Q_{2i} - m_i a_{i2})$$

$$\sum_{i=1}^{3} m_i(y_{2i}A_{2i-k} - y_{2i-1}A_{2ik})\dot{u}_1 - \dot{u}_{3+k} = -G_k + \lambda_k q_k + \sum_{i=1}^{3} m_i(A_{2i-k}a_i + A_{2ik}a_{i2})$$

$$(k = 1, \ldots, v)$$

Initial Conditions

Given: $x_1(0)$, $x_2(0)$, $x_3(0)$; $\dot{x}_1(0)$, $\dot{x}_2(0)$, $\dot{x}_3(0)$

Needed: $z_1(0)$, $z_2(0)$, $\theta(0)$, $u_1(0)$, $u_2(0)$, $u_3(0)$; $q_k(0)$, $u_{3+k}(0)$ $\quad (k = 1, \ldots, v)$

$6 + 2v$ unknowns

Equations:

$$z_1(0) - x_{2i}(0)\theta(0) + \sum_{k=1}^{v} A_{2i-k}q_k(0) = x_{2i-1}(0) - \dot{x}_{2i-1}$$

$$z_2(0) + x_{2i}(0)\theta(0) + \sum_{k=1}^{v} A_{2ik}q_k(0) = x_{2i}(0) - \dot{x}_{2i}$$

$$-y_{2i}(0)u_1(0) + u_3(0) + \sum_{k=1}^{v} A_{2i-k}u_{3+k}(0) = \dot{x}_{2i-1}(0) - \dot{x}_{2i}(0)\theta(0)$$

$$-y_{2i-1}(0)u_1(0) + u_3(0) + \sum_{k=1}^{v} A_{2ik}u_{3+k}(0) = -\dot{x}_{2i-1}(0)\theta(0) + \dot{x}_{2i}(0)$$

$$(i = 1, 2, 3)$$

12 equations

If $v < 3$, the number of equations is greater than the number of unknowns.

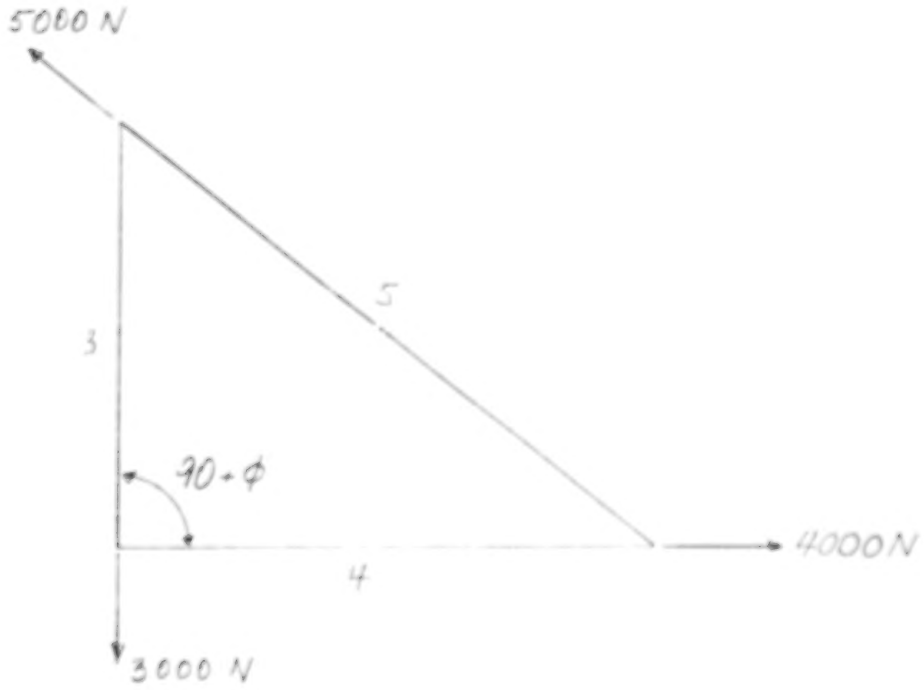

Figure 3

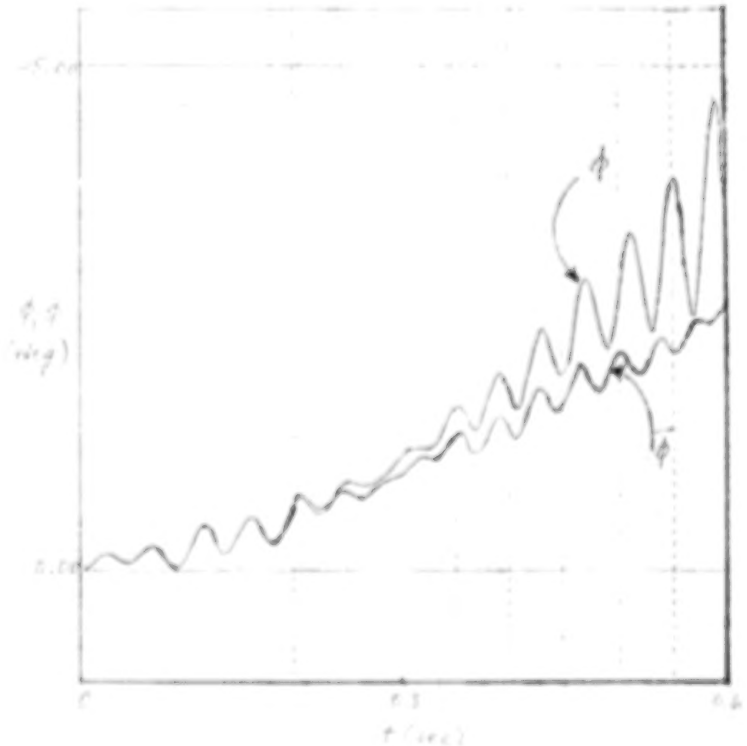

Figure 4 (φ = exact; $\bar{\phi}$ = linear solution)

BLANK PAGE

ATTENDEES

NASA Langley Research Center
Hampton, VA

J. L. Allen
Dr. E. S. Armstrong
G. P. Beasley
W. J. Boyer
M. L. Brumfield
Dr. M. F. Card
S. R. Cole
R. S. Dunning
H. A. Hamer
Dr. G. C. Horner
E. B. Lightner
U. M. Lovelace
Dr. R. C. Montgomery
J. R. Newsom
R. A. Russell
A. A. Schy
Dr. J. D. Shaughnessy
L. W. Taylor, Jr.
T. M. Weller (NSF)

Jet Propulsion Laboratory
Pasadena CA

D. B. Schaechter
Dr. A. F. Tolivar

NASA Goddard Space Flight Center
Greenbelt, MD

J. P. Young

Stanford University
Stanford, CA

Dr. H. Ashley
Dr. A. E. Byrson, Jr.
Dr. R. H. Cannon, Jr.
Dr. T. R. Kane

City University of New York
New York, NY

Dr. F. E. Thau

University of Houston
Houston, TX

Dr. E. D. Denman

North Carolina A & T
University
Greensboro, NC

Dr. E. Abu-Saba

Massachusetts Institute of Technology
Cambridge, Ma

Dr. E. F. Crawley
Dr. W. E. VanderVelde

Virginia Polytechnic Institute
and State University
Blacksburg, VA

Dr. C. R. Johnson, Jr.
D. Lawrence

University of Virginia
Charlottesville, VA

Dr. W. D. Pilkey

University of Maryland
College Park, MD

Dr. S. H. Wang

Honeywell, Inc.
Minneapolis, MN

C. W. Farnham
Dr. C. S. Greene
W. T. Herring
R. Pope

Structural Dynamics Research Corp.
Milford, OH

T. Savell

Ford Aerospace & Communications Corp.
Detroit, MI

C. T. Plescia

1. Report No.	2. Government Accession No.	3. Recipient's Catalog No.
NASA CP-2187		

4. Title and Subtitle	5. Report Date
STRUCTURAL DYNAMICS AND CONTROL OF LARGE SPACE STRUCTURES	June 1981
	6. Performing Organization Code: 506-54-93-01

7. Author(s)	8. Performing Organization Report No.
E. Burton Lightner, compiler	L-14609
	10. Work Unit No.

9. Performing Organization Name and Address	11. Contract or Grant No.
NASA Langley Research Center Hampton, VA 23665	
	13. Type of Report and Period Covered: Conference Publication

12. Sponsoring Agency Name and Address	14. Sponsoring Agency Code
National Aeronautics and Space Administration Washington, DC 20546	

15. Supplementary Notes

16. Abstract

This publication documents the proceedings of the Workshop on the Structural Dynamics and Control of Large Space Structures held at the NASA Langley Research Center (LaRC). The focus of the workshop was the basic research program assembled by LaRC to address the fundamental technology deficiencies that were identified in several studies on large space systems (LSS) conducted by NASA in the last several years. The program consists of an in-house effort, university grants, and industry contracts. The staffs of the respective participants were assembled at the workshop to review the current state of research in the control technology for large structural systems and to plan the efforts that would be pursued by their respective organizations. This document contains the more important slides used by the participants with text where necessary for clarity. The workshop was held on October 30-31, 1980.

17. Key Words (Suggested by Author(s))	18. Distribution Statement
Control systems Large space structures Structural dynamics	Unclassified - Unlimited Subject Category 15

19. Security Classif. (of this report)	20. Security Classif. (of this page)	21. No. of Pages	22. Price
Unclassified	Unclassified	138	A07

For sale by the National Technical Information Service, Springfield, Virginia 22161

NASA-Langley, 1981

90%

END